Thu. Sep 5, 2019

Poster Place

Poster Session | Postharvest Machinery

[5-1130-P] Postharvest Machinery (5th)

11:30 AM - 12:30 PM Poster Place (Entrance Hall)

[5-1130-P-14] **Detection of Outliers in Pre-processing of Datasets for Recognition of Classifiers Using Partial Least Squares Discriminant Analysis**

*Miki Fujii[1], Ryozo Noguchi[2], Tofael Ahamed[2], Takuma Genkawa[3] (1. Graduate School of Life and Environmental Sciences, University of Tsukuba(Japan), 2. Faculty of Life and Environmental Sciences, University of Tsukuba(Japan), 3. Food Research Institute, NARO(Japan))

11:30 AM - 12:30 PM

Poster Session | Postharvest/Food Technology and Process Engineering

[5-1130-P] Postharvest/Food Technology and Process Engineering (5th)

11:30 AM - 12:30 PM Poster Place (Entrance Hall)

[5-1130-P-01] **Development of dumpling rich in barley flour with gluten added**

*Masatsugu Tamura[1], Naoya Takahashi[1], Takahiro Saito[1], Satomi Akutsu[2], Yoshihiro Hoshi[3], Takemi Okamoto[3] (1. Utsunomiya Univ.(Japan), 2. Tochigi Industrial Promotion Center(Japan), 3. Industrial Technology Center of Tochigi Pref.(Japan))

11:30 AM - 12:30 PM

[5-1130-P-02] **Palm Oil based Wax Coating Maintained Postharvest Quality of Thai Lime cv. Paan Pichit#1**

*Varit Srilaong[1], Nutthachai Pongprasert[1], Songsin Photchanachai[1], Panida Boonyaritthongchai[1], Kornkanok Aryusuk[2] (1. Division of Postharvest Technology, School of Bioresources and Technology, King Mongkut's University of Technology Thonburi(Thailand), 2. Division of Biochemical Technology, School of Bioresources and Technology, King Mongkut's University of Technology Thonburi(Thailand))

11:30 AM - 12:30 PM

[5-1130-P-03] **Development of Blueberry Wine with High Content of Polyphenol**

*Hongpu Wang[1], Yutaka Kitamura[2], Mito Kokawa[2] (1. Graduate school of Life and Environmental Sciences, Tsukuba Univ.(Japan), 2. Faculty of Life and Environmental Sciences, Tsukuba Univ.(Japan))

11:30 AM - 12:30 PM

[5-1130-P-04] **Effects of Heating under Pasteurization Conditions on Mechanical and Electrical Properties of Mung Bean Sprout**

*Hayato Ogino[1], Haruki Ando[1], Satoshi Iwamoto[1], Teppei Imaizumi[1] (1. Gifu University(Japan))

11:30 AM - 12:30 PM

[5-1130-P-05] **Study on Non-Destructive Measurements to Predict Sugar Content of Melons Using a DLP Based Miniature Spectrometer**

*Chao-Yin TSAI[1], Pin-Chih Fang[1], Yi-Tzu Shen[1], Yung-Huei Chang[1], Han-Chun Hsu[1], Suming Chen[1] (1. Department of Bio-Industrial Mechatronics Engineering, National Taiwan University(Taiwan))

11:30 AM - 12:30 PM

[5-1130-P-06] **Effect of Lactic acid bacteria fermentation on the microbial diversity, physico-chemical properties, and organic acid profile of *pindang damulag*, a fermented carabeef**

*Michael Angelo Santos Esteban[1], Lotis Mopera[1], Maria Cynthia Oliveros[1], Erlinda Dizon[1] (1. University of the Philippines Los Banos(Philippines))

11:30 AM - 12:30 PM

[5-1130-P-07] **Properties of Rice Starch-Based Film Incorporated with Zinc Oxide Nanoparticles**

KHALISHAH RAHMA SAFIRA[1,2], *SAROAT RAWDKUEN[2] (1. Department of Food Science and Technology, Faculty of Agricultural Technology and Engineering, Bogor Agricultural University(Indonesia), 2. Unit of Innovative Food Packaging and Biomaterials, School of Agro-Industry, Mae Fah Luang University(Thailand))

11:30 AM - 12:30 PM

[5-1130-P-08] **Effect of pulsed electric field treatment on drying rate and quality changes of spinach**

in hot air drying

*Koya Yamakage[1], Takahiro Yamada[1], Takahiro Orikasa[2,3], Katsuyuki Takahashi[2,4], Shoji Koide[3], Koichi Takaki[2,4], Hitoshi Aoki[5], Junichi Kamagata[5] (1. Graduate School of Arts and Science, Iwate University(Japan), 2. Agri-Innovation Center, Iwate University(Japan), 3. Faculty of Agriculture, Iwate University(Japan), 4. Faculty of Science and Engineering, Iwate University(Japan), 5. Nichirei Foods Inc.(Japan))

11:30 AM - 12:30 PM

[5-1130-P-09] **Prospects of Biogas Production From The Manure of Dairy Cattle Fed on Iron-supplemented Ration**

*Mohamed Farghali[1,2], Maejima Mayumi[3], Kuramoto Syo[3], Aoki Satoshi[4], Yasui Seiichi[5], Sayoko Takashima [1], Hijiri Ono[1], Yuhendra AP[1], Takaki Yamashiro[6], Moustafa M. Ahmed[2], Saber Kotb[2], Masahiro Iwasaki[1], Kazutaka Umetsu[1] (1. Graduate School of Animal and Food Hygiene, Obihiro University of Agriculture and Veterinary Medicine(Japan), 2. Department of Animal and Poultry Hygiene &Environmental Sanitation, Faculty of Veterinary Medicine, Assiut University(Egypt), 3. Maezawa Engineering service Inc.(Japan), 4. Maezawa Industries Inc.(Japan), 5. Hokkaido Air Water Inc.(Japan), 6. Tokachi Agri Works (Japan))

11:30 AM - 12:30 PM

[5-1130-P-10] **Anaerobic Digestion of Bean Sprouts Waste**

*Yuki Yamamoto[1], Yuki Mizuya[2], Takaki Yamashiro[3], Fetra J Andriamanohiarisoamanana[1,4], Yoshiteru Takeuchi[5], Kazutaka Umetsu[1] (1. Graduate school of Obihiro University of Agriculture and Veterinary Medicine(Japan), 2. Obihiro University of Agriculture and Veterinary Medicine(Japan), 3. Tokachi Agri Works(Japan), 4. Graduate School of Agricultural Science, Kobe University(Japan), 5. Biomass Research(Japan))

11:30 AM - 12:30 PM

[5-1130-P-11] **Optimization of Orange-Fleshed Sweet Potato (*Ipomoea batatas* var. Kinerot) Flour Processing for Carotenoid Retention**

James Ryan D. Aranzado[1], *Loraine C. Bainto[1], Dennis Marvin O. Santiago[1] (1. Institute of Food Science and Technology, College of Agriculture and Food Science, University of the Philippines Los Baños(Philippines))

11:30 AM - 12:30 PM

[5-1130-P-12] **Temporal Transition of Spatial Dependence of Weeds in Grassland**

*Katsuyuki Tanaka[1], Ayako Oide[1], Hideo Minagawa[1] (1. Kitasato University(Japan))

11:30 AM - 12:30 PM

[5-1130-P-13] **RNA-Seq analysis of the transcriptome and genes expression profile during the browning of Lotus Root (*Nelumbo nucifera*)**

*Kanjana Worarad[1], Haruka Norii[1], Yuya Muchizuki[1], Takashi Ishii[2], Keiko Shinohara[3], Takao Miyamoto [4], Eiichi Inoue [1] (1. Ibaraki University(Japan), 2. Ibaraki Agricultural Center, Horticultural Research Institute (Japan), 3. Tokushima Agriculture, Forestry and Fisheries Technology Support Center(Japan), 4. Renkon3kyodai Co.Ltd(Japan))

11:30 AM - 12:30 PM

Poster Session | Food Quality

[5-1130-P] Food Quality (5th)

11:30 AM - 12:30 PM Poster Place (Entrance Hall)

[5-1130-P-15] **Effect of Blending at Different Stages of Winemaking on the Quality of Mixed Fruit Wine**

*Claire Solis Zubia[1], Erlinda Ignacio Dizon[1] (1. University of the Philippines Los Banos(Philippines))

11:30 AM - 12:30 PM

[5-1130-P-16] **Pest Control of *Tetranychus urticae* by Branched Fatty Acids**

*Mai Nagano[1], Akitaka Teshima[1], Toshinari Koda[2], Hiroshi Morita[1] (1. The University of Kitakyushu(Japan), 2. Nissan Chemical corporation(Japan))

11:30 AM - 12:30 PM

[5-1130-P-17] **Evaluation of Quality and Structural Properties of Bread Containing Edible Cricket**

*Kiko Kuroda[1], Tatsuya Oshima[1], Teppei Imaizumi[1] (1. Gifu Graduate School of Applied

Biological Sciences and Faculty of Applied Biological Sciences(Japan))
11:30 AM - 12:30 PM

Poster Session | Food Safety

[5-1130-P] Food Safety (5th)

11:30 AM - 12:30 PM Poster Place (Entrance Hall)

[5-1130-P-18] **Key Process Variables Affecting the Formation of Chlormequat Compounds During Baking of Cereal Products**
*Adam Ekielski[1] (1. Warsaw University of Life Sciences(Poland))
11:30 AM - 12:30 PM

[5-1130-P-19] **Acaricidal effects of Linear fatty acids against *Tyrophagus putrescentiae***
*Kosuke Matsuoka[1], Toshinari Koda[2], Hiroshi Morita[1] (1. The University of Kitakyushu(Japan), 2. Nissan Chemical Corporation(Japan))
11:30 AM - 12:30 PM

[5-1130-P-20] **Improvement of the Cleanability of Milk Soil on a Highly Smooth Surface of Stainless Steel Tubing**
*Ikko Ihara[1], Homi Takato[1], John K Schueller[2], Gen Yoshida[1], Kazutaka Umetsu[3], Hitomi Yamaguchi[2] (1. Kobe University(Japan), 2. University of Florida(United States of America), 3. Obihiro University of Agriculture and Veterinary Medicine(Japan))
11:30 AM - 12:30 PM

Poster Session | Others (including the category of JSAM and SASJ)

[5-1130-P] Other Categories (5th)

11:30 AM - 12:30 PM Poster Place (Entrance Hall)

[5-1130-P-21] **Screening and Identification of Endophytic Bacteria from Thai Organic Rice for Plant Growth Promotion**
*Somkid Deejing[1], Witchayaporn Pawong[1] (1. Program in biotechnology, Faculty of Science, Maejo University, Sansai, Chiang Mai(Thailand))
11:30 AM - 12:30 PM

[5-1130-P-22] **Data Extraction for Pig Weight Prediction Model**
*Khin Dagon Win[1], Kikuhito Kawasue[1], Hsu Lai Wai[1], Kumiko Yoshida[2] (1. University of Miyazaki(Japan), 2. KOYO Plant Service(Japan))
11:30 AM - 12:30 PM

[5-1130-P-23] **Power Tiller's Wheel Structure and its Oscillatory Effects on Subsoiling Operation**
*Oyetayo Olukorede Oyebode[1], Koichi Shoji[1] (1. Graduate School of Agricultural Science, Kobe University(Japan))
11:30 AM - 12:30 PM

[5-1130-P-24] **Proposal of temperature control technology in pot cultivation for the citrus fruits**
*Ryuta IBUKI[1], Yoshimichi Yamashita[2], Sachie Horii[2], Norihiro Hoshi[2], Madoka Chiba[1] (1. Miyagi University(Japan), 2. National Agriculture and Food Research Organization(Japan))
11:30 AM - 12:30 PM

[5-1130-P-25] **Investigation by Driving Simulation of Tractor Overturning Accidents Caused by Steering Instability**
*Masahisa Watanabe[1], Kenshi Sakai[1] (1. Tokyo University of Agriculture and Technology(Japan))
11:30 AM - 12:30 PM

[5-1130-P-26] **Classification of Salinity Damaged Spring Potato (Solanum tuberosum) using Hyperspectral Imagery based on Decision Tree Classifier**
*KyungSuk Kang[1], Sae Rom Jun[1], Si Hyeong Jang[1], Jun Woo Park[1], Hye Young Song[1], Ye Seong Kang[1], Chan Seok Ryu[1], Su Hwan Lee[2] (1. GNU(Korea), 2. RDA(Korea))
11:30 AM - 12:30 PM

[5-1130-P-27] **Classification for Fire Blight Disease Infection Area using Vegetation Index and Background Segmentation based on Multispectral Image**
*Jun-woo Park[1], Chan-seok Ryu[1], Ye-seong Kang[1], Sae-Rom Jean[1], Si-Hyeong Jang[1], Hye-Young Song[1], Kyung-Suk Kang[1] (1. GNU(Korea))
11:30 AM - 12:30 PM

[5-1130-P-28] **The Static Load Test for Tractor Attached Three-Point Hitch Type Dynamometerd**
*Hyo-Geol Kim[1], Sung-Bo Shim[2], Yeon-Soo Kim[1], Young-Joo Kim[1], Sang-Dae Lee[1] (1. Korea Institute of Industrial Technology(Korea), 2. Gyeongsang National University(Korea))

11:30 AM - 12:30 PM

[5-1130-P-29] **Isolation and Identification of Acetic Acid Bacteria from Philippine Fermented Rice Cake Batters by 16S rRNA Gene Sequence Analysis**

Audrey Mae Villamin Orillaza[1], Honey Bhabes R Iñigo[1], *Baby Richard Ragudo Navarro[1] （1. Institute of Food Science and Technology, College of Agriculture and Food Science, University of the Philippines Los Baño s(Philippines)）

11:30 AM - 12:30 PM

[5-1130-P-30] **Estimation of Greenhouse Gas Emissions from Poultry Farming Systems for a Broiler Meat Production and an Egg Production in Japan using a Life Cycle Assessment**

*Tatsuo Hishinuma[1], Tetsuya Hoshino[1], Atsuo Ikeguchi[1], （1.Utsunomiya Univ.(Japan)）

11:30 AM - 12:30 PM

Poster Session | Postharvest Machinery

[5-1130-P] Postharvest Machinery (5th)

Thu. Sep 5, 2019 11:30 AM - 12:30 PM Poster Place (Entrance Hall)

[5-1130-P-14] Detection of Outliers in Pre-processing of Datasets for Recognition of Classifiers Using Partial Least Squares Discriminant Analysis

*Miki Fujii[1], Ryozo Noguchi[2], Tofael Ahamed[2], Takuma Genkawa[3] （1. Graduate School of Life and Environmental Sciences, University of Tsukuba(Japan), 2. Faculty of Life and Environmental Sciences, University of Tsukuba(Japan), 3. Food Research Institute, NARO(Japan)）

11:30 AM - 12:30 PM

11:30 AM - 12:30 PM (Thu. Sep 5, 2019 11:30 AM - 12:30 PM Poster Place)

[5-1130-P-14] Detection of Outliers in Pre-processing of Datasets for Recognition of Classifiers Using Partial Least Squares Discriminant Analysis

*Miki Fujii[1], Ryozo Noguchi[2], Tofael Ahamed[2], Takuma Genkawa[3] (1. Graduate School of Life and Environmental Sciences, University of Tsukuba(Japan), 2. Faculty of Life and Environmental Sciences, University of Tsukuba(Japan), 3. Food Research Institute, NARO(Japan))

Keywords: Pre-Processing, Dataset for Recognition of Classifiers, Machine Learning, Multivariate Analysis

In recent years, smart agriculture has received increasing attention in Japan. Image recognition is used to confirm the growth of vegetables and to determine the proper harvest timing. In machine learning, the choice of images used for the data set affects the accuracy rate of recognition of classifiers. Generally, collected data sets are pre-processed by analysts according to their experience and knowledge. Among them, there are images that could be outliers that adversely affect the accuracy rate. In this study, pre-processing was performed to datasets with objective indicators using partial least squares discriminant analysis (PLS-DA), which is one of the multivariate analyses. In datasets, 300 images of lemon and 300 images of strawberry were used. All images were 75x75 pixels in size. In first test, recognition of classifiers was performed on this dataset by Support Vector Machine (SVM). Of all the data, 75% was set as training data and 25% was randomly set as test data. The rate at which images are correctly classified is defined as the accuracy rate. Also, the images of the dataset were resized from 2x2 pixels to 64x64 pixels, and the same verification was performed. Verification was performed 100 times at each pixel condition. The outliers were detected by PLS-DA before recognition of classifiers by SVM. The objective variable of the data of the lemon images were set to 1, and data of strawberry images were set to 0. The threshold value was determined to be 0.5. In the model of PLS-DA, data of lemon images whose predicted values showed a value of 0.5 or more and data of strawberry images whose predicted values showed 0.5 or less were detected as outliers. Data detected as outliers were removed from the dataset and then image recognition was performed in the same flow as the first test. First test was conducted and noted that SVM had 91.6% ~ 96.5% accuracy rates in each pixel images. It means recognition of classifiers was performed almost accurately. Focusing on the increase in the number of pixels, the accuracy rate continued to improve up to 8x8 pixels images and stayed about 96% after that. At 2x2 pixels images, its standard deviation shows 7.6% (maximum accuracy rate: 98.0%, minimum accuracy rate: 51.7%) and its coefficient of variation shows 0.083. On the other hand, 4x4 pixels and more pixels images showed 1.4 ~ 1.8% standard deviation and less than 0.009 coefficient of variation. Comparing these two, the accuracy rate varied widely for each test when using 2x2 pixels images for testing. Second test was conducted and noted that PLS-DA for preprocessing and performed SVM had more than 99% accuracy regardless of the number of pixels. Images detected as outliers were less than 6% (4 images ~ 17 images) in each pixel image. The t test between the first test and the second test showed that the accuracy rate was significantly improved in all pixel conditions. And the coefficient of variation in each pixel images showed less than 0.009. In particular, in the 2x2 pixels images, the value of the coefficient of variation decreased significantly. This means that it proved removal of outliers can suppress variation in accuracy rate. From the above, by detection of outliers to remove from dataset using PLS-DA, it proved that the accuracy rate of recognition of classifiers could be significantly improved from 96% to 99%, and the variation in accuracy rate values could also be suppressed. In the machine-learning algorithm for training and testing, the developed outlier detection method can be implemented to increase the accuracy of validation.

Poster Session | Postharvest/Food Technology and Process Engineering

[5-1130-P] Postharvest/Food Technology and Process Engineering (5th)

Thu. Sep 5, 2019 11:30 AM - 12:30 PM Poster Place (Entrance Hall)

[5-1130-P-01] Development of dumpling rich in barley flour with gluten added

*Masatsugu Tamura[1], Naoya Takahashi[1], Takahiro Saito[1], Satomi Akutsu[2], Yoshihiro Hoshi[3], Takemi Okamoto[3] (1. Utsunomiya Univ.(Japan), 2. Tochigi Industrial Promotion Center(Japan), 3. Industrial Technology Center of Tochigi Pref.(Japan))

11:30 AM - 12:30 PM

[5-1130-P-02] Palm Oil based Wax Coating Maintained Postharvest Quality of Thai Lime cv. Paan Pichit#1

*Varit Srilaong[1], Nutthachai Pongprasert[1], Songsin Photchanachai[1], Panida Boonyaritthongchai[1], Kornkanok Aryusuk[2] (1. Division of Postharvest Technology, School of Bioresources and Technology, King Mongkut's University of Technology Thonburi(Thailand), 2. Division of Biochemical Technology, School of Bioresources and Technology, King Mongkut's University of Technology Thonburi(Thailand))

11:30 AM - 12:30 PM

[5-1130-P-03] Development of Blueberry Wine with High Content of Polyphenol

*Hongpu Wang[1], Yutaka Kitamura[2], Mito Kokawa[2] (1. Graduate school of Life and Environmental Sciences, Tsukuba Univ.(Japan), 2. Faculty of Life and Environmental Sciences, Tsukuba Univ.(Japan))

11:30 AM - 12:30 PM

[5-1130-P-04] Effects of Heating under Pasteurization Conditions on Mechanical and Electrical Properties of Mung Bean Sprout

*Hayato Ogino[1], Haruki Ando[1], Satoshi Iwamoto[1], Teppei Imaizumi[1] (1. Gifu University(Japan))

11:30 AM - 12:30 PM

[5-1130-P-05] Study on Non-Destructive Measurements to Predict Sugar Content of Melons Using a DLP Based Miniature Spectrometer

*Chao-Yin TSAI[1], Pin-Chih Fang[1], Yi-Tzu Shen[1], Yung-Huei Chang[1], Han-Chun Hsu[1], Suming Chen[1] (1. Department of Bio-Industrial Mechatronics Engineering, National Taiwan University(Taiwan))

11:30 AM - 12:30 PM

[5-1130-P-06] Effect of Lactic acid bacteria fermentation on the microbial diversity, physico-chemical properties, and organic acid profile of *pindang damulag*, a fermented carabeef

*Michael Angelo Santos Esteban[1], Lotis Mopera[1], Maria Cynthia Oliveros[1], Erlinda Dizon[1] (1. University of the Philippines Los Banos(Philippines))

11:30 AM - 12:30 PM

[5-1130-P-07] Properties of Rice Starch-Based Film Incorporated with Zinc Oxide Nanoparticles

KHALISHAH RAHMA SAFIRA[1,2], *SAROAT RAWDKUEN[2] (1. Department of Food Science and Technology, Faculty of Agricultural Technology and Engineering, Bogor Agricultural University(Indonesia), 2. Unit of Innovative Food Packaging and Biomaterials, School of Agro-Industry, Mae Fah Luang University(Thailand))

11:30 AM - 12:30 PM

[5-1130-P-08] Effect of pulsed electric field treatment on drying rate and quality changes of spinach in hot air drying

*Koya Yamakage[1], Takahiro Yamada[1], Takahiro Orikasa[2,3], Katsuyuki Takahashi[2,4], Shoji Koide[3], Koichi Takaki[2,4], Hitoshi Aoki[5], Junichi Kamagata[5] （1. Graduate School of Arts and Science, Iwate University(Japan), 2. Agri-Innovation Center, Iwate University(Japan), 3. Faculty of Agriculture, Iwate University(Japan), 4. Faculty of Science and Engineering, Iwate University(Japan), 5. Nichirei Foods Inc.(Japan)）

11:30 AM - 12:30 PM

[5-1130-P-09] Prospects of Biogas Production From The Manure of Dairy Cattle Fed on Iron-supplemented Ration

*Mohamed Farghali[1,2], Maejima Mayumi[3], Kuramoto Syo[3], Aoki Satoshi[4], Yasui Seiichi[5], Sayoko Takashima [1], Hijiri Ono[1], Yuhendra AP[1], Takaki Yamashiro[6], Moustafa M. Ahmed[2], Saber Kotb[2], Masahiro Iwasaki[1], Kazutaka Umetsu[1] （1. Graduate School of Animal and Food Hygiene, Obihiro University of Agriculture and Veterinary Medicine(Japan), 2. Department of Animal and Poultry Hygiene &Environmental Sanitation, Faculty of Veterinary Medicine, Assiut University(Egypt), 3. Maezawa Engineering service Inc.(Japan), 4. Maezawa Industries Inc.(Japan), 5. Hokkaido Air Water Inc.(Japan), 6. Tokachi Agri Works (Japan)）

11:30 AM - 12:30 PM

[5-1130-P-10] Anaerobic Digestion of Bean Sprouts Waste

*Yuki Yamamoto[1], Yuki Mizuya[2], Takaki Yamashiro[3], Fetra J Andriamanohiarisoamanana[1,4], Yoshiteru Takeuchi[5], Kazutaka Umetsu[1] （1. Graduate school of Obihiro University of Agriculture and Veterinary Medicine(Japan), 2. Obihiro University of Agriculture and Veterinary Medicine(Japan), 3. Tokachi Agri Works(Japan), 4. Graduate School of Agricultural Science, Kobe University(Japan), 5. Biomass Research(Japan)）

11:30 AM - 12:30 PM

[5-1130-P-11] Optimization of Orange-Fleshed Sweet Potato (*Ipomoea batatas* var. Kinerot) Flour Processing for Carotenoid Retention

James Ryan D. Aranzado[1], *Loraine C. Bainto[1], Dennis Marvin O. Santiago[1] （1. Institute of Food Science and Technology, College of Agriculture and Food Science, University of the Philippines Los Baños(Philippines)）

11:30 AM - 12:30 PM

[5-1130-P-12] Temporal Transition of Spatial Dependence of Weeds in Grassland

*Katsuyuki Tanaka[1], Ayako Oide[1], Hideo Minagawa[1] （1. Kitasato University(Japan)）

11:30 AM - 12:30 PM

[5-1130-P-13] RNA-Seq analysis of the transcriptome and genes expression profile during the browning of Lotus Root (*Nelumbo nucifera*)

*Kanjana Worarad[1], Haruka Norii[1], Yuya Muchizuki[1], Takashi Ishii[2], Keiko Shinohara[3], Takao Miyamoto [4], Eiichi Inoue [1] （1. Ibaraki University(Japan), 2. Ibaraki Agricultural Center, Horticultural Research Institute (Japan), 3. Tokushima Agriculture, Forestry and Fisheries Technology Support Center(Japan), 4. Renkon3kyodai Co.Ltd(Japan)）

11:30 AM - 12:30 PM

11:30 AM - 12:30 PM (Thu. Sep 5, 2019 11:30 AM - 12:30 PM Poster Place)

[5-1130-P-01] Development of dumpling rich in barley flour with gluten added

*Masatsugu Tamura[1], Naoya Takahashi[1], Takahiro Saito[1], Satomi Akutsu[2], Yoshihiro Hoshi[3], Takemi Okamoto[3]
（1. Utsunomiya Univ.(Japan), 2. Tochigi Industrial Promotion Center(Japan), 3. Industrial Technology Center of Tochigi Pref.(Japan)）

Keywords: Barley, Dumpling, β-glucan, Total polyphenol, Texture

This study aimed to develop dumplings with high barley content, by the incorporation of less than 10% gluten. To 100 g of barley flour, 5% and 10% gluten, and 50%, 60%, 65%, 70% and 75% water, respectively, were added. The mixture was kneaded, left for 3 hours to allow dough development, cut to form raw barley dumpling skin, and then baked for analysis of color, texture, β-glucan content and total polyphenol content. Cooked barley dumplings with mincemeat filling were prepared for sensory evaluation. In addition, wheat dumplings were also prepared and examined, for comparison. The barley dumpling skin had significantly lower L* and higher a* when compared with wheat dumpling skin. No significant difference in firmness was observed between baked wheat dumpling skins (2.07 N) and burley dumpling skins with added 10% gluten and 65%, 70% and 75% moisture (1.82–2.28 N). The burley dumpling skin with 10% gluten and 70% moisture, used to prepare the meat dumplings, displayed the closest texture to that of the baked wheat dumpling skin. A higher β-glucan content (2.2% vs. 0.2% dry basis) and total polyphenol content (183.2 vs. 86.4 mg gallic acid equivalents/g dry weight) were provided by baked barley dumpling than the baked wheat dumpling. The sensory test revealed no difference between baked barley and wheat dumplings, except for appearance. The proposed method provides barley dumpling with high functional components and palatability.

Poster Session | Postharvest/Food Technology and Process Engineering
[5-1130-P] Postharvest/Food Technology and Process Engineering (5th)
Thu. Sep 5, 2019 11:30 AM - 12:30 PM Poster Place (Entrance Hall)

[5-1130-P-02] Palm Oil based Wax Coating Maintained Postharvest Quality of Thai Lime cv. Paan Pichit#1

*Varit Srilaong[1], Nutthachai Pongprasert[1], Songsin Photchanachai[1], Panida Boonyaritthongchai[1], Kornkanok Aryusuk[2] (1. Division of Postharvest Technology, School of Bioresources and Technology, King Mongkut's University of Technology Thonburi(Thailand), 2. Division of Biochemical Technology, School of Bioresources and Technology, King Mongkut's University of Technology Thonburi(Thailand))

Keywords: Coating, Palm oil wax, Lime, Postharvest, Quality

Immature green lime fruit cv. Pann Pichit#1 is widely consumption in Thailand as an ingredient of Thai' s dish. Most of consumers prefer to have immature green lime due to its enriches with special aromatic compound, taste and flavor. Thus, to maintain the green color of lime fruit is very important for retarding quality losses. Peel yellowing is one of a major problem in lime fruit during postharvest period which lead to reduction of fruit qualities thus the inhibiting or delaying of chlorophyll breakdown is needed. There are several kind of postharvest technology to prolong storage life and maintain green color of fresh produces and one of them is coating technique by using natural based wax. According to Thailand produces a lot of palm oil and a byproduct from palm oil industry, palm oil wax, has potential to use as a wax based to form coating material. Thus, this research aimed to use palm oil based wax coating for maintaining quality of immature green lime cv. Pann Pichit#1. Lime fruit were harvested from commercial orchard and coated with palm oil based wax (PW) and commercial wax (CW), and then stored at 13°C. Uncoated fruit was set as a control. Changes of lime fruit qualities including fresh weight loss, browning spot, chlorophyll content, ascorbic acid content and acetaldehyde content were investigated at 5 days interval. The results found that lime fruit coated with PW showed the lowest water loss compared with that of CW coated and the control, respectively. The percentage of peel browning spot occurrence was also reduced in the fruit coated with PW while the application of CW induced a browning spot to higher level than the control. This result was concomitant with the incidence of peel browning. Lime fruit coated with both PW and CW delayed the chlorophyll breakdown in the same trend while the continuously degradation of chlorophyll was observed in the control. There was no consistent change of ascorbic acid content in all treatments, anyway the content was slightly change from the initial until the end of storage. The accumulation of acetaldehyde in lime juice was initially observed on day 10 in all treatments and then declined throughout the end of storage with slightly difference among the treatments. From the results indicated that PW has potential to apply with immature green lime fruit during postharvest period. In addition, the use of byproduct from palm oil industry for formulating a coating material will support the zero waste policy and also added a value of byproduct.

Palm Oil based Wax Coating Maintained Postharvest Quality of Thai Lime cv. Paan Pichit#1

Varit Srilaong[1,*], Nutthachai Pongprasert[1], Songsin Photchanachai[1], Panida Boonyaritthongchai[1] and Kornkanok Aryusuk[2]

[1]Postharvest Technology Division, School of Bioresources and Technology,
King Mongkut's University of Technology Thonburi, Bangkok, Thailand
[2]Biochemical Technology Division, School of Bioresources and Technology,
King Mongkut's University of Technology Thonburi, Bangkok, Thailand

*Corresponding author: varit.sri@mail.kmutt.ac.th

ABSTRACT

Immature green lime fruit cv. Pann Pichit#1 is widely consumption in Thailand as an ingredient of Thai's dish. Most of consumers prefer to have immature green lime due to its enriches with special aromatic compound, taste and flavor. Thus, to maintain the green color of lime fruit is very important for retarding quality losses. Peel yellowing is one of a major problem in lime fruit during postharvest period which lead to reduction of fruit qualities thus the inhibiting or delaying of chlorophyll breakdown is needed. There are several kind of postharvest technology to prolong storage life and maintain green color of fresh produces and one of them is coating technique by using natural based wax. According to Thailand produces a lot of palm oil and a byproduct from palm oil industry, palm oil wax, has potential to use as a wax based to form coating material. Thus, this research aimed to use palm oil based wax coating for maintaining quality of immature green lime cv. Pann Pichit#1. Lime fruit were harvested from commercial orchard and coated with palm oil based wax (PW) and commercial wax (CW), and then stored at 13°C. Uncoated fruit was set as a control. Changes of lime fruit qualities including fresh weight loss, browning spot, chlorophyll content, ascorbic acid content and acetaldehyde content were investigated at 5 days interval. The results found that lime fruit coated with PW showed the lowest water loss compared with that of CW coated and the control, respectively. The percentage of peel browning spot occurrence was also reduced in the fruit coated with PW while the application of CW induced a browning spot to higher level than the control. This result was concomitant with the incidence of peel browning. Lime fruit coated with both PW and CW delayed the chlorophyll breakdown in the same trend while the continuously degradation of chlorophyll was observed in the control. There was no consistent change of ascorbic acid content in all treatments, anyway the content was slightly change from the initial until the end of storage. The accumulation of acetaldehyde in lime juice was initially observed on day 10 in all treatments and then declined throughout the end of storage with slightly difference among the treatments. From the results indicated that PW has potential to apply with immature green lime fruit during postharvest period. In addition, the use of byproduct from palm oil industry for formulating a coating material will support the zero waste policy and also added a value of byproduct.

Keywords: Coating, Palm oil wax, Lime, Postharvest, Quality

1. INTRODUCTION

Lime (*Citrus auranifolia* Swingle) is considered as a unique fruit endowed with high flavor and acidity often used to accent the flavor of various Thai foods and beverages. Nutritionally, lime fruit are an excellent source of vitamin C, dietary fiber and contain numerous other nutrients in small quantities. The green peel of the fruit is a very important indicator of quality in terms of a potential to attract premium prices in the market especially in Thailand (Pranamornkith et al., 2010). During postharvest period (storage, transportation and retailing), the fruit is highly predisposed to postharvest yellowing as a result of chlorophyll degradation (Srilaong et al., 2011). The loss in the green color affects the quality attributes as well as the market value of lime. It is therefore important to investigate techniques that delay chlorophyll catabolism and how it is suppressed. In addition, the desiccation of lime fruit

due to transpiration during postharvest period is another problem. This leads to unacceptable external quality. From the above mentioned, it is really need a postharvest technique to overcome yellowing and wilting problems in lime fruit.

Literature gleaned from several authors elucidates that many postharvest techniques can delay senescence and retard quality losses of horticultural products. One of them is the application of coating material to maintain postharvest life of fresh produces. Natural materials that used to produce coating materails can be divided into three categories including hydrocolloids (polysaccharides, proteins), lipids (fatty acids, waxes), and composites (Navarro-Tarazaga, et al., 2008). Among lipids, waxes are the most attractive and promising coating materials for fruits and vegetables. The wax-based coatings are known to have a good barrier property against moisture transfer. In addition, it has been used to reduce respiration, improve appearance of fruits and vegetables by generating a shiny skin (Morillon, et al, 2002). Carnauba and candelilla are among the plant waxes that commonly used as a component in coating materials (Puttalingamma, 2014). However, these waxes are very expensive. Thus, an alternative wax based is becoming more intensive focused. In Thailand, wax is widely used in citrus with a purpose of prolong storage life and also for shiny appearance to attract the consumer. In each year, Thailand imported a wax for citrus around 500-700 tons which cost 60-84 million baht/year. It is quite big amount of investment in citrus business. Recently, many researchers try to formulate a wax from palm oil by using a byproduct from palm oil industry and found a potential to use for coating of seed (Pinkrajay et al., 2019). However, until now no report studies the effect of palm oil based wax on prolonging a storage life of fresh produces. Thus, the objective of this research was to investigate the effect of palm oil based wax coating on quality changes of lime fruit in comparison with a commercial coating solution during storage at low temperature. In addition, this research aimed to promote the zero waste concept by using a byproduct from palm oil industry to do value added product.

2. MATERIALS AND METHODS

2.1 Lime fruit preparation

Immature green lime fruit were harvested from commercial orchard in Samutprakarn province, Thailand and then transported to laboratory within 30 min. Fruit were selected for uniformity of color, size and shape, and also free from diseases and defects. The selected lime fruit were washed with running tap water and dipped in 150 ppm sodium hypochlorite solution for 5 min, and then air-dried at 25^{o}C.

2.2 Coating application

Fruit prepared from 2.1 were divided into 3 groups and each group has 200 fruits. Then, the lime fruit from each group were coated with commercial wax (CW) and palm oil based wax (PW), respectively. All coated fruit were subjected to air-dry at 25^{o}C. The control group was uncoated fruit. The CW concentration was prepared according to the recommendation for citrus as mentioned on label. The PW was prepared by using byproduct from palm oil industry and the formulation was developed by Division of Biochemical Technology, School of Bioresources and Technology, King Mongkut's University of Technology Thonburi, Bangkok, Thailand. The mixture and protocol of PW preparation could not inform in this report according to it will be applied for patent. All of lime fruit were stored in a cold room at 13^{o}C (90-95%RH). The experimental design was completely randomized design (CRD) with 5 replications. LSD was analyzed for significant difference among treatment.

2.3 Analytical parameters

2.3.1 Weight loss

Individual weight loss in 24 fruits were registered and expressed as the percentage loss of initial weight.

2.3.2 Browning severity and percentage

Browning severity was evaluated in 24 fruits per treatment. The different degrees of browning severity were rated as 1 = none, 2 = 0.1-5% browning severity on lime surface, 3 = 5.1-10% browning severity on lime surface, 4 = 10.1-15% browning severity on lime surface and 5 = browning severity on lime surface more than 15.1%. Results were converted to an average index (1–5). The fruit was calculated for the total fruit (n = 24) per treatment at each storage time as:

$$\% \text{ Browning} = (\text{number of fruit browning} / \text{ total number of fruit}) \times 100$$

2.3.3 Total chlorophyll content

Total chlorophyll content was determined by the method of Inskeep and Bloom (1985). 1 gram of flavedo tissue from lime peel were added with 20 ml N,N-Dimethylformamide. Then incubated in dark condition at 4ºC for 24 hour. The chlorophyll extract was measured as chlorophyll *a*, *b* and total chlorophyll content in a UV-visible spectrophotometer, at 664 and 647 nm.

2.3.4 Ascorbic acid content

Ascorbic acid content was determined according the method of Kapur et al. (2012) with some modifications. Two ml of juice was taken into 10 ml of 5% meta-phosphoric acid then mixed and filtrated with whatman #01 filter paper and clear sample was taken. 0.2 ml of 0.02% indophenol solution was added with 0.4 ml of sample extract and incubated 2-3 min until it became a stable reddish-pink color. After that, 0.4 ml of 2% thiourea and 0.2 ml of 2% DNP solution were added and then incubated 1 hour at 50ºC in a hot water bath. Then, 1 ml of 85% sulfuric acid was added and then incubated at room temperature for 30 min. The absorbance was determined at 540 nm using visible spectrophotometer (SP-830 plus, Metertech). A standard curve was prepared using standard ascorbic acid with concentrations of 20, 40, 60, 80, 100 mg/L

2.3.5 Acetaldehyde content

Acetaldehyde content was determined by Fuggate et al. (2010) with some modifications. 10 ml of lime juice added in 18 ml container (Precision Scientific, Chicago, IL, USA) and then incubated in a water bath at 50°C for 15 min. One-milliliter headspace samples were injected into a GC-2014 Shimadzu equipped with 80/100 Am mesh Porapack Q column. Chromatographic parameters were: detector: FID; helium as gas carrier; column temperature: 200ºC; injector port temperature: 120ºC.

3. RESULTS AND DISCUSSION

The quality of lime fruit with and without coating treatments stored at 13ºC for 30 days was observed and showed results as in following:

3.1 Weight loss

Fresh weight loss of lime fruit in all treatments increased with a progress of storage time (Fig. 1). Fruit without coating (control) showed the highest weight loss and reached a level of 5% on day 25 which started to observe skin wilting. This agree with the previous reported about a level of water loss at higher than 5% induces external quality loss in fresh produces (Wills et al., 1998). While the coated fruit showed lower fresh weight loss compared with the control. Fruit coated with PW has significantly lower water loss compared with that of coated with CW throughout storage and found the percentage of weight loss was lower than the control about 50%. The results indicated that PW coating could reduce transpiration of lime fruit due to the coating technique can generate modified atmosphere condition in the fruit and led to decrease of respiration rate. It showed a similar result of the study in tomato fruit that found reduction of respiration rate in cellulose based coated fruit (Tosati et al., 2015).

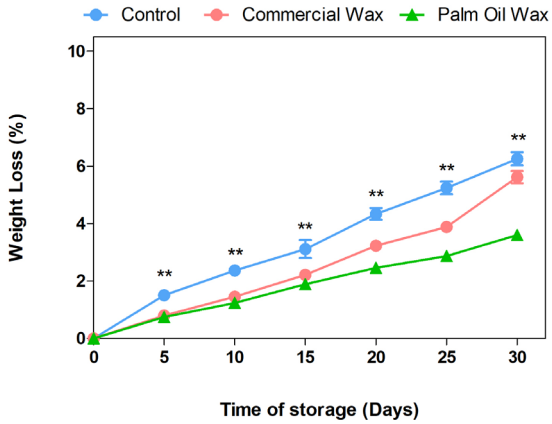

Figure 1. Weight loss of lime fruit coated with commercial wax (CW) and palm oil based wax (PW) compared with the uncoated control during storage at 13ºC for 30 days. The error bar indicates ±SE (n=5).

3.2 Browning spot

3.2.1 Browning spot severity

Browning on the peel of lime fruit was found from day 15 in all treatments and the severity was increased with the progress of storage time (Fig. 2). The severity of browning spot was lowered in lime fruit coated with PW compared with that of other treatments. Interestingly, the browning severity of the CW coated fruit was induced and reached higher level than that of other treatments from day 15 until the end of storage. This might be due to a toxicity of the commercial wax which has adverse effect on lime fruit appearance. The results were concomitant with the percentage of browning spot in Table 1. The browning spot is a sign of senescence on the peel of lime fruit after storage for a certain of time. This may relate with the percentage of water loss, a higher water loss in the control and CW coated fruit showed higher browning severity than the PW coated. PW is classified in a group of edible coating material thus it is not harmful to fruit itself and also consumer (Navarro-Tarazaga, et al., 2008).

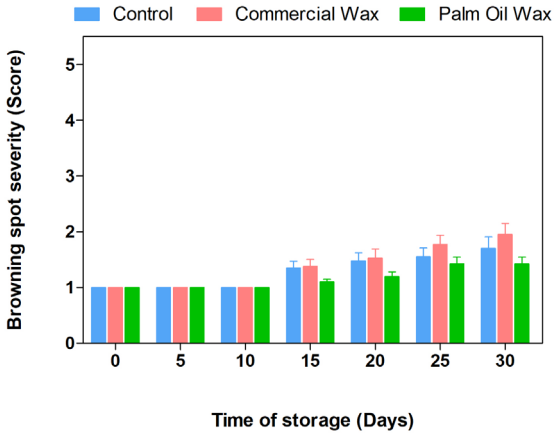

Figure 2. Browning spot severity on the peel of lime fruit coated with commercial wax (CW) and palm oil based wax (PW) compared with the uncoated control during storage at 13°C for 30 days. The error bar indicates ±SE (n=5).

3.2.2 Percentage of peel browning spot

The percentage of peel browning spot of lime fruit was exhibited in the same trend with the severity of browning spot (Table 1). The highest percentage of brown spot was recorded in lime fruit coated with CW, while those coated PW alleviated the percentage of browning until day 20 of storage and then increased to a similar level with that of control. From the results, it seems PW coating has ability to delay browning disorder on fruit peel. The limitation of gas transmission (oxygen) from PW film might play an important role to reduce the oxidative process of phenolic compounds by polyphenol oxidase enzyme to form brown pigment. As in the browning mechanism needs oxygen for oxidation of phenol (Massantini and Mencarelli, 2007).

Table 1. Percentage of browning spot on the peel of lime fruit coated with commercial wax (CW) and palm oil based wax (PW) compared with the uncoated control during storage at 13°C for 30 days.

Treatment	% of peel browning spot						
	Time of storage (Days)						
	0	5	10	15	20	25	30
Control	0.00	0.00	0.00	25.0	25.0	27.5	27.5
Commercial Wax	0.00	0.00	0.00	25.0	27.5	45.0	45.0
Palm Oil Wax	0.00	0.00	0.00	10.0	15.0	30.0	30.0

3.3 Total chlorophyll content

Total chlorophyll content in the peel of lime fruit in all treatments declined from 30-40 mg/100 gFW to less than 10 mg/100 gFW at the end of storage period (Fig. 3). However, the application of PW delayed the reduction of total chlorophyll content in lime during the first 10 days of storage and thereafter it showed the same trend of change as in the fruit coated with CW. Lime fruit coated with both CW and PW maintained higher total chlorophyll content from day 15 to day 30 of storage compared with the control. The catabolism of chlorophyll could initiate by oxidative process and also exogenous ethylene (Kaewsuksaeng, 2011). As above mentioned, coating material can control gas permeability through the fruit thus it limits the oxygen for oxidation and also protect the fruit from exogenous ethylene. In addition, coating technique also retards the respiration process and also delay ethylene production in the fruit thus minimizes the degradation of chlorophyll.

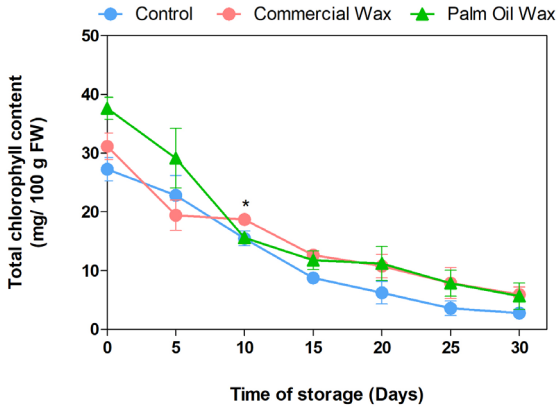

Figure 3. Total chlorophyll content in the peel of lime fruit coated with commercial wax (CW) and palm oil based wax (PW) compared with the uncoated control during storage at 13°C for 30 days. The error bar indicates ±SE (n=5).

3.4 Ascorbic acid content

Ascorbic acid content in lime juice was slightly change from the initial until the end of storage especially in the control and CW coated fruit which showed the same trend during storage (Fig. 4). However, the content in lime fruit coated with PW was temporary increased at day 5 and decreased thereafter to similar level with that of other treatments, and then increased again on day 25 and declined at the end of storage. Normally the change of ascorbic acid content in fresh produce is related with the percentage of water loss (Lee and Kader, 2000). From the results of this experiment, a bit higher ascorbic acid content in PW coated fruit might be a response of lower water loss.

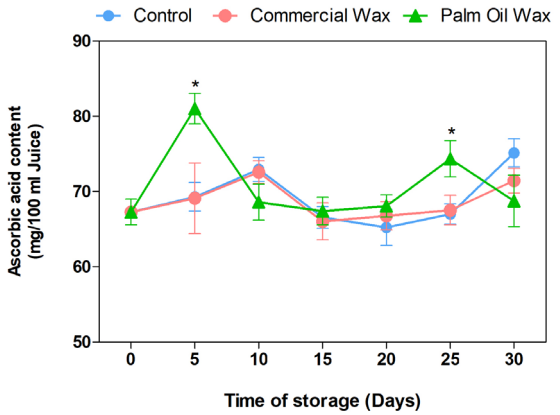

Figure 4. Ascorbic acid content in the juiceof lime fruit coated with commercial wax (CW) and palm oil based wax (PW) compared with the uncoated control during storage at 13°C for 30 days. The error bar indicates ±SE (n=5).

3.5 Acetaldehyde content

The acetaldehyde content in coated fruit is one of indicator to inform fruit quality and anaerobic respiration process which led to fermentation. The acetaldehyde content in lime juice from all treatments was not significant difference from the initial until day 10 (Fig. 5). A sharp increase of the acetaldehyde content on day 10 to level of 2.5 ppm was detected in all treatments, this might be the adaptation of lime fruit to low temperature storage. The previous study reported that low temperature induces the alcohol dehydrogenase enzyme activity in rice as a defense mechanism to stress condition and led to accumulation of alcohol (Kato-Noguchi, 2007). However, it could not detect any off-flavor by smelling in all treatments until from day 10 until the end of storage. This indicates that both of CW and PW were not induced anaerobic respiration process in lime fruit during a month storage.

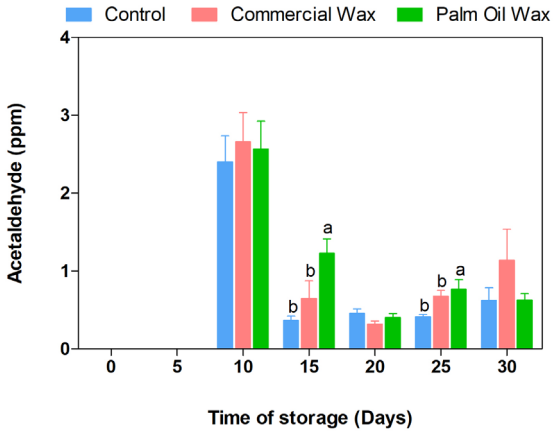

Figure 5. Acetaldehyde content in the juice of lime fruit coated with commercial wax (CW) and palm oil based wax (PW) compared with the uncoated control during storage at 13ºC for 30 days. The error bar indicates ±SE (n=5).

4. CONCLUSION

The application of palm oil based wax coating has potential to maintain postharvest quality of immature green lime fruit through reduction of water loss, chlorophyll breakdown and browning disorder. A proper commercial wax must be concerned for coating of immature green lime fruit to avoid a toxic component that may induce brown spot development on fruit surface.

ACKNOWLEDGMENT

The authors would like to thanks to National Research Council of Thailand for granting a budget of this research in fiscal year of 2017.

REFERENCES

Fuggate, P., C. Wongs-Aree, S. Noichinda and S. Kanlayanarat. 2010. Quality and volatile attributes of attached and detached 'Pluk Mai Lie' papaya during fruit ripening. *Scientia Horticulturae*, 126. 120-129.

Inskeep, W.P. and P. R. Bloom. 1985. Extinction Coefficients of Chlorophyll a and b in N,N-Dimethylformamide and 80% Acetone. *Plant Physiology*, 77: 483-485.

Kaewsuksaeng, S. 2011. Chlorophyll degradation in horticultural crops. *Walailak Journal of Science and Technology*, 8(1): 9-19.

Kapur, A., A. Hasković, A. Čopra-Janićijević, L. Klepo, A. Topcagic, I. Tahirovic and E. Sofić. 2012. Spectrophotometric analysis of total ascorbic acid content in various fruits and vegetables. *Bulletin of the Chemists and Technologists of Bosnia and Herzegovina*, 38: 40-43.

Kato-Noguchi, H. 2007. Submergence acclimation to low-temperature stress in rice roots. *Plant Production Science*, 10(3): 297-302.

Lee, S.K. and A.A. Kader. 2000. Preharvest and postharvest factors influencing vitamin C content of horticultural crops. *Postharvest Biology and Technology*, 20: 207–220.

Massantini, R. and F. Mencarelli. 2007. Understanding and management of browning in fresh whole and light processed fruits. *Fresh produce*, 1(2): 94-100.
Morillon, V., F. Debeaufort, G. Blond, M. Capelle and A. Voilley. 2002. Factors affecting the moisture permeability of lipid based edible films: A review, *Critical Reviews in Food Science and Nutrition*, 42(1): 67-89.
Navarro-Tarazaga, M. L., M. A. Del Rio, J. M. Krochta and M. B. Pe´rez-Gago. 2008. Fatty acid effect on hydroxypropyl methylcellulose-beeswax edible film properties and postharvest quality of coated 'Ortanique' mandarins. *Journal of Agricultural and Food Chemistry*, 56: 10689-10696.
Pinkrajay, R., A. Nakornsadet, K. Aryusuk, N. Jeyashoke, S. Photchanachai and K. Krisnangkura. 2018. Palm oil wax esteremulsion used as seed and fruit coating. In Proceedings of the 12th SEATUC Symposium, Universitas Gadjah Mada, Yogyakarta, Indonesia, 12-13 March, 815-820.
Puttalingamma, V. 2014. Edible coatings of carnauba wax a novel method for preservation and extending longevity of fruits and vegetables- A Review, *Journal of Food Safety*, 16: 1-5.
Srilaong, V., S. Aiamla-or, A. Soontornwat, M. Shigyo and N. Yamauchi. 2011. UV-B irradiation retards chlorophyll degradation in lime (*Citrus latifolia* Tan.) fruit. *Postharvest Biology and Technology*, 59: 110-112.
Tosati, V. J., D. de Oliveira, L. A. Lerin, C. I. G. L. Sarantópoulos and A. R. Monteiro. 2015. Respiration rate of cherry tomatoes and gas permeability of hydroxypropylmethyl cellulose-based coating. *International Journal of Emerging Technology and Advanced Engineering*, 5(3): 281-287.
Wills, R., B. McGlasson, D. Graham and D. Joyce. 1998. Postharvest: An Introduction to the Physiology and Handling of Fruit. Vegetable and Ornamentals. 4th ed. Hyde Park Press, Australia.

11:30 AM - 12:30 PM (Thu. Sep 5, 2019 11:30 AM - 12:30 PM Poster Place)

[5-1130-P-03] Development of Blueberry Wine with High Content of Polyphenol

*Hongpu Wang[1], Yutaka Kitamura[2], Mito Kokawa[2] (1. Graduate school of Life and Environmental Sciences, Tsukuba Univ.(Japan), 2. Faculty of Life and Environmental Sciences, Tsukuba Univ.(Japan))
Keywords: blueberry wine, micro wet milling, alcohol production, polyphenol, anthocyanin, antioxidant activity

Rabbit-eye blueberry (*Vaccinium virgatum*) is suitable to be produced into wine because of high content of sugar and phenolic compounds. However, to obtain clear wine, pomace is produced after wine processing. It is a kind of by-product, including skin, seeds and some pulps, which contains most of bioactive compounds. In the research, micro wet milling technology (MWM) was used to improve reserved content of bioactive compounds such as polyphenol in the final product and increase taste of wine. Rabbit-eye blueberry (harvested from Ibaraki, Japan) was used to ferment wine by wine yeast. The soluble solids content was enriched up to 21˚ Brix before fermentation to obtain a potential alcohol level of approximately 12%vol. Fermentation was conducted to finish after 35 days when soluble solids content reached a constant level (between 6-7˚ Brix). MWM was used to decrease particle size into micro scale after fermentation. Blueberry wine were evaluated for total phenolic content (TPC) using Folin-Ciocalteu method, total anthocyanin content (TAC) using pH differential method, antioxidant activity using the radical scavenging capacity (DPPH) method and some physicochemical properties such as pH, ˚ brix. The total polyphenol content and antioxidant activity were increased by MWM compared with conventional processing, which means it is possible to produce blueberry wine with high content of polyphenol and increase utilization of pomace by MWM.

11:30 AM - 12:30 PM (Thu. Sep 5, 2019 11:30 AM - 12:30 PM Poster Place)

[5-1130-P-04] Effects of Heating under Pasteurization Conditions on Mechanical and Electrical Properties of Mung Bean Sprout

*Hayato Ogino[1], Haruki Ando[1], Satoshi Iwamoto[1], Teppei Imaizumi[1] (1. Gifu University(Japan))
Keywords: impedance, pasteurization condition, electrical property, mechanical property, mung bean sprout

Heat pasteurization using hot water is easy to introduce in small-scale facilities. However, heat treatments often degrade tissue structure and decrease texture of vegetables. Although cell membrane structure, which makes turgor pressure, is one of the most important factors to determine vegetable texture, heat-resisting properties of the structure is not well clarified yet. To date, impedance measurement has been used to evaluate cell membrane state. In this study, we mainly investigated such an electrical properties of mung bean sprout heated under pasteurization conditions, and evaluated relationships with its quality.Mung bean sprout is used in this study. A beaker containing 300 mL of distilled water was controlled at temperatures of 50, 60, 65 and 70 degree in a water bath. After measuring weight of mung bean sprout, it was put into a net and immersed in the beaker for 0 - 60 sec. Then, the sprout was immediately cooled in iced water for 30 sec. For the heated mung bean sprout, mechanical and electrical properties were measured. In order to measure the mechanical properties, a creepmeter (TPU-2D, Yamaden Co., Ltd.), equipped with a wedge-shaped plunger or a knife-shaped plunger, was used. The wedge-shaped and the knife-shaped ones were moved at 1

mm/sec for compression test and 10 mm/sec for shear test, respectively. For the impedance measurement, two needle electrodes (diameter: 0.25 mm) connected to a LCR tester (IM3536, HIOKI) were inserted into the sample. In this study, equivalent circuit analysis was conducted on the measured impedance values, and cell membrane capacitance, intracellular resistance and extracellular resistance were obtained. In addition, cell membrane structure was observed by using a confocal laser scanning microscope. In this study, two kinds of mechanical properties were evaluated for heated sprouts. While the compression force of the sample did not change a lot, significant differences were appeared on the shear force especially at 65 degree. In impedance measurement, measured values showed an arc when resistance and reactance were plotted on vertical and horizonal axis, respectively. Top coordinate of the arc decreased as the heating temperature risen. Additionally, an equivalent circuit model was well fitted to the measured values. The cell membrane capacitance decreased by the heating. Also, the extracellular resistance showed a decreasing tendency at heating above 60 degree. These changes seemed to relate with cell membrane damage which observed by the confocal laser scanning microscope. Consequently, our study indicated that impedance measurement was a good way to estimate texture and tissue structure of mung bean sprout. These findings will contribute to quality control of vegetables during heat processings.

Poster Session | Postharvest/Food Technology and Process Engineering
[5-1130-P] Postharvest/Food Technology and Process Engineering (5th)
Thu. Sep 5, 2019 11:30 AM - 12:30 PM Poster Place (Entrance Hall)

[5-1130-P-05] Study on Non-Destructive Measurements to Predict Sugar Content of Melons Using a DLP Based Miniature Spectrometer

*Chao-Yin TSAI[1], Pin-Chih Fang[1], Yi-Tzu Shen[1], Yung-Huei Chang[1], Han-Chun Hsu[1], Suming Chen[1] (1. Department of Bio-Industrial Mechatronics Engineering, National Taiwan University(Taiwan))
Keywords: Digital Light Processing, Micromirror, Spectrometer, Near Infrared

Spectrometers based on digital light processing (DLP) design replace the traditional linear array detector with a micromirror array for wavelength selection. It has the advantages of lower cost and higher performance through the use of a larger and cheaper single element detector. In this study, a commercially available DLP based spectrometer and mobile phone were used. The former was used as a measurement tool; the latter was used as a control panel with APP. Spectra and sugar content of 151 samples were measured at the different parts of eight melons. Peel and flesh measuring modes had been conducted and one laboratory spectrophotometer (Model: NIRS 6500) was also used to measure the spectra of two modes together with DLP based spectrometer. WinISI spectral analysis software was used to build a cross validation model with MPLSR method. The best DLP spectrometer’s model of SEC, RSQ, SECV, 1-VR for peel and flesh modes were 0.598, 0.786, 0.735, 0.681 when mathematic treatment was done in (1,2,2,1) model and 0.614, 0.781, 0.745, 0.677 when mathematic treatment was done in (1,12,12,1) model, respectively. The best NIRS 6500 spectrophotometer’s model of SEC, RSQ, SECV, 1-VR for peel and flesh modes were 0.544, 0.823, 0.702, 0.705 when mathematic treatment was done in (1,4,4,1) model and 0.413, 0.898, 0.512, 0.841 when mathematic treatment was done in (1,10,10,1) model, respectively. Observing the two apparatuses model’s result, the performance of DLP spectrometer is worse when compared with NIRS6500 spectrophotometer; but it is enough for industrial applications.

Study on Non-Destructive Measurements to Predict Sugar Content of Melons Using a DLP Based Miniature Spectrometer

Chao-Yin Tsai, Pin-Chih Fang, Yi-Tzu Shen, Yung-Huei Chang, Han-Chun Hsu, Suming Chen*

Department of Bio-Industrial Mechatronics Engineering, National Taiwan University, Taiwan

*Corresponding author: schen@ntu.edu.tw

ABSTRACT

Spectrometers based on digital light processing (DLP) design replace the traditional linear array detector with a micromirror array for wavelength selection. It has the advantages of lower cost and higher performance through the use of a larger and cheaper single element detector. In this study, a commercially available DLP based spectrometer and mobile phone were used. The former was used as a measurement tool; the latter was used as a control panel with APP. Spectra and sugar content of 151 samples were measured at the different parts of eight melons. Peel and flesh measuring modes had been conducted and one laboratory spectrophotometer (Model: NIRS 6500) was also used to measure the spectra of two modes together with DLP based spectrometer. WinISI spectral analysis software was used to build a cross validation model with MPLSR method. The best DLP spectrometer's model of SEC, RSQ, SECV, 1-VR for peel and flesh modes were 0.598, 0.786, 0.735, 0.681 when mathematic treatment was done in (1,2,2,1) model and 0.614, 0.781, 0.745, 0.677 when mathematic treatment was done in (1,12,12,1) model, respectively. The best NIRS 6500 spectrophotometer's model of SEC, RSQ, SECV, 1-VR for peel and flesh modes were 0.544, 0.823, 0.702, 0.705 when mathematic treatment was done in (1,4,4,1) model and 0.413, 0.898, 0.512, 0.841 when mathematic treatment was done in (1,10,10,1) model, respectively. Observing the two apparatuses model's result, the performance of DLP spectrometer is worse when compared with NIRS6500 spectrophotometer; but it is enough for industrial applications.

Keywords: Digital Light Processing, Micromirror, Spectrometer, Near Infrared

11:30 AM - 12:30 PM (Thu. Sep 5, 2019 11:30 AM - 12:30 PM Poster Place)

[5-1130-P-06] Effect of Lactic acid bacteria fermentation on the microbial diversity, physico-chemical properties, and organic acid profile of *pindang damulag*, a fermented carabeef

*Michael Angelo Santos Esteban[1], Lotis Mopera[1], Maria Cynthia Oliveros[1], Erlinda Dizon[1] （1. University of the Philippines Los Banos(Philippines)）

Keywords: carabeef, fermentation, lactic acid bacteria, pindang damulag

Fermented carabeef or *pindang damulag* is a native traditional food from Pampanga, Philippines. It is produced through the action of naturally growing lactic acid bacteria (LAB) via fermentation for 1 week at room temperature. The study aimed to determine the changes on the microbial diversity, physico-chemical properties, and organic acid profile of *pindang damulag* brought by the lactic acid bacteria fermentation. Procurement and processing of *pindang damulag* was based on the method of known makers from Pampanga, Philippines, but minor revisions were made to address the food safety concerns of the researcher. During fermentation, all targeted groups of microorganisms (fungi, common bacteria, coliforms, acid producing bacteria and LAB) grew significantly until the 3rd day. After day 3, only acid producing bacteria and LAB grew significantly. There was also a significant decrease in total soluble solids (TSS) from day 0 to day 3 (30.31 – 28.17˚ Brix), while titratable acidity (TA) and pH were found to be statistically constant (3.5% @ pH 5.97 – 3.6% @ pH5.9). Moreover, significant decrease in TSS (24.89, 22.76, and 20.53˚ Brix) and pH (5.60, 4.93, and 4.53) were observed, while TA increased significantly (4.5, 5.6, 6.6%) during days 5, 7, and 9. Moisture content, on the other hand, increased significantly from day 0 to day 1 (64.5759 ± 1.5085 – 66.1952 ± 1.2023) but remained statistically constant until day 9 (65.6447 ± 0.8445). The *L** value also decreased significantly from day 0 to day 1 (26.99 – 23.48) but increased significantly at day 3 and day 7 (28.60 – 34.12). The *a** value increased significantly from day 0 to day 1 (10.92 – 16.90) but remained statistically constant until day 9 (17.77). While *b** value remained statistically constant throughout fermentation. After the culture dependent phenotypic tests, some LAB isolates were found to be heterofermentative, which also reflected on the predominance of other organic acids such as citric acid (448.70 mg/100g), acetic acid (1724 mg/100g) other than the lactic acid (4440 mg/100g) alone. Therefore, LAB was found to have a major role in the food safety, food quality and overall profile of *pindang damulag*.

Poster Session | Postharvest/Food Technology and Process Engineering
[5-1130-P] Postharvest/Food Technology and Process Engineering (5th)
Thu. Sep 5, 2019 11:30 AM - 12:30 PM Poster Place (Entrance Hall)

[5-1130-P-07] Properties of Rice Starch-Based Film Incorporated with Zinc Oxide Nanoparticles

KHALISHAH RAHMA SAFIRA[1,2], *SAROAT RAWDKUEN[2] (1. Department of Food Science and Technology, Faculty of Agricultural Technology and Engineering, Bogor Agricultural University(Indonesia), 2. Unit of Innovative Food Packaging and Biomaterials, School of Agro-Industry, Mae Fah Luang University(Thailand))
Keywords: Antimicrobial packaging, Nanocomposite film, Nanoparticle, Rice starch, Zinc oxide

This study aimed to develop rice starch based antimicrobial film as an active food packaging with zinc oxide nanoparticles (ZnO-NPs) incorporation. ZnO-NPs were synthesized by hydrothermal method and their formation was confirmed by using XRD analysis. The synthesized ZnO-NPs showed an average size of $\leq$100 nm with spherical shape under the scanning electron microscope (SEM). The nanoparticles were studied against two foodborne pathogens bacteria; *Staphylococcus aureus* and *Escherichia coli* at different concentrations (0 – 5 %, w/v) and found effective against both microorganisms. The ZnO-NPs (3%, w/w) was selected for the incorporation into rice starch-based (5%) antimicrobial film with sorbitol as plasticizer via solution casting method. Physical, mechanical, chemical, and antimicrobial properties of the films were examined. Presence and distribution of nanoparticles in the film were confirmed with SEM and FTIR. Incorporation of zinc oxide nanoparticles significantly decreased ($p<0.05$) the transparency (2.64 ± 0.01), solubility (19.22 ± 0.39%), WVP (0.04 ± 0.00 x 10^{-10} g m/m^2 Pa s), and elongation at break (37.18 ± 2.61%), while increased the lightness (89.73 ± 0.06) and tensile strength (9.14 ± 0.78 MPa) of the film were observed ($p<0.05$). The rice starch/ZnO-NPs nanocomposite films showed antibacterial activity against *S. aureus* and *E. coli*. These results suggest that rice starch/ZnO-NPs nanocomposite film can be used as active packaging materials.

Rice Starch-Based Film Incorporated with Zinc Oxide Nanoparticles

Khalishah Rahma Safira[1,2], Saroat Rawdkuen[2*]

[1]Department of Food Science and Technology, Faculty of Agricultural Technology and Engineering,
Bogor Agricultural University, Indonesia
[2]Unit of Innovative Food Packaging and Biomaterials, School of Agro-Industry,
Mae Fah Luang University, Thailand

*Corresponding author: saroat@mfu.ac.th

ABSTRACT

This study aimed to develop rice starch-based antimicrobial film with zinc oxide nanoparticles (ZnO-NPs) incorporation. ZnO-NPs were synthesized by hydrothermal method and their formation was confirmed by using XRD analysis. The synthesized ZnO-NPs showed an average size of ≤ 100 nm with spherical shape under the scanning electron microscope (SEM). The nanoparticles were studied against two foodborne pathogens bacteria; *Staphylococcus aureus* and *Escherichia coli* at different concentrations (1, 3, and 5 %, w/v) and found effective against both microorganisms. The ZnO-NPs (3 %, w/w) was selected for the incorporation into rice starch-based (5 %) antimicrobial film with sorbitol as plasticizer via solution casting method. Physical, mechanical, chemical and antimicrobial properties of the films were examined. Presence and distribution of nanoparticles in the film were confirmed with SEM and FTIR. Incorporation of ZnO-NPs significantly decreased ($p<0.05$) the transparency (2.64 ± 0.01), solubility (19.22 ± 0.39 %), WVP (0.04 ± 0.00 x 10^{-10} g m/m^2 Pa s), and elongation at break (37.18 ± 2.61 %), while increased the lightness (89.73 ± 0.06) and tensile strength (9.14 ± 0.78 MPa) of the film were observed ($p<0.05$). The rice starch/ZnO-NPs film showed antibacterial activity against tested bacteria. These results suggest that rice starch/ZnO-NPs film can be used as an active packaging material.

Keywords: Antimicrobial packaging, Nanocomposite film, Nanoparticles, Rice starch, Zinc oxide

1. INTRODUCTION

Recently, there is an increasing concern for the microbial safety of food products. Food deterioration is mainly caused due to microbial activity. Growth of spoilage microorganisms, spoilage bacteria, mold, and yeast can reduce the quality of food products during storage. It will shorten the shelf life of the foods and lead to food waste and economic losses. Besides, the contamination of pathogenic microorganism in the foods can cause foodborne illnesses. The Center for Disease and Control and Prevention has estimated there are 48 million people are sick, 128000 are hospitalized and 3000 die every year due to foodborne illnesses (CDC, 2018).

Food packaging is essential for maintaining quality and providing the safety of food products. The current trend of the food packaging system is concerning about developing more innovative approaches to inhibit pathogenic microbial activities in foods (Sung et al., 2013). One of the packaging technology that has been developed is active biodegradable packaging. According to Kaewprachu and Rawdkuen (2016), active packaging is a system in which the product, the package, and the environment interact in a positive way to extend shelf life or improve microbial safety or sensory properties while maintaining the quality of food products. Antimicrobial packaging is the type of active packaging which can kill or inhibit the growth of microorganism by releasing the antimicrobial agents from the food packaging system.

The incorporation of inorganic materials in nanoscale is a great opportunity to use as antimicrobial agents due to their high surface area, thus it can present strong antibacterial activity (Espitia *et al.*, 2012). Zinc oxide nanoparticles (ZnO-NPs) is one of the metallic oxide nanoparticles that have been explored to incorporate into food packaging materials as an antimicrobial agent. They have better stability compared to organic agents and exhibit antibacterial activity against Gram-positive and Gram-negative bacteria as well as fungi (Espitia *et al.*, 2012; Kanmani and Rhim, 2014). Moreover,

ZnO is currently listed as generally recognized as safe (GRAS) material by the Food and Drug Administration and is used as a food additive (U.S. Food and Drug Administration, 2018).
The renewable biopolymer can be used as a carrier of active antimicrobial agents. It can be obtained from local sources such as polysaccharides, proteins, and lipids. Among the variety of polysaccharides have been used, starch is one of the most abundant natural polysaccharide raw material, inexpensive, renewable, and non-toxic (Jiménez et al., 2012; Kotharangannagari and Krishnan, 2016). Rice starch is an attractive raw material because its major components, such as amylose and amylopectin can act as barriers in packaging materials (Phattaraporn et al., 2011) and they have been used to produce biodegradable films to partially or entirely replace plastic polymers (Detduangchan et al., 2014). Unfortunately, films prepared from rice starch products have disadvantages including low mechanical properties and lack of efficient barrier against high polarity compounds due to the highly hydrophilic character of rice starch polymers (Wittaya, 2012). Besides its antimicrobial activity, the incorporation of nanoparticles into biopolymer films can be a new alternative technique for improving the film properties.
Previous work had been done about the incorporation of ZnO-NPs in the food active packaging system. Suyatma et al., (2014) reported that the use of ZnO-NPs as Nano-filler could increase functional properties of pectin film in view of tensile strength, water vapor barrier, and antimicrobial capacity. Therefore, this study aimed to develop rice starch based antimicrobial film as an active food packaging with zinc oxide nanoparticles incorporation because only rice starch film doesn't inherent antimicrobial activity and it susceptible to microbial growth. Furthermore, this study was to investigate the characteristics of rice starch film with ZnO-NPs incorporation.

2. MATERIALS AND METHODS

2.1 Materials

All chemicals were obtained from Scientific and Technological Instruments Center Store, Mae Fah Luang University (Chiang Rai, Thailand). Sodium hydroxide and zinc chloride were used for the preparation of ZnO nanoparticles. Rice starch and liquid sorbitol were used for film preparation were obtained from the Food Packaging Laboratory, Mae Fah Luang University (Chiang Rai, Thailand). Nutrient broth (NB) and Mueller-Hinton agar (MHA) were used for the antimicrobial assay. Foodborne pathogenic microorganisms, *Staphylococcus aureus* TISTR 746 and *Escherichia coli* TISTR 527 were obtained from culture collection center (Mae Fah Luang University, Chiang Rai, Thailand). All chemicals and solvent used were analytical grade.

2.2 Preparation and Characterization of Zinc Oxide Nanoparticles

The ZnO nanoparticles were prepared by hydrothermal synthesis according to Akbar and Anal (2014). Aqueous solutions (100 mL) with a molar concentration of 0.2 M and zinc chloride solution 0.1 M were prepared. Sodium hydroxide (0.2 M, 100 mL) solution was added dropwise to aqueous zinc chloride (0.1 M, 100 mL) solution under constant stirring (100 rpm). The mixture solution was heated at 60 ºC for 2 h in a water bath. Following the heating, the reaction mixture was left standing overnight (12 h) at 24 ºC and filtered through Whatman filter number one. The precipitate result was kept in a hot air oven at 60 ºC for 48 h to ensure the complete formation of ZnO nanoparticles. The powdered nanoparticles will be used for further experiments. X-ray diffraction (XRD) patterns were observed in the range of 2Θ values from 20º-80º with PANalytial X'Pert Pro MPD, X-ray diffractometer. Morphology and size of nanoparticles were observed under scanning electron microscope SEM (LEO, 1450 VP) with magnification range 5000-20000x, resolution 200 Å and an acceleration voltage of 20 kV. Samples were coated with gold before observation.

2.3 The Antimicrobial Activity of Zinc Oxide Nanoparticles

Zinc oxide nanoparticles solution were prepared following Nafchi et al. (2012) with slight modification. ZnO nanoparticles were dispersed in distilled water at different concentrations (1, 3, and 5 %; w/v), stirred for 1 h at 60 ºC, and then sonicated in an ultrasonic bath (Marconi model, Unique

USC 35 kHz) for 30 min at 60 ºC. The solution was used for further studies of antimicrobial activity against target foodborne pathogens *S. aureus* and *E. coli* with the disk diffusion method.
A disk diffusion method was used following Shahverdi et al. (2007) with modifications. The filter paper disk was cut into 6 mm-diameter disks. Each paper disk was further immersed in the freshly prepared ZnO-NPs solution at different concentrations (1 %, 3 %, and 5 %; w/v). The disks were removed and dried, followed by sterilized under UV for 30 min. A single colony of each test strain was grown overnight in nutrient broth medium on a rotary shaker (200 rpm) at 37 °C. The inocula were prepared by diluting the overnight cultures with 0.85 % NaCl to a 0.5 McFarland turbidity (approximately 1.5 x 10^8 CFU/mL). A sterile cotton swab was used to inoculate the surface of Mueller Hinton agar plate rotating the plate every 60° to ensure homogeneous growth. The prepared disks containing different amounts of ZnO-NPs were placed on Mueller Hinton agar plates. The plates were then incubated at 37 ºC for 24 h. After that, the plates were examined for the zone of inhibition of the film discs. Inhibition zone (diameter) of the disc was calculated in mm as follows:

Inhibition zone = diameter of inhibition area – diameter of disc area

All samples were performed in duplicate. The best antimicrobial activity of the ZnO nanoparticles concentration will be selected for further film development.

2.4 Preparation of Rice Starch/ZnO-NPs Nanocomposite Film

The nanocomposite films were prepared by using solution casting method according to Nafchi et al. (2012) with modifications. ZnO nanoparticles were dispersed in distilled water at 3 % (w/w of rice starch) stirred at 60 ºC for 1 h, and then sonicated in an ultrasonic bath (Marconi model, Unique USC 35 kHz) at 60 ºC for 30 min. The solution was used to prepare the aqueous starch dispersion at 5 % (w/v). Sorbitol at 30 % (w/w of rice starch) was added as plasticizers in accordance with Laohakunjit and Noomhorm (2004). Starch nanocomposites were heated to 75±5 °C and held for 45 min to allow gelatinization. Upon completion of starch gelatinization, the film-forming solution (FFS) was cooled to 45 °C. A portion (4.04±0.02 g) of the FFS was cast on onto a rimmed silicone resin plate (50×50 mm) and then evaporated at room temperature for 24 h before dried with a ventilated oven environmental chamber at 25±0.5 °C and 50±5 % relative humidity (RH) for another 24 h. The obtained dried films were manually peeled. Control films were prepared similarly but without the addition of nanoparticles.

2.5 Characterization of Rice Starch-based Nanocomposite Film

2.5.1 Morphological Observation and FT-IR

The morphological features and nanoparticles distribution pattern of the ZnO nanoparticles loaded films will be characterized by using SEM. According to Suyatma et al. (2014), film specimens were scratched on the top surface before being mounted on an aluminum stub and were covered with double-sided carbon tape then sputter coated with gold to enhance surface conductivity. Samples will be viewed in SEM at 20 kV with 5000x magnification on the surface.
FTIR spectra of the films were analyzed following Nafchi et al. (2012). FTIR spectra of the films were recorded using an attenuated total reflection (ATR) method in FTIR Spectrum GX (Perkin Elmer). The thin films were applied directly onto the ZnSe ATR cell. The spectrum was recorded at wave number 650-4000 cm^{-1}. For each spectrum, 64 consecutive scans at 4 cm^{-1} resolutions were averaged to reduce spectral noise.

2.5.2 Thickness and Mechanical Properties of The Films

The thickness of the film samples was measured using a hand-held micrometer (Dial Thickness Gauge 7301, Mitutoyo Corporation, Kanagawa, Japan). Nine random measurements were taken from each film sample of the ten film samples were used for thickness determination and the average values were used as the film thickness.
The mechanical properties of the film samples were measured according to Rawdkuen et al. (2012). Prior to testing the mechanical properties, the films were conditioned for 48 h at 50±5 % RH at 25 °C. The tensile strength (TS) and elongation at break (EAB) were determined by using a Universal Testing

Machine (Instron, 5566). Ten samples (20×50 mm) with an initial grip length of 30 mm were used for testing. The cross-head speed was set at 30 mm/min with 100 N load.

2.5.3 Surface Color and Transparency

Surface color of the film samples was measured following Kanmani and Rhim (2014) using a Chroma meter (Hunter Lab MiniScan EZ) with a white color plate (L* = 93.09, a* = -1.07, and b* = 2.40) as a standard background for color measurement. The CIE color values (L*, a*, and b*) were determined by the average of five readings from each film sample. The total color difference (ΔE) was calculated as follows:

$$\Delta E = [(\Delta L^*)^2 + (\Delta a^*)^2 + (\Delta b^*)^2]^{0.5}$$

where ΔL*, Δa*, and Δb* were the difference between the color of the standard plate and film samples, respectively.

The ultraviolet and visible light barrier properties of the films were measured according to Rawdkuen *et al.* (2012) at selected wavelengths between 200 and 800 nm by using a UV-Vis spectrophotometer. The film transparency was calculated by the following equation:

Transparency = $\log T_{600}/x$

where T_{600} was the fractional transmittance at 600 nm, and x is the film thickness (mm). This experiment was performed in triplicate.

2.5.4 Moisture Content (MC)

Moisture content (MC) of the films was determined following Shankar et al. (2016) with slight modification. Each film was cut into 2×2 cm and dried at 105 °C for 24 h using hot air oven. The weight loss of each film was measured as MC and expressed as percent MC based on the initial weight of the film. This experiment was performed in triplicate.

2.5.5 Film Solubility

The film solubility was determined according to the method of Rawdkuen et al. (2012) with slight modification. The dried film samples were weighed and placed in a 50 mL centrifuge tube containing 10 mL of distilled water. The mixture was shaken at a speed of 250 rpm using a shaker for 24 h. The un-dissolved debris was then removed by centrifugation at 3000 rpm for 20 min. The pellet was dried at 105 °C for 24 h and weighed. The weight of the solubilized dry matter was calculated by subtracting its difference from the initial weight of the dry matter. It was then expressed as a percentage of the total weight. This experiment was performed in triplicate.

2.5.6 Water Vapor Permeability (WVP)

The film water vapor permeability (WVP) was measured following Shankar et al. (2016) with slight modification. The films were sealed onto a permeation cup containing silica gel (0 % RH) and sealed to prevent the leakage of water vapor. The cups were then placed in a humidity chamber controlled at 50 % RH and 25 °C. The weight loss of the cup was measured every hour for 8 h to determine the water vapor transmission rate (WVTR) (g/m^2s) of the film, then the WVP of the film was calculated in g m/m^2 Pa s as follows:

$$WVP = (WVTR \times L)/\Delta p$$

where L was the thickness of the film (m) and Δp was partial water vapor pressure difference (Pa) across the film.

2.5.7 Antimicrobial Activity of Films

The evaluation of the antimicrobial activity of the rice starch film containing zinc oxide nanoparticles was carried out by using two test microorganisms: *S. aureus* (Gram-positive, TISTR 746) and *E. coli* (Gram-negative, TISTR 527). The rice starch film was also tested as a control. Antimicrobial activity tests were carried out by using the agar disk diffusion method according to Ramos et al. (2012) with modifications. Disks cut from films (5 mm) were sterilized under UV for 30 min. A single colony of each test strain was grown overnight in nutrient broth medium on a rotary shaker (200 rpm) at 37 °C. The inocula were prepared by diluting the overnight cultures with 0.85 % NaCl to a 0.5 McFarland turbidity (approximately 1.5 x 10^8 CFU/mL). A sterile cotton swab was used to inoculate the surface

of Mueller Hinton agar plate rotating the plate every 60° to ensure homogeneous growth. The prepared disks were placed on Mueller–Hinton agar plate. The petri dishes were then incubated at 37 °C for 24 h. Sterile water and antibiotic were used as negative and positive control, respectively. The antimicrobial activity of each material was evaluated by observing the growth inhibition zone and measuring the diameter (mm) by a ruler. Tests were carried out in duplicate. Inhibition zone (diameter) of the discs was calculated in mm as follows:

Inhibition zone = diameter of inhibition area – diameter of film area

2.6 Statistical Analysis

Data were expressed as means ± standard deviation. The data were also subjected to analysis of variance (ANOVA) and Duncan's multiple range tests using SPSS 25.0 for Windows. The significance level of $p<0.05$ was considered significantly different.

3. RESULTS AND DISCUSSION

3.1 Preparation and Characterization of Zinc Oxide Nanoparticles

XRD analysis was used to determine the structural characterization of the nanoparticles. The ZnO nanoparticles formation was confirmed by XRD. XRD patterns of synthesized ZnO nanoparticles is presented in Figure. 1. The XRD spectra showed sharp diffraction peaks at 31.92°, 34.56°, 36.44°, 47.70°, 56.78°, 62.99°, 66.49°, 68.12°, 69.14°, 72.67°, and 77.07° of 2Θ, corresponds to (100), (002), (101), (102), (103), (200), (112), (201), (004), and (202) crystal planes. All diffraction peaks indicate the ZnO wurtzite hexagonal structure found in the standard reference data (ICSD 029272, 01-075-0576, Zincite).

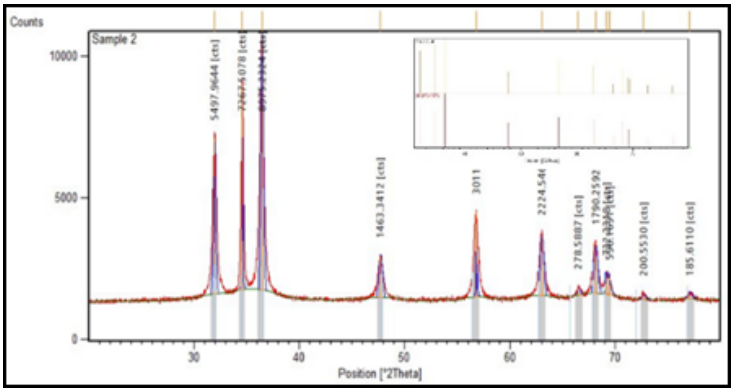

Figure 1. XRD spectra of synthesized ZnO-NPs.

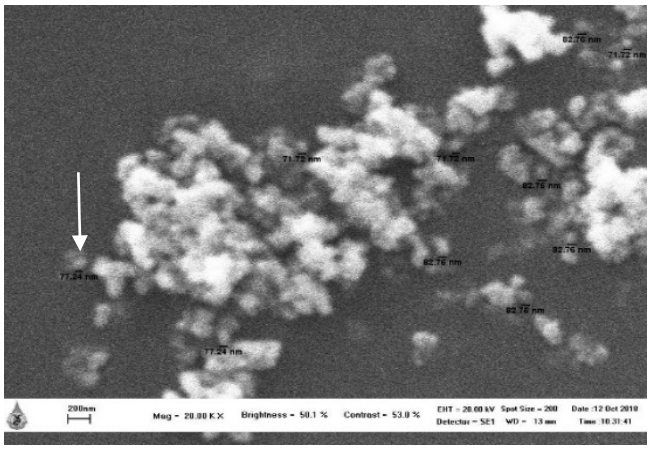

Figure 2. SEM micrograph of synthesized ZnO-NPs with magnification 20000x.

The particle size measurement and morphology of the nanoparticles were observed under SEM (Figure. 2) at magnification 20000x. Single nanoparticles indicated with the arrows sign in the figure. The synthesized ZnO-NPs showed an average size (diameter) of 79.25 nm with a spherical shape. Akbar and Anal (2014) reported that the particle size of ZnO-NPs synthesis using hydrothermal method was around 50 nm with a spherical shape. The size and shape of nanoparticles depend on several factors, such as the type of precursor and the solvent used as well as chemical and physical conditions (pH, temperature) in the reaction (Espitia et al., 2012).

3.2 Antimicrobial Activity of Zinc Oxide Nanoparticles

The preliminary test of ZnO nanoparticles antimicrobial activity were tested against the Gram-positive (*S. aureus*) and Gram-negative (*E. coli*) bacteria. The paper disk containing different concentration of ZnO nanoparticles showed a clear zone against the target bacteria. The clear zone of ZnO nanoparticles against the target bacteria is illustrated in Figure. 3. Its antimicrobial properties are associated to several mechanisms including the release of antimicrobial ions (Zn^{2+}), the interaction of nanoparticles with microorganisms, subsequently damaging the integrity of bacterial cell and the formation of ROS by the effect of light radiation (Espitia et al. 2012). Li et al. (2011) found that the toxicity of Nano-ZnO was mainly attributed to the released Zn^{2+} ions. Akbar and Anal (2014) observed that the nanoparticles have a high impact on the cell surface integrity, which responsible to make the cell wall porous, and the target bacterial cells with ruptured bodies are clearly noted in the electron micrograph.

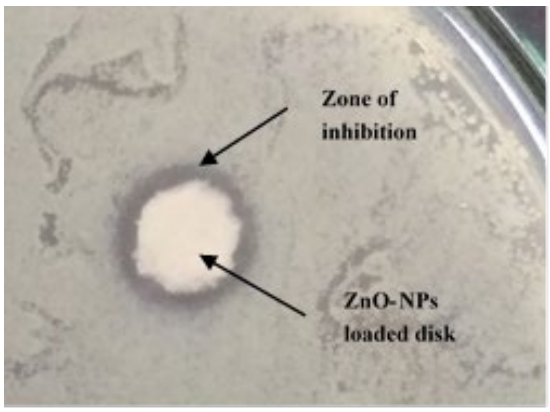

Figure 3. Zone of inhibition of ZnO-NPs loaded paper disk against the target bacteria on Mueller Hinton agar plate.

Particle size and shape may affect its antimicrobial activity. Song et al. (2010) found that 10–30 nm spherical ZnO particles were slightly highly toxic than three rod-like ZnO particles. Nair et al. (2009) also found that antibacterial activity toward *E. coli* increased as the particle size decreased because the smaller sized particles would be expected to have a higher surface charge because of the increased surface area per unit volume.

Table 1. The result of the disk diffusion method of synthesized ZnO-NPs.

Treatment	Zone of inhibition (mm)	
	S. aureus	*E. coli*
1% ZnO NPs	1.50 ± 0.71^{a}	0.00 ± 0.00^{a}
3% ZnO NPs	3.00 ± 0.00^{b}	1.25 ± 0.35^{b}
5% ZnO NPs	4.00 ± 0.00^{b}	3.00 ± 0.00^{c}

Results were represented as means of replicates ± standard deviation. Values with different superscripts in the column are significantly different ($p<0.05$).

The higher concentrations of ZnO nanoparticles showed higher antibacterial activity against the target bacteria (Table 1). According to Li et al. (2011), the Zn^{2+} ions concentration increased with the increasing concentration of ZnO-NPs, thus it resulted in higher toxicity towards tested bacteria. Akbar and Anal (2014) reported that the antimicrobial effect of the ZnO-NPs increased with the increase of ZnO-NPs concentration because nanoparticles are responsible to make the cell wall porous. However, the 1 % concentration of ZnO-NPs was not effective to inhibit the growth of *E. coli* (approximately 1.5 x 108 CFU/mL) after 24 h of incubation. This result might be attributed to *E. coli* can excrete large amounts of extracellular polymer substances during growth to resist toxicity, thus *E. coli* could still survive with low concentrations of ZnO-NPs (Li et al. 2011). There was no significant difference in the inhibition zone of *S. aureus* at 3 % and 5 % ZnO-NPs concentration. A similar result also found by Pamuji (2014), the incorporation of 3 % ZnO-NPs has a significant effect on antibacterial properties of tapioca starch film against *E. coli*, *B. cereus*, and *S. aureus*. Therefore, the 3 % of zinc oxide nanoparticles is the optimum concentration to inhibit the growth of tested bacteria and it was selected to further use in active film development.

3.3 Characterization of Rice Starch-based Nanocomposite Film

3.3.1 Morphological Observation and FT-IR

FT-IR analysis was performed to examine the interactions between rice starch polymer and ZnO NPs as shown in Figure. 4. A broad absorption band of rice starch film 3263.27 cm^{-1} was attributed to the stretching of hydroxyl (O-H) groups (Li et al. 2011). The peak at 2923.83 cm^{-1} was the C-H stretching, while the peak at 1367.28 cm^{-1} was the O-H of water (Bourtoom and Chinnan, 2008). According to Kizil et al. (2002), water adsorbed in the amorphous region of starches could be identified as a broad infrared band with a peak at 1637 cm^{-1}, as a result of the vibration of water molecules adsorbed in the nanocrystalline region of the starch. The IR peaks for rice starch at 1076.72 and 1015.46 cm^{-1} were assigned to the anhydroglucose ring of the O–C stretch (Matmin et al., 2018), whereas the band obtained at 994.91 cm^{-1} was attributed to the vibrations originating from the C-O-C of α-1,4 glycosidic linkages (Kizil et al., 2002). Other vibrational bands in the fingerprint region, at 667.47, 704.36 and 759.83 cm^{-1}, were due to the skeletal mode vibrations of the pyranose ring in the glucose unit (Matmin et al., 2018).

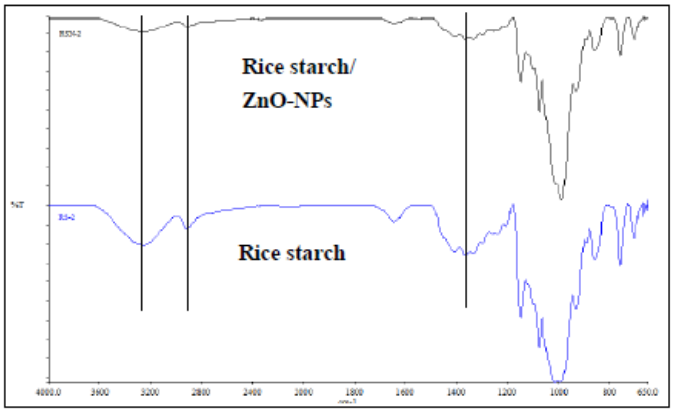

Figure 4. FTIR spectra of rice starch and rice starch film incorporated with 3% ZnO-NPs.

No new functional group was added after the ZnO-NPs incorporation. It indicated an only physical interaction between the ZnO- N and the film matrix occurs (Nafchi et al., 2012). However, some of the peaks were shifted to higher and lower wave number with ZnO-NPs incorporation may be due to certain interactions between ZnO NPs and biopolymer matrix (Anitha et al., 2013).
The presence of ZnO nanoparticles in the film was observed under SEM, illustrated in Figure. 5. The nanoparticles in the rice starch film indicated with the arrows sign in the figure. The neat rice starch film was smooth and had a compact surface, while rice starch/ZnO-NPs films showed rough surface

and the ZnO nanoparticles were distributed through the film surface. Similar surface morphologies of nanocomposite films with ZnO-NPs incorporation such as agar/ZnO-NPS, carrageenan/ZnO-NPs, CMC/ZnO-NPs (Kanmani and Rhim, 2014), and gelatin/ZnO-NPs (Shankar et al., 2016).

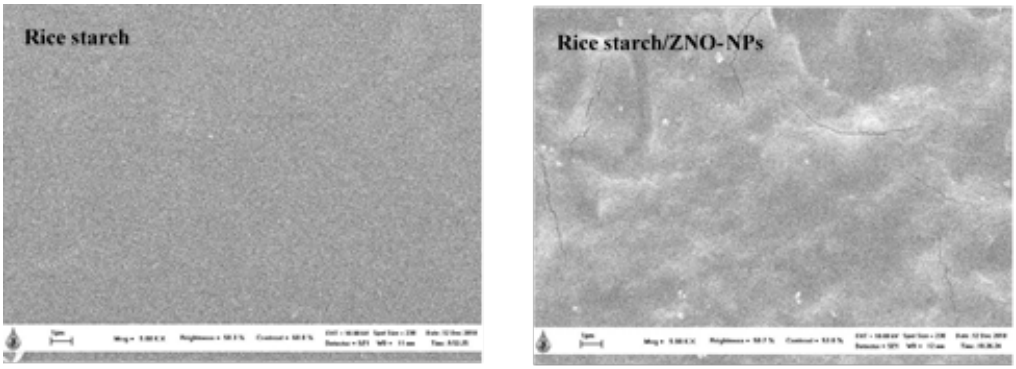

Figure 5. SEM micrograph of rice starch film and rice starch film incorporated with ZnO-NPs on the surface with magnification 20000x.

3.3.2 Thickness and Mechanical Properties of The Films

The thickness and mechanical properties of the films are shown in Table 2. The thickness of neat rice starch films was 70.00 µm, which was not significantly ($p>0.05$) changed after blending with ZnO nanoparticles. A contrary result was found by Kanmani and Rhim (2014) who reported that the thickness of various biopolymer films increased with the addition of ZnO NPs.

Table 2. Thickness, tensile properties, moisture content, film solubility, and water vapor permeability of rice starch film and rice starch film incorporated with ZnO-NPs.

Films	Thickness (µm)	TS (MPa)	EAB (%)	MC (%)	Film solubility (%)	WVP (x 10^{-10} g m/ m^2 Pa s)
Rice starch	70.00 ± 2.13^a	5.00 ± 0.44^a	76.62 ± 5.68^b	11.95 ± 1.48^a	27.12 ± 1.33^b	0.06 ± 0.01^b
Rice starch/ZnO-NPs	69.50 ± 3.32^a	9.14 ± 0.78^b	37.18 ± 2.61^a	12.55 ± 1.12^a	19.22 ± 0.39^a	0.04 ± 0.00^a

Results were represented as means of replicates ± standard deviation. Values with different superscripts in the column are significantly different ($p<0.05$).

The mechanical properties (TS and EAB) of rice starch film greatly influenced after incorporation with ZnO-NPs ($p<0.05$). The TS of the rice starch film increased from 5.00 MPa to 9.14 MPa after ZnO-NPs incorporation. In contrast, the EAB decreased from 76.62 % to 37.18 % after ZnO-NPs incorporation. It was expected to improve the tensile strength of rice starch films by incorporating ZnO-NPs. Tensile strength (TS) is a measure of film integrity and elongation at break (EAB) is a quantitative representation of the ability to stretch of the films. A Similar result was found by Suyatma et al. (2014) who reported that the incorporation of ZnO- NPs into pectin films would raise TS and slightly reduce EAB. The increase in mechanical strength of the rice starch/ZnO-NPs composite film might be due to the interaction formed by the hydrogen bond between ZnO-NPs and rice starch. The mechanical properties of the films are closely related to the distribution and density of the intra and intermolecular interactions between the polymer chains in the film matrix (Shankar et al., 2016).

3.3.3 Surface Color and Transparency

The color characteristics of the films are summarized in Table 3. Apparently, the neat rice starch films were translucent with a whitish tint (Figure. 6). However, the rice starch/ZnO-NPs film was changed appearance to milky white and more opaque. It indicated the formation of ZnO nanoparticles (Shankar et al., 2014). The lightness (Hunter L-value) of rice starch film was 86.73, but it increased significantly ($p<0.05$) after incorporation with ZnO-NPs. Hunter a and b values (indicating greenness-

redness and blueness-yellowness, respectively) of rice starch/ ZnO-NPs film were not significantly different ($p>0.05$). Consequently, the total color difference (ΔE) of rice starch/ZnO-NPs film (3.38) decreased compared with the neat rice starch film (6.37).

Table 3. Color parameters of rice starch film and rice starch film incorporated with ZnO-NPs.

Films	L*	a*	b*	ΔE
Rice starch	86.73 ± 0.83^{a}	-1.17 ± 0.15^{a}	2.63 ± 0.35^{a}	6.37 ± 0.83^{b}
Rice starch/ZnO-NPs	89.73 ± 0.06^{b}	-0.90 ± 0.21^{a}	2.11 ± 0.04^{a}	3.38 ± 0.04^{a}

Results were represented as means of replicates ± standard deviation. Values with different superscripts in the column are significantly different ($p<0.05$).

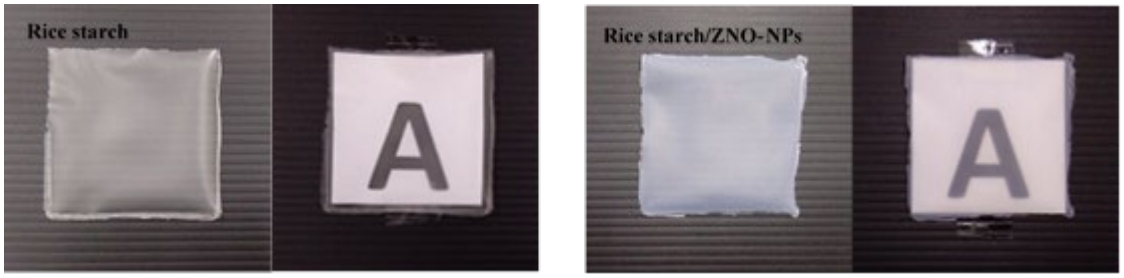

Figure 6. Appearance of rice starch film and rice starch film incorporated with ZnO-NPs.

Optical properties of films are an important attribute that influences its appearance, marketability, and their suitability for various applications (Rawdkuen et al., 2012). Light transmission in UV (200–280 nm) and visible ranges (350–800 nm), as well as the transparency of the film samples, are shown in Table 4. Generally, all films exhibited lower light transmission in the UV range than in the visible range. The light transmission of the film was decreased significantly by the formation of nanocomposite with ZnO ($p<0.05$). It indicated that the ZnO-NPs in the film matrices prevented the passage of UV light. This result was consistent with Kanmani and Rhim (2014) who observed low transmissions of light in the UV range of various biopolymer incorporated with ZnO-NPs. For film transparency, there were significant differences between treatments and the control were observed ($p<0.05$). This result was also confirmed by the surface morphology with different backgrounds of the films in Figure. 6. The higher transparency value indicated that the film was less transparent. It was found that incorporating ZnO-NPs into the rice starch-based film affected the transparency of the resulting films. Based on the optical properties of the film, the application of rice starch film incorporated with ZnO-NPs may be limited to certain food products (e.g. meatball).

Table 4. Light transmission and transparency value of rice starch film and rice starch film incorporated with ZnO-NPs.

Films	% Transmittance								Transparency value
	T_{200}	T_{280}	T_{350}	T_{400}	T_{500}	T_{600}	T_{700}	T_{800}	
Rice starch	0.07	22.57	34.77	37.98	42.44	45.37	48.06	50.48	2.81 ± 0.01^{b}
Rice starch/ZnO-NPs	0.03	3.28	4.07	14.05	24.56	30.83	35.49	39.26	2.64 ± 0.01^{a}

Results were represented as means of replicates ± standard deviation. Values with different superscripts in the column are significantly different ($p<0.05$).

3.3.4 Moisture Content (MC)

The moisture content of the films is shown in Table 2. The rice starch/ZnO-NPs film exhibited slightly higher MC (12.55 %) compared with the control films (11.95 %), however, they were not significantly different ($p>0.05$). It indicated there was no significant change to the total solid of the films after incorporation with ZnO-NPs. The difference in moisture content may be caused by the drying process of the film. A similar result was found by Kanmani and Rhim (2014), who reported that moisture content of various biopolymer films slightly increased with the addition of ZnO-NPs.

3.3.5 Film Solubility

The solubility of the rice starch incorporated with ZnO-NPs in term of water solubility is shown in Table 2. The control film showed the higher film solubility (27.12 %), while decreased significantly ($p<0.05$) in the film incorporated with ZnO-NPs (19.22 %). A similar result was found by Nafchi et al. (2012), who incorporated ZnO nano-rods to sago starch film significantly decreased the solubility of the biocomposites. This result may be attributed to the interactions between ZnO and starch in the biopolymer film structure. Furthermore, it can be caused by the hydrophobic nature of ZnO-NPs. Nafchi et al. (2012) reported that increasing the ZnO-NPs content of films increased the hydrophobicity of the films may be due to the formation of more hydrogen bonds the ZnO-NPs and the matrix components.

3.3.6 Water vapor permeability (WVP)

The results of WVP studies are presented in Table 2. The incorporation of ZnO NPs into the rice starch film significantly decreased ($p<0.05$) the WVP of the rice starch films. The WVP results indicated that the water vapor barrier property of the nanocomposite films was improved compared with the control films. The increased water vapor barrier property may be attributed to the water vapor impermeable nanoparticles and the formation of a tortuous path for passage of water molecules by ZnO NPs addition in the polymer matrix since ZnO could disperse well in the matrix (Yu et al., 2009). Due to their small size, the nanoparticles might enhance the water vapor resistance of the films because they can increase the compactness of the films and they can prevent the formation of intermolecular hydrogen bonding amongst starch molecules which can reduce the water vapor diffusion through the film (Shi et al., 2013). The significant decrease in WVP after the incorporation of ZnO-NPs may be attributed to the greater water resistance of ZnO-NPs compared with the pure rice starch film (Nafchi et al., 2012). Kanmani and Rhim (2014) found that the WVP of incorporation of ZnO NPs into the various polymer films clearly decreased the WVP. Nafchi et al. (2012) also found that the incorporation of ZnO-N into sago starch film decreased the WVP of the film.

3.3.7 Antimicrobial Activity of Films

The ZnO nanoparticles incorporation into rice starch film showed a clear zone against the target bacteria (Table 5). The clear zone of active films against the target bacteria is illustrated in Figure. 7. Rice starch films used as a control (without ZnO nanoparticles) showed no clear zone against the tested bacteria. Results indicate that the antimicrobial activity of rice starch/ZnO-NPs film should be attributed to the ZnO-NPs because the control film didn't show antibacterial activity against tested bacteria. The inactivation of bacteria by ZnO involves mainly direct interaction between ZnO nanoparticles and the surface of cells, affecting the permeability of the membrane, allowing the internalization of nanoparticles and inducing oxidative stress in bacterial cells, resulting in the inhibition of cell growth (Espitia et al., 2012).

Table 5. The result of the disk diffusion method of the film.

Films	Zone of inhibition (mm)	
	S. aureus	*E. coli*
Rice starch	0.00 ± 0.00^{a}	0.00 ± 0.00^{a}
Rice starch/ZnO-NPs	4.50 ± 0.71^{b}	2.50 ± 0.71^{b}

Results were represented as means of replicates ± standard deviation. Values with different superscripts in the column are significantly different ($p<0.05$).

Tankhiwale and Bajpai (2012) found that petri plate supplemented with ZnO-loaded SCP film shows a clear zone of inhibition around the film which indicates that ZnO nanoparticles must have diffused away from the film, thus causing bacterial cell death and forming a clear zone of inhibition around the film. Li et al. (2011) were observed the cytoplasmic membranes deformed, wherein some cells swelled

and the intracellular substances leaked out under Zn stress, thus Zn^{2+} ions dissolved from ZnO were considered as the primary cause for ZnO ecotoxicity.

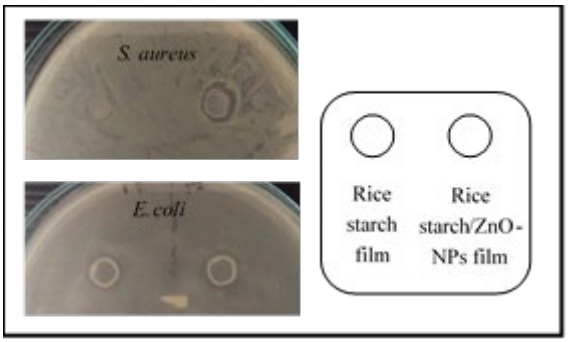

Figure 7. Antimicrobial activity of the film against *S. aureus* and *E. coli*.

The observed inhibition zone of the ZnO-NPs loaded film showed that *S. aureus* inhibition zone was larger than *E. coli* inhibition zone. It indicates rice starch/ZnO-NPs film had higher antibacterial activity against Gram-positive *S. aureus* than Gram-negative *E. coli*. A similar result also found by Anitha et al. (2013), Banoee et al. (2010), Kanmani and Rhim (2014), and Li et al. (2009). This result may be attributed to the different structure and thickness of the membrane cell wall between *S. aureus* and *E. coli*. The Gram-positive *S. aureus* is composed of multi-layers of peptidoglycan which has plenty of pores that could render them more susceptible to the intracellular transduction by the nanoparticles leading to cell disruption, while the cell wall of Gram-negative *E. coli* is relatively thin mainly consisting of peptidoglycan and an outer layer of lipopolysaccharide, lipoprotein, and phospholipids, which would be less prone to the attack of the nanoparticles (Anitha et al. 2013).

4. CONCLUSION

The ZnO-NPs were successfully obtained through hydrothermal synthesis with an average size of 79.25 nm and spherical shape. The synthesized ZnO-NPs showed antimicrobial activity against tested bacteria (*S. aureus* and *E. coli*). The optimum concentration to inhibit the growth of tested bacteria was 3 % and it was used to develop antimicrobial nanocomposite films. ZnO-NPs were successfully incorporated into rice starch film through a solution casting method. The ZnO-NPs were distributed on the surface of the nanocomposite film. Significant changes in color, transparency, mechanical properties, solubility, and water vapor permeability were observed. Incorporation of ZnO NPs into rice starch film showed an antimicrobial effect against *S. aureus* and *E. coli*. Based on these results, rice starch/ZnO-NPs nanocomposite film had the potential to be used as biodegradable antimicrobial packaging. Nevertheless, further studies such as an application part for the real foods are needed to analyze their potential performance.

ACKNOWLEDGMENTS

The authors warmly thank School of Agro-Industry, Mae Fah Luang University for financial support.

REFERENCES

Akbar, A. and Anal, A.K. (2014). Zinc oxide nanoparticles loaded active packaging, a challenge study against Salmonella typhimurium and Staphylococcus aureus in ready-to-eat poultry meat. *Food Control*, **38**, 88–95.

Anitha, S., Brabu, B., John Thiruvadigal, D., Gopalakrishnan, C. and Natarajan, T.S. (2013). Optical, bactericidal and water repellent properties of electrospun nano-composite membranes of cellulose acetate and ZnO. *Carbohydrate Polymers*, **97**, 856–863.

Banoee, M., Seif, S., Nazari, Z.E., Jafari-Fesharaki, P., Shahverdi, H.R., Moballegh, A., Moghaddam, K.M. and Shahverdi, A.R. (2010). ZnO nanoparticles enhanced antibacterial activity of ciprofloxacin against Staphylococcus aureus and Escherichia coli. *Journal of Biomedical Materials Research Part B: Applied Biomaterials*, **93B**, 557–561.

Bourtoom, T. and Chinnan, M.S. (2008). Preparation and properties of rice starch-chitosan blend biodegradable film. *LWT - Food Science and Technology*, **41**, 1633–1641.

CDC. (2018). Foodborne illnesses and germs [Internet document] URL https://www.cdc.gov/foodsafety/foodborne-germs.html. Accessed 26/06/2019.

Detduangchan, N., Sridach, W. and Wittaya, T. (2014). Enhancement of the properties of biodegradable rice starch films by using chemical crosslinking agents. *International Food Research Journal*, **21**, 1225–1235.

Detduangchan, N. and Wittaya, T. (2011). Effect of UV-Treatment on Properties of Biodegradable Film From Rice Starch. *International Journal of Materials and Metallurgical Engineering*, **5**, 829–834.

Espitia, P.J.P., Soares, N. de F.F., Coimbra, J.S. dos R., Andrade, N.J. de, Cruz, R.S. and Medeiros, E.A.A. (2012). Zinc Oxide Nanoparticles: Synthesis, Antimicrobial Activity and Food Packaging Applications. *Food and Bioprocess Technology*, **5**, 1447–1464.

Jiménez, A., Fabra, M.J., Talens, P. and Chiralt, A. (2012). Edible and Biodegradable Starch Films : A Review. *Food Bioprocess Technology*, **5**, 2058–2076.

Kaewprachu, P. and Rawdkuen, S. (2016). Application of Active Edible Film as Food Packaging for Food Preservation and Extending Shelf Life. In: *Microbes in Foods and Health*. Pp. 185–205. Springer International Publishing Switzerland.

Kanmani, P. and Rhim, J.W. (2014). Properties and characterization of bionanocomposite films prepared with various biopolymers and ZnO nanoparticles. *Carbohydrate Polymers*, **106**, 190–199.

Kizil, R., Irudayaraj, J. and Seetharaman, K. (2002). Characterization of irradiated starches by using FT-Raman and FTIR spectroscopy. *Journal of Agricultural and Food Chemistry*, **50**, 3912–3918.

Kotharangannagari, V.K. and Krishnan, K. (2016). Biodegradable hybrid nanocomposites of starch/lysine and ZnO nanoparticles with shape memory properties. *Materials and Design*, **109**, 590–595.

Laohakunjit, N. and Noomhorm, A. (2004). Effect of plasticizers on mechanical and barrier properties of rice starch film. *Starch/Staerke*, **56**, 348–356.

Li, M., Zhu, L. and Lin, D. (2011). Toxicity of ZnO nanoparticles to escherichia Coli: Mechanism and the influence of medium components. *Environmental Science and Technology*, **45**, 1977–1983.

Li, X., Xing, Y., Jiang, Y., Ding, Y. and Li, W. (2009). Antimicrobial activities of ZnO powder-coated PVC film to inactivate food pathogens. *International Journal of Food Science and Technology*, **44**, 2161–2168.

Matmin, J., Affendi, I., Ibrahim, S.I. and Endud, S. (2018). Additive-free rice starch-assisted synthesis of spherical nanostructured hematite for degradation of dye contaminant. *Nanomaterials*, **8**.

Nafchi, A.M., Alias, A.K., Mahmud, S. and Robal, M. (2012). Antimicrobial, rheological, and physicochemical properties of sago starch films filled with nanorod-rich zinc oxide. *Journal of Food Engineering*, **113**, 511–519.

Nair, S., Sasidharan, A., Divya Rani, V. V., Menon, D., Nair, S., Manzoor, K. and Raina, S. (2009). Role of size scale of ZnO nanoparticles and microparticles on toxicity toward bacteria and osteoblast cancer cells. *Journal of Materials Science: Materials in Medicine*, **20**, 235–241.

Pamuji, M.W. (2014). *Development of bionanocomposite film based from cassava starch and nanoparticle ZnO with glycerol as platicizer*.

Phattaraporn, T., Waranyou, S. and Thawien, W. (2011). Effect of palm pressed fiber (PPF) surface treatment on the properties of rice starch films. *International Food Research Journal*, **18**, 287–302.

Ramos, M., Jiménez, A., Peltzer, M. and Garrigós, M.C. (2012). Characterization and antimicrobial activity studies of polypropylene films with carvacrol and thymol for active packaging. *Journal of Food Engineering*, **109**, 513–519.

Rawdkuen, S., Suthiluk, P., Kamhangwong, D. and Benjakul, S. (2012). Mechanical, physico-chemical, and antimicrobial properties of gelatin-based film incorporated with cathecin-lysozyme. *Chemistry Central Journal*, **6**, 1–10.

Shahverdi, A.R., Fakhimi, A., Shahverdi, H.R. and Minaian, S. (2007). Synthesis and effect of silver nanoparticles on the antibacterial activity of different antibiotics against Staphylococcus aureus and Escherichia coli. *Nanomedicine: Nanotechnology, Biology, and Medicine*, **3**, 168–171.

Shankar, S., Tanomrod, N., Rawdkuen, S. and Rhim, J. (2016). Preparation of pectin / silver nanoparticles composite films with UV-light barrier and properties. *International Journal of Biological Macromolecules*, **92**, 842–849.

Shankar, S., Teng, X. and Rhim, J. (2014). Effects of concentration of ZnO nanoparticles on mechanical, optical, thermal, and antimicrobial properties of gelatin / ZnO nanocomposite films. *Korean Journal of Packaging Science and Technology*, **20**, 41–49.

Shi, A.M., Wang, L.J., Li, D. and Adhikari, B. (2013). Characterization of starch films containing starch nanoparticles Part 1: Physical and mechanical properties. *Carbohydrate Polymers*, **96**, 593–601.

Song, W., Zhang, J., Guo, J., Zhang, J., Ding, F., Li, L. and Sun, Z. (2010). Role of the dissolved zinc ion and reactive oxygen species in cytotoxicity of ZnO nanoparticles. *Toxicology Letters*, **199**, 389–397.

Sung, S., Sin, L.T., Tee, T., Bee, S., Rahmat, A.R., Tan, A.-C. and Vikhraman, M. (2013). Antimicrobial agents for food packaging applications. In: *Trends in Food Science and Technology*. Elsevier Ltd.

Suyatma, N.E., Ishikawa, Y. and Kitazawa, H. (2014). Nanoreinforcement of pectin film to enhance its functional packaging properties by incorporating zno nanoparticles. *Advanced Materials Research*, **845**, 451–456.

Tankhiwale, R. and Bajpai, S.K. (2012). Biointerfaces preparation, characterization and antibacterial applications of ZnO-nanoparticles coated polyethylene films for food packaging. *Colloids and Surfaces B: Biointerfaces*, **90**, 16–20.

Thakur, R., Pristijono, P., Golding, J.B., Stathopoulos, C.E., Scarlett, C.J., Bowyer, M., Singh, S.P. and Vuong, Q. V. (2018). Development and application of rice starch based edible coating to improve the postharvest storage potential and quality of plum fruit (Prunus salicina). *Scientia Horticulturae*, **237**, 59–66.

Thakur, R., Saberi, B., Pristijono, P., Golding, J., Stathopoulos, C., Scarlett, C., Bowyer, M. and Vuong, Q. (2016). Characterization of rice starch-ι-carrageenan biodegradable edible film. Effect of stearic acid on the film properties. *International Journal of Biological Macromolecules*, **93**, 952–960.

U.S. Food and Drug Administration. (2018). GRAS Substances (SCOGS) Database [Internet document] URL https://www.accessdata.fda.gov/scripts/fdcc/?set=SCOGSandsort=Sortsubstanceandorder=ASCandstartrow=1andtype=basicandsearch=zinc oxide. Accessed 20/12/2018.

Wittaya, T. (2012). Rice Starch-Based Biodegradable Films: Properties Enhancement. In: *Structure and Function of Food Engineering*. Pp. 103–134. IntechOpen.

Yu, J., Yang, J., Liu, B. and Ma, X. (2009). Preparation and characterization of glycerol plasticized-pea starch / ZnO – carboxymethylcellulose sodium nanocomposites. *Bioresource Technology*, **100**, 2832–2841.

11:30 AM - 12:30 PM (Thu. Sep 5, 2019 11:30 AM - 12:30 PM Poster Place)

[5-1130-P-08] Effect of pulsed electric field treatment on drying rate and quality changes of spinach in hot air drying

*Koya Yamakage[1], Takahiro Yamada[1], Takahiro Orikasa[2,3], Katsuyuki Takahashi[2,4], Shoji Koide[3], Koichi Takaki[2,4], Hitoshi Aoki[5], Junichi Kamagata[5] (1. Graduate School of Arts and Science, Iwate University(Japan), 2. Agri-Innovation Center, Iwate University(Japan), 3. Faculty of Agriculture, Iwate University(Japan), 4. Faculty of Science and Engineering, Iwate University(Japan), 5. Nichirei Foods Inc.(Japan))
Keywords: pulsed electric field, spinach, drying rate, L-ascorbic acid, potassium

Although hot air drying is a commonly method for vegetable preservation, it has various disadvantages, including a slow drying rate. To increase the drying rate, hot water (HW) pretreatment is often applied during dried vegetable production using hot air. However, HW pretreatment can result in the elution of water-soluble components. Therefore, we examined the application of pulsed electric field (PEF) technology before drying as a waterless treatment to overcome the disadvantages of HW pretreatment. We measured the moisture content and quality changes in spinach (residual ratios of L-ascorbic acid (L-AsA) and potassium (K)) after drying with PEF, HW and control (CONT) treatments. The drying rates were faster for PEF and HW than for CONT. The residual ratios of L-AsA and K were higher for PEF than for HW. Our results indicated that PEF was more effective than HW as a pretreatment method before drying with respect to the drying rate and the maintenance of water-soluble components. This pretreatment approach has potentially applications for the productions of high-quality dried vegetables.

11:30 AM - 12:30 PM (Thu. Sep 5, 2019 11:30 AM - 12:30 PM Poster Place)

[5-1130-P-09] Prospects of Biogas Production From The Manure of Dairy Cattle Fed on Iron-supplemented Ration

*Mohamed Farghali[1,2], Maejima Mayumi[3], Kuramoto Syo[3], Aoki Satoshi[4], Yasui Seiichi[5], Sayoko Takashima [1], Hijiri Ono[1], Yuhendra AP[1], Takaki Yamashiro[6], Moustafa M. Ahmed[2], Saber Kotb[2], Masahiro Iwasaki[1], Kazutaka Umetsu[1] (1. Graduate School of Animal and Food Hygiene, Obihiro University of Agriculture and Veterinary Medicine(Japan), 2. Department of Animal and Poultry Hygiene &Environmental Sanitation, Faculty of Veterinary Medicine, Assiut University(Egypt), 3. Maezawa Engineering service Inc.(Japan), 4. Maezawa Industries Inc.(Japan), 5. Hokkaido Air Water Inc.(Japan), 6. Tokachi Agri Works (Japan))
Keywords: iron supplement, animal feed, biogas, manure, anaerobic digestion

Anaerobic digestion (AD) is a promising bio-technology for energy recovery from organic wastes. This study provides a novel method for the enhanced AD of dairy manure (DM) without pre/post-treatment by the direct supplementation of special natural ash from soil called Mineraso (MS) to the feed of lactating Holstein dairy cattle (HDC). MS is chiefly composed of approximately 84.8% of iron hydroxide. MS was supplemented at rates of 0 (F1), 25 (F2), and 50 (F3) g/head of HDC/day for two months. Thereafter, the manure of each group of HDC was collected and examined for iron concentrations prior to the batch AD experiments. The results revealed that the amounts of iron excreted in manure were reduced by 63.64% and 68.42%, respectively. Interestingly, the supplementation of MS at concentrations of 25 and 50 g/head of HDC improved biogas yields from DM by 21.90% and 40.05%, respectively than the control (no MS supplementation). Additionally, the equivalent dosages of MS improved methane yield by 25.87% and 46.51%, respectively. The highest cumulative production of biogas and CH_4 was 1.11 and 0.63 L/gVS removed, respectively, which was achieved by F3 supplement, while the corresponding values in the case of

F1 were 0.79 and 0.43 L/gVS removed. Therefore, the supplementation of animals with iron-containing MS might represent a sustainable and practical approach to enhancing CH_4 yields.

Poster Session | Postharvest/Food Technology and Process Engineering
[5-1130-P] Postharvest/Food Technology and Process Engineering (5th)
Thu. Sep 5, 2019 11:30 AM - 12:30 PM Poster Place (Entrance Hall)

[5-1130-P-10] Anaerobic Digestion of Bean Sprouts Waste

*Yuki Yamamoto[1], Yuki Mizuya[2], Takaki Yamashiro[3], Fetra J Andriamanohiarisoamanana[1,4], Yoshiteru Takeuchi[5], Kazutaka Umetsu[1] (1. Graduate school of Obihiro University of Agriculture and Veterinary Medicine(Japan), 2. Obihiro University of Agriculture and Veterinary Medicine(Japan), 3. Tokachi Agri Works(Japan), 4. Graduate School of Agricultural Science, Kobe University(Japan), 5. Biomass Research(Japan))

Keywords: bean sprouts, anaerobic digestion, biogas , acid fermentation, elements addition

Wastes from food represents a critical issue globally. Bean sprouts, which are a familiar diet in Japan, are directly linked to the problem. In Ibaraki, a prefecture of japan, around 20% of the whole bean sprouts are disposed as a waste, therefore, their use as substrates for the Anaerobic digestion (AD) is of great challenge. Therefore, this study was considered to explore the potential of batch and continuous fermentation on the AD of bean sprouts wastes. In batch experiment, the biogas yields of boiled bean sprouts after 20 days were 2.4-times higher than raw bean sprouts. The continuous mesophilic experiments (38 ^{o}C) were conducted in three different experiments. The first experiment proposed a long period stable process after 30 days, with higher biogas yields from the mixtures of bean sprouts and return digestate than the use of bean sprout alone. The second experiment aimed to explore the impact of acid fermentation on the AD process, while the third experiment was involved the addition of trace element and different organic lading rates of bean sprouts. The results showed that acid fermentation enhanced biogas yield after 50 days by 1.5 time than no acid fermentation digester. Additionally, in third experiment, the B digester with 100g bean sprout, 200g return digestate, and 0.16g of iron, cobalt and nickel additives was produced higher organic decomposition rate of 71.02 % than the corresponding A digester (with 75g, 150g, and 0.12g, respectively) and C digesters (with 150g, 300g, and 0.24g, respectively). Therefore, the AD of bean sprouts wastes might represent a hygienic approach for their disposal with the advantage of large amounts of CH_4 production, especially when using a mixture of bean sprouts and a return digestate as a substrate. Additionally, acid fermentation, appropriate organic loading rate, and trace elements additions improved biogas production.

Anaerobic Digestion of Bean Sprouts Waste

Yuki Yamamoto[1], Yuki Mizuya[2], Takaki Yamashiro[3], Fetra J Andriamanohiarisoamanana[1,4], Yoshiteru Takeuchi[5], Kazutaka Umetsu[1*]

[1] Graduate school of Obihiro University of Agriculture and Veterinary Medicine,
[2] Obihiro University of Agriculture and Veterinary Medicine,
[3] Tokachi Agri Works,
[4] Graduate School of Agricultural Science, Kobe University,
[5] Biomass Research

*umetsu@obihiro.ac.jp

ABSTRACT

Wastes from food represents a critical issue globally. Bean sprouts, which are a familiar diet in Japan, are directly linked to the problem. In Ibaraki, a prefecture of japan, around 20% of the whole bean sprouts are disposed as a waste, therefore, their use as substrates for the Anaerobic digestion (AD) is of great challenge. Therefore, this study was considered to explore the potential of batch and continuous fermentation on the AD of bean sprouts wastes. In batch experiment, the biogas yields of boiled bean sprouts after 20 days were 2.4-times higher than raw bean sprouts. The continuous mesophilic experiments (38^{o}C) were conducted in three different experiments. The first experiment proposed a long period stable process after 30 days, with higher biogas yields from the mixtures of bean sprouts and return digestate than the use of bean sprout alone. The second experiment aimed to explore the impact of acid fermentation on the AD process, while the third experiment was involved the addition of trace element and different organic lading rates of bean sprouts. The results showed that acid fermentation enhanced biogas yield after 50 days by 1.5 time than no acid fermentation digester. Additionally, in third experiment, the B digester with 100g bean sprout, 200g return digestate, and 0.16g of iron, cobalt and nickel additives was produced higher organic decomposition rate of 71.02 % than the corresponding A digester (with 75g, 150g, and 0.12g, respectively) and C digesters (with 150g, 300g, and 0.24g, respectively). Therefore, the AD of bean sprouts wastes might represent a hygienic approach for their disposal with the advantage of large amounts of CH_4 production, especially when using a mixture of bean sprouts and a return digestate as a substrate. Additionally, acid fermentation, appropriate organic loading rate, and trace elements additions improved biogas production.

Keywords: Bean sprouts, Anaerobic Digestion, Biogas, Acid Fermentation, Elements Addition

1. INTRODUCTION

Methane fermentation, also referred to as anaerobic fermentation is a decomposition reaction of organic matter that proceeds under anaerobic conditions. The organic matter is decomposed by microorganisms belonging to the methanogen group to generate methane (CH_4) gas from hydrogen and carbon dioxide gas (Paritosh et al., 2017).

In recent years, from the standpoint of environmental protection view, CH_4 fermentation has been positioned as the main method of manure treatment, and in Japan efforts are also being made from both aspects of effective utilization of livestock manure and utilization of methane energy as natural bio-energy source. In addition, large amounts of waste biomasses such as sewage sludge, garbage and livestock excrement can be used as materials to be digested, with a global environmental protection. By the action of anaerobic bacteria, energy recovery from biomass organic matter to CH_4 leads to saving of electricity, reduce the use of fossil fuel and reduce of CO_2 and other greenhouse gases emissions. Moreover, the digestate which is a methane fermentation residue has the advantage to be used as a fertilizer to substitute the chemicals one to offer a safe and high-quality crop growth (Tatsuya Noike et al 2009).

Currently, about 1.3 billion tons of food, which is one-third of the world's food production, is discarded every year, especially in industrialized countries (FAO, 2011). In Japan, about 17 million

tons of food waste are discharged annually. Among them, 5 to 8 million tons of originally eaten food is discarded as food loss each a year.
Japan's food loss is about twice the amount of food aid to worldwide. This is comparable to Japan's rice production, and corresponds to the domestic supply of food for Namibia, Liberia, and the Democratic Republic of Congo, to which Japan has provided ODA assistance. About one-fourth of the food before the expiration date is discarded as a food waste (WFP, FAOSTAT" Food balance sheets" 2009)
Bean sprouts are familiar foods to Japanese food culture since ancient times. They are characterized by their potential nutrients such as starch, fat and protein, which stored in seeds, also their cells and tissues are made to grow while releasing energy at the stage of bean sprouting (Hedges and Lister, 2006.). In addition to the nutrients inherent in seeds, it is considered a special vegetable that produces new nutrients. Bean sprouts have been produced and consumed in large numbers in the past 25 years. Because stable production is possible regardless of the weather, the production and consumption of bean sprouts increase to compensate for the shortage of vegetables when the amount of supply of other vegetables decreases due to irregular weather (Bean sprout producers association, 2017).
However, up to 20% of the total production of bean sprouts in Ibaraki prefecture are not be sold and discarded as a waste. Therefore, in this study, we thought it could be effectively used as a material for anaerobic digestion to produce methane. In this context, batch and continuous experiments were conducted aimed to verify whether the bean waste was effective as methane fermentation material. In batch fermentation tests, raw and boiled bean sprouts were used as materials. In the continuous experiment, three study items were set up. The first is to explore the potential of continuous methane fermentation on bean sprouts as a substrate, the second is to examine the effectiveness of acid fermentation, and the third is to investigate the impacts of trace element addition on HRT and appropriate organic substance loading. HRT refers to the number of days of hydraulic retention time for which the substrate is in the fermenter. The organic load represents the weight of organic entering the fermenter. HRT and organic matter load are factors that determine the volume of the digester.

2. MATERIALS AND METHODS

2.1 Materials

2.1.1 Bean sprouts

Raw bean sprouts that collect from Ibaraki prefecture and boiled bean sprouts were used as a substrate for digestion. In the batch experiment, three runs of raw bean sprouts, boiled bean sprouts, and inoculum, which were collected from an active food processing biogas plant were set up. In the continuous experiment, ground bean sprouts were used based on the results of the batch experiment. The TS% and VS% of raw and boiled bean sprouts were 11.89, 11.22 and 11.22, 10.71, respectively.

2.1.2 Return digestate

The discharged digestate from the fermenter in the continuous experiment was mixed with bean sprouts substrate and used as the input material for the next day, and acid fermentation was performed until the input.

2.1.3 Trace elements

It is considered to be a substance necessary for the activity of microorganisms involved in methane fermentation. Among them, iron, cobalt and nickel were added at rates of 0.16, 0.12, and 0.24 g, respectively. In order to facilitate mixing, the three elements were made into an aqueous solution and mixed immediately before feeding into the fermenter.

2.1.4 Inoculum

Inoculum was collected from a food factory in Shihoro-cho, Hokkaido. The TS% and VS% of inoculum was 1.57 and 1.05, respectively.

2.2 Methods

2.2.1 Batch experiment

In this experiment, 700 g of materials were added into a 1L polyethylene digester. The fermentation conditions were operated in mesophilic temperature at 38 ° C. The experimental period was setup to 20 days, and stirring was performed manually once a day. Measurement of biogas volume and biogas component were carried out daily, TS% and VS% of materials, pH samples were measured before and after fermentation.

2.2.2 Continuous experiment

In this study, continuous experiments were performed as following: experiment 2-1, to investigate the methane fermentation using bean sprouts as material, experiment 2-2, to examine of the effectiveness of acid fermentation, and experiment 2-3, to determine the effect of HRT, trace element input, and the appropriate organic load rate. In Experiment 2-1, RUN A was used only bean sprouts as a material and RUN B, which used bean sprouts and return digester as a material, were setup. In Experiment 2-2, RUN A using bean sprouts from acid fermenter digester and a return digest solution as a material, and RUN B mixed with bean sprouts and a return digester on the day without acid fermentation were set. In Experiment 2-3, RUN A, B, and C, which used bean sprouts and the digestate and different amounts trace elements as materials, were set. The details of experimental design were shown in table 1, 2 and 3. In each experiment, one 10 L stainless fermenter was used per RUN. The fermenter was sealed and kept anaerobic, and placed in a water bath at 38 ° C mesophilic temperature. The input materials were stirred manually at least 1 min per day. The biogas volume was measured daily before the input of materials, and the biogas was collected once a week in a gas bag to measure the methane concentration. The weight and pH of the excreted digestate were measured daily, while total solid (TS%) and the volatile organic solid (VS%) were measured once a week (the measurement method will be described later). In the continuous experiment 2-2 A, the materials were exposed to acid fermentation before use. The material was put in 1L of polybin for mesophilic fermentation at 38°C., and acid fermentation was carried out for the input material from the next day onwards.

Table 1 Experimental 2-1 design, TS, VS, HRT

	materials	TS(%)	VS(%)	HRT(d)
RUN A	Bean sprouts 200g	15.93	15.31	50
RUN B	Bean sprouts 200g＋Return digestate 500g	3.26	3.05	15

Table 2 Experimental 2-2 design, TS, VS, HRT

	materials	TS(%)	VS(%)	HRT(d)
RUN A	Bean sprouts 100 g ＋Return digestate 300 g (acid fermentation)	3.89	3.17	25
RUN B	Bean sprouts 100 g ＋Return digestate 300 g (no acid fermentation)	5.13	4.53	25

Table 3 Experimental 2-3 design, TS, VS, HRT, organic loading

	materials	TS (%)	VS (%)	HRT (d)	organic loading (g-VS/L/d)
RUN A	Bean sprouts 75 g ＋Return digestate 150 g ＋Trace elements 0.12 g	6.09	5.38	44	2.75
RUN B	Bean sprouts 100 g ＋Return digestate 200 g ＋Trace elements 0.16g	5.58	4.68	33	4.26
RUN C	Bean sprouts 150 g ＋Return digestate 300 g ＋Trace elements0.24g	5.11	4.41	22	9.02

2.3 Parameter analysis

2.3.1 Biogas volume and composition

Biogas was collected in gas bags and its volume was measured by using wet gas flow meter (Shinagawa meter). The biogas was sampled with a gas bag, and the content ratio of H_2, O_2, N_2, CO_2, CH_4 in the biogas was analyzed with a gas chromatograph (SHIMAZU GC-14A). Before and after the batch test, the total solids (TS%), volatile solids, (VS%), and pH, in each biodigester were determined. Standard process (section 2540G) was followed to calculate the TS and VS contents (APHA, 2005). The pH was considered using a Horiba (D-55) pH meter.

2.3.2 Volatile fatty acid(mg/L)

It analyzed by the high-performance liquid chromatograph (HPLC: Shimadzu LC-10AD). An ion exclusion column was used and the column temperature was 45 ° C. The mobile phase was a 5 mM aqueous solution of p-toluene sulfonic acid at a flow rate of 0.8 mL/min. The buffer phase was a mixture of 20 mM Bis-Tris and 100 μM ethylenediaminetetraacetic acid in an aqueous solution of the mobile phase at a flow rate of 0.8 mL / min. For sample pretreatment, we added 6 mL of 10% tungstic acid and 6 mL of 2 / 3N sulfuric acid to 3 g of each sample, homogenized (10000 rpm, 5 min), centrifuged (10000 rpm, 20 min), then the collected supernatant was filtered with a membrane filter. A mixed solution of 1000 mg / L, 500 mg / L and 250 mg / L of formic acid, acetic acid, propionic acid and butyric acid, respectively, was used as a standard substance.

3. RESULTS AND DISCUSSION

3.1 Batch experiment

3.1.1 Cumulative biogas volume

As shown in figure 1, in batch raw bean sprouts experiment (RUN II), the biogas was generated up to 2 days after the start of the test, but no more gas was generated thereafter. However, in batch boiled bean sprouts experiment (RUN III), it was found that RUN III generated gas until 14 days after the start of the test, and generated about 2.4 times the gas volume of RUN II.

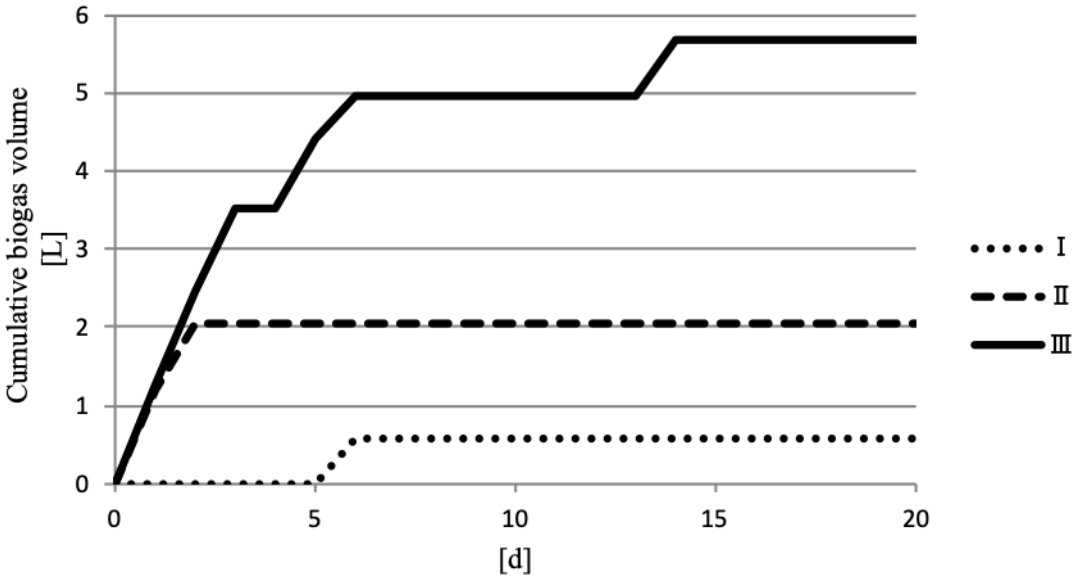

Figure 1 Cumulative biogas volume

3.1.2 Biogas component

In RUN II, the generation of gas ceased two days after the start of the test, so the generation of methane and carbon dioxide was insufficient. RUN III, fermentation was performed smoothly by 14 days after the start of the test, and methane and carbon dioxide were accordingly produced, and the methane concentration was about 1.6 times that of RUN II (Table 4)

Table 4 Biogas components

	CH_4(%)	CO_2(%)
RUN Ⅱ	32.89	35.37
RUN Ⅲ	54.72	23.39

3.1.3 Organic matter decomposition rate

The decomposition rate of organic matter was significantly higher in RUN III than RUN II. As the factor, it is considered that the fermentation period is longer RUN III, and the fermentation was performed smoothly (Table 5).

Table 5 Organic matter decomposition rate

	Before (VS%)	After (VS%)	Organic matter decomposition rate (%)
RUN Ⅱ	2.26	1.43	36.73
RUN Ⅲ	2.83	0.93	67.14

3.2 Continuous experiment

3.2.1 effect of continuous methane fermentation from bean sprouts as a material

Seven days after the start of the experiment in RUN A, the amount of gas decreased sharply and the generation of gas stopped. In addition, the optimum pH of the methane fermenter in methanogenesis is supposed to be 6.5 to 8.2, but when the amount of gas decreases, the pH shows a very low value of

4.39. Here too, it was determined that it was difficult to continue the fermentation, using only the bean sprouts as a material. On the other hand, RUN B which used bean sprouts and return digester as a material continued to generate gas until 25 days as shown in figure 2.

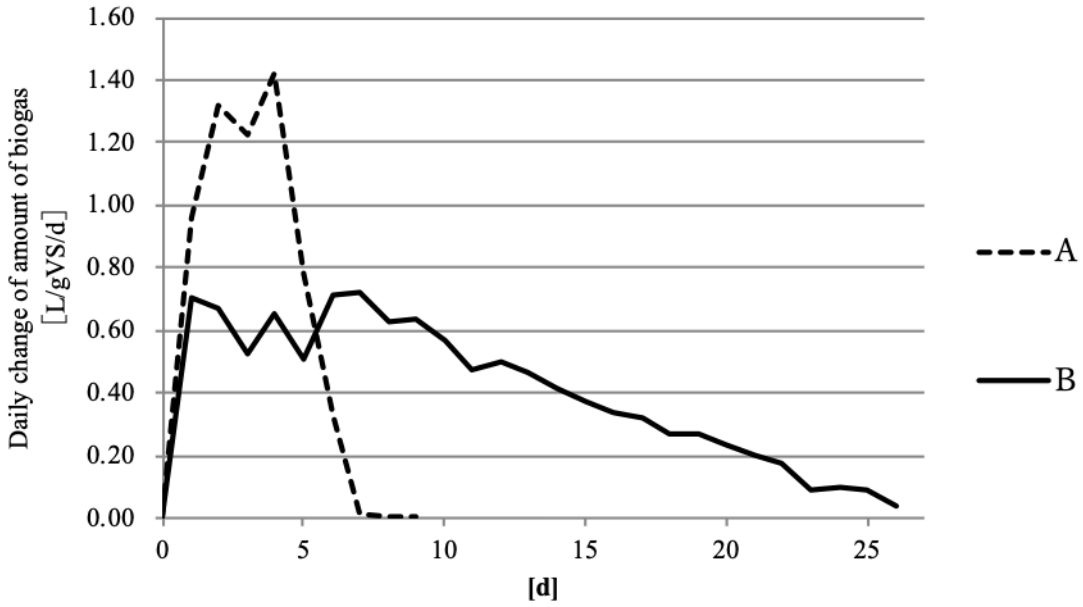

Figure 2 Daily change of amount of biogas

3.2.2 The effectiveness of acid fermentation

3.2.2.1 Amount of biogas and methane concentration per input VS

The acid fermentation RUN A produced more biogas than the RUN B, which did not undergo acid fermentation as shown in table 6. Moreover, since the average methane concentration was higher in RUN A than RUN B, it was found that an increase in methane concentration can be expected by performing acid fermentation.

Table 6 Amount of biogas and methane concentration per input VS

Materials	Average amount of biogas per input VS (L/g-VS/d)	Average CH_4 (%)
A Bean sprouts + Return digestate (acid fermentation)	0.65 (±0.032)	69.31 (±1.336)
B Bean sprouts + Return digestate (no acid fermentation)	0.43 (±0.010)	63.18 (±1.592)

3.2.2.2 pH

Through the experiment, the average value of pH for each test area was 7.74 for RUN A and 7.62 for RUN B, and no difference was found in the input materials. Moreover, both were in the range of optimal pH.

3.2.2.3 Organic matter decomposition rate

In the organic matter decomposition rate, RUN B was 1.6 times higher than RUN A. This can be attributed to that the material which carried out acid fermentation is used in RUN A; therefore, it is thought that their organic matter is decomposed at the stage of acid fermentation.

3.2.2.4 VFA

Since the acid fermentation is performed, the volatile organic acid concentration of the material in RUN A is high. Therefore, by performing methane fermentation, volatile organic acids were

decomposed, and a reduction of approximately 40.50% was observed. On the other hand, RUN B, the volatile organic acid was not decomposed well and an increase of about 27.13% after digestion as observed in figure 3.

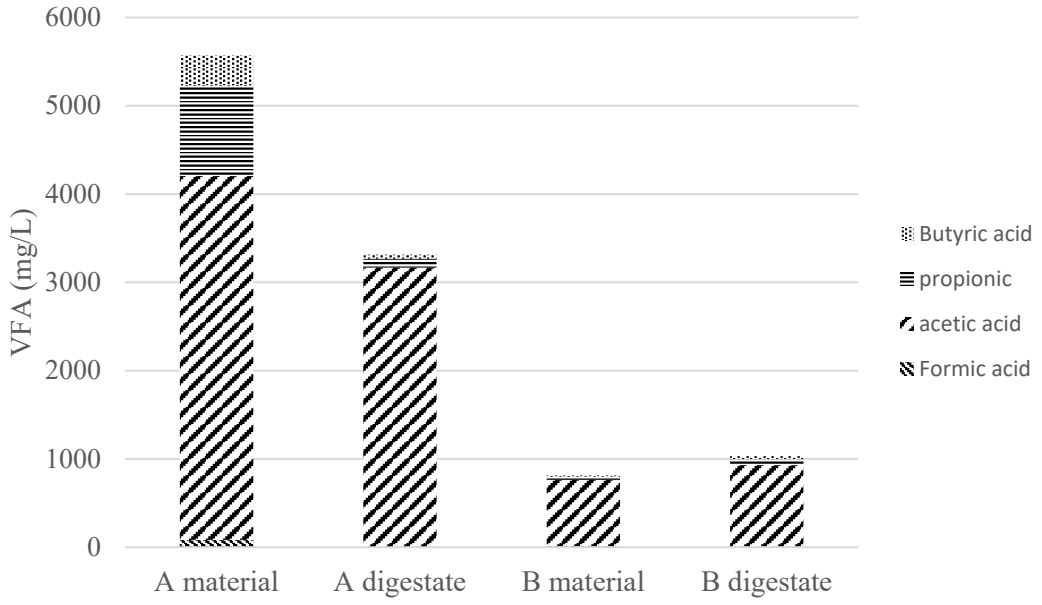

Figure 3 VFA

3.2.3 Impacts of trace element input HRT, and appropriate organic substance load

3.2.3.1 Biogas production per input VS

RUN A, B and C, to which trace elements were added, were higher and stable than biogas produced from RUN B of experiment 2-1 (without the addition of trace elements) as presented in figure 4.

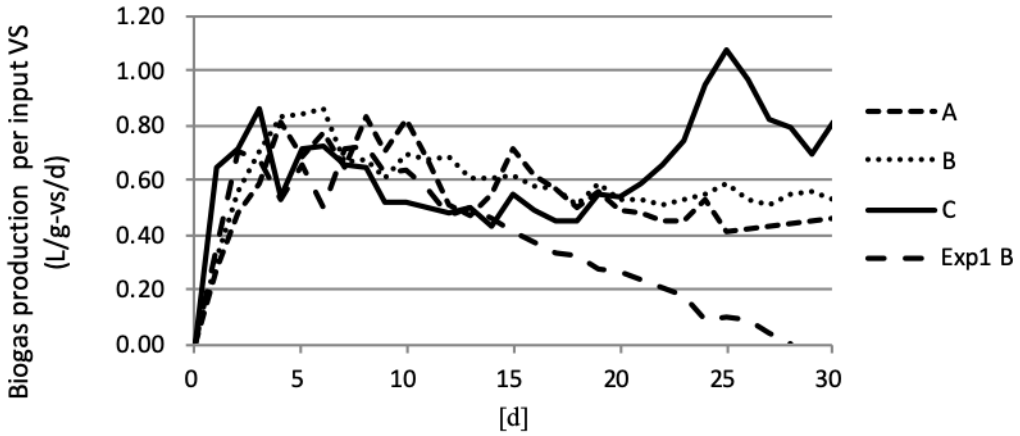

Figure 4 Biogas production per input VS

3.2.3.2 pH

The average value of the digestate pH for each RUN was 7.64 for RUN A, 7.65 for RUN B, 7.78 for RUN C, and no difference was found in the input materials. Also, all were within the optimum pH range.

3.2.3.3 Organic matter decomposition rate

As shown in table 7, RUN B showed the highest organic matter decomposition rate. From this, it was found that HRT around 33 days, organic load 4.26g-VS / L / d is suitable for continuous methane fermentation of bean sprout waste for 10L fermenter.

Table 7 Organic matter decomposition rate

Materials	Organic matter decomposition rate (%)	HRT (d)	Organic loading (g-VS/L/d)
A Bean sprouts 75 g ＋ Return digestate 150 g ＋Trace elements 0.12 g	62.94	44	2.75
B Bean sprouts 100 g ＋Return digestate 200 g ＋Trace elements 0.16g	71.02	33	4.26
C Bean sprouts 150 g ＋Return digestate 300 g ＋Trace elements0.24g	59.06	22	9.02

3.2.3.4 VFA

Organic matter decomposition rate was observed in all RUN. Decrease of 77.07% in RUN A, 78.94% in RUN B and 82.90% in RUN C was observed.

4. CONCLUSION

It was found that after boiling, the sprout produces about 2.4 times the amount of gas than fresh sprout. This is thought to have a positive effect on gas production as it was hydrolyzed the nutrients such as starch, fat and protein stored in seeds by the heat action.

In continuous fermentation, it is recommended to use a mixture of bean sprout and return digest as a raw material than single bean sprout for effective AD process. Additionally, by performing acid fermentation, more biogas is generated, and this due to the action of acid-fermented to decompose the protein (acetic acid) contained in the bean sprout, and in turn this is used as the input material. Therefore, it is thought that not only acid fermentation is appropriate for bean sprouts but also for methane fermentation of other food wastes to enhance their output gas production potential.

Biogas production was sustained by the addition of trace elements, but it was found that the decomposition rate of organic matter was lower when the trace elements amount was too small or too large. In addition, it has become clear that it is necessary to set the HRT (hydraulic retention days) and the organic substance load appropriate for the volume of the fermenter.

Based on the above results and considerations, it is thought that methane fermentation using bean sprouts is possible. In addition, we think that there is need to consider whether it can be applied to food waste including other garbage.

ACKNOWLEDGMENT

We deeply grateful to bean sprout manufacturing plant in Ibaraki prefecture for providing the research material for this experiment.

REFERENCES

APHA, 2005. Standard methods for the examination of water and wastewater.

Noike Tatsuya (2009). Methane fermentation. Technical bulletin publication book, Japanese version.

FAO "Global Food Loses and Food Waste (2011)" http://www.fao.org/food-loss-and-food-waste/en/"

Hedges, L., Lister, C., 2006. Nutritional attributes of legumes (2) Sprouted beans and seeds. Crop Food Res. Confid. Rep. No. 1795 1–30.

Bean sprout producer's association, 2017 (http://www.moyashi.or.jp/nutrition/)

Paritosh, K., Kushwaha, S. K., Yadav, M., Pareek, N., Chawade, A., & Vivekanand, V. (2017). Food waste to energy: an overview of sustainable approaches for food waste management and nutrient recycling. BioMed research international, 2017.

11:30 AM - 12:30 PM (Thu. Sep 5, 2019 11:30 AM - 12:30 PM Poster Place)

[5-1130-P-11] Optimization of Orange-Fleshed Sweet Potato (*Ipomoea batatas* var. Kinerot) Flour Processing for Carotenoid Retention

James Ryan D. Aranzado[1], *Loraine C. Bainto[1], Dennis Marvin O. Santiago[1] (1. Institute of Food Science and Technology, College of Agriculture and Food Science, University of the Philippines Los Baños(Philippines))
Keywords: orange-fleshed sweet potato , response surface methodology, carotenoid retention, flour processing

Orange-fleshed sweet potato (OFSP) is a rich source of carotenoids which upon body intake, is converted to Vitamin A. This raw material is commonly processed into popular food ingredients such as flour, however, the conversion process renders carotenoids susceptible to degradation. To maximize the retention of carotenoids in OFSP, optimized processing conditions must be determined using appropriate tool. In the study, response surface methodology was used to optimize the different process parameters involved in the production of sweet potato flour which will yield the desired level of identified responses related to its carotenoid content. Factor levels of processing conditions including slab thickness (ST), blanching time (Bt), blanching temperature (BT), and drying temperature (DT) were varied to determine their effect on selected responses namely vitamin A value, *L*a*b** color values, and antioxidant activity. The optimized values obtained for the independent variables were 1.55 mm, 1.46 minutes, 100˚ C, and 50˚ C for ST, Bt, BT, and DT, respectively. Sweet potato flour produced under these conditions displayed maximized Vitamin A value (3810.09 IU per gram), *a** (16.04) and *b** (38.42) values, and antioxidant activity (81.19% DPPH inhibition) with minimized *L** value (78.93). These experimental values were within the predicted interval of the responses which proves the applicability of the model.

Poster Session | Postharvest/Food Technology and Process Engineering
[5-1130-P] Postharvest/Food Technology and Process Engineering (5th)
Thu. Sep 5, 2019 11:30 AM - 12:30 PM Poster Place (Entrance Hall)

[5-1130-P-12] Temporal Transition of Spatial Dependence of Weeds in Grassland

*Katsuyuki Tanaka[1], Ayako Oide[1], Hideo Minagawa[1] (1. Kitasato University(Japan))

Keywords: Spatial Modeling, Rumex obtusifolius.L, Grassland

Grasslands with high yield have a large percentage of grass as the main component and a low percentage of weeds and bare land. Especially, Broad−Leaved Bock (*Rumex obtusifolius.*L) has high seed productivity and regeneration ability and is recognized as a highly harmful weed. In order to control the amount, it is necessary to grasp the growing point. In this study, we clarified changes in spatial dependence by examining the spatial modeling by using the time-series distribution survey data from 2015 to 2018.

Temporal Transition of Spatial Dependence of Weeds in Grassland

Katsuyuki Tanaka, Ayako Oide*, Hideo Minagawa

Division of Environmental Bioscience, Kitasato University, Japan

*Corresponding author: oideayak@vmas.kitasato-u.ac.jp

ABSTRACT

Grassland with high yield are characterized as the high composition of grass and low composition of weeds and bare land. Among the weed, especially, Broad−Leaved Bock (*Rumex obtusifolius*.L) has high seed productivity and regeneration ability and is recognized as a highly harmful weed. In order to control the amount of Broad−Leaved Bock, it is necessary to grasp the growing point effectively.

In this study, we clarified the temporal changes in spatial dependence of weeds occurrence by examining the semi-variogram model to multi temporal vegetation survey dataset, observed from 2015 to 2018. As the result, the significant trend of spatial dependence was indicated. From these results, this study proposed the practical and effective strategy for weeding in grassland, that is, preferential spot weeding to large individual or the cluster controlling for the dense crowded area within the range of space dependency

Keywords: Forage corn UAV, Precision Agriculture Remote sensing

1. INTRODUCTION

Grassland with high yield are characterized as the high composition of grass and low composition of weeds and bare land. To rid of these noxious weeds from grassland, it's growing spot is need to be identified first. However, the growing spots of these noxious weeds is not constant, and often appears in completely different place after harvesting. Therefore, the field manager needs to identify these weeds one by one on site to proceed the weeding works, which requires a great deal of labor and time.

There are many studies aimed at efficient weed control, focusing on weed detection(Ayumi Nakatsubo et,al, 2013), but few studies focus on the dynamics of weeds expansion inside grassland.

Therefore, this study aims to clarify the change of spatial dependence in weed occurrence in the grassland using semi-variance analysis, which is a method of spatial statistics. In this study, the *Rumex obtusifolius*.L which has especially high seed productivity and regeneration ability are targeted among several weeds which appears in grassland.

2. MATERIALS AND METHODS

2.1 Study Site

The study site is established in the second field of Field Science Center (FSC) Towada Farm, Kitasato University Faculty of Veterinary Medicine. 50m survey zone was established in the both north-south and north-south directions, respectively, and divided by a 2 m square mesh, providing a total of 2500 small sections.

2.2 Vegetation Survey

The distributing position of *Rumex obtusifolius*.L (hereinafter, referred to as RO) in settled test site was identified using quadrats divided into 1.0m x 1.0m. Table 1 shows the survey dates for each fiscal year. According to the weighted scoring method depends on the diameter (R) of the equivalent circle including the tip of the leaf, each sampling point have been divided into three categories, that is, small ($0 \leqq R < 0.2$ m), middle ($0.2 (R < 0.4$ m), large ($R \geqq 0.4$ m), and is scored 1,3,5 respectively. Then the scores were counted by each section which is consists of 0.5 m square mesh to standardize.

Table 1. Date of survey in each fiscal year

Fiscal year	First harvest	Second harvest	Third harvest
2015	30-April	7-July	3-September
2016	30-April	7-July	9-September
2017	26-April	5-July	15-September
2018	21-May	16-July	17-November

2.3 Semi-Variance Analysis

The spatial dependence was examined by applying semi-variance analysis to the standardized score for each small mesh. Semi-variogram was calculated by using the definition of two-dimensional analysis. After that, a sphere model was applied for the semi-variogram to find three semi-variogram parameters, which is nugget, sill and range. Nugget is the parameter which shows the variation that appears even when the distance between the two becomes zero. The value of the semi-variance (γ) at the point of semi-variance (γ) becomes constant is called the sill. Range is the spatial distance when the semi-variance (γ) becomes constant. The range shows the limit of space dependence. Therefore, in this study, the spatial dependence of RO is indicated as the semi-variance parameter of range.

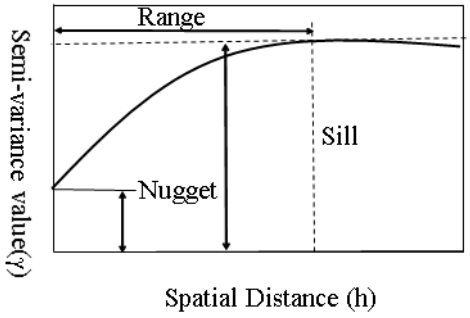

Figure 1. General semi-variogram model

2.4 Statistic Test

In order to check if there is spatial dependence within the range, each section have been categorized to 3 groups by the centered score as shown in Table 2. Then each group were examined by the following two examination methods. Firstly, the significant difference between the mean of expected values of weighted scores within 2 spatial distances segments, that is, 3 m from the center, 3 m to 10 m from the center, was examined by a t-test. Second, when the score of the center in the 3m range is different, the significant difference in the mean value of each expected t-value was examined by the t-test. For examining these two statistical tests, the 500 section sample data was randomly extracted from total 2,500 sections.

Table 2. 3 Groups categorized by the centered score

Group	Centered score
G1	0
G2	1~2
G3	3~12

3. RESULTS AND DISCUSSION

3.1 Distribution Plot

The result of vegetation survey in each fiscal year have been plotted to the map by categorizing to three types by the diameter size. Figure 2 shows an example from the survey result of 3rd crop in 2018.

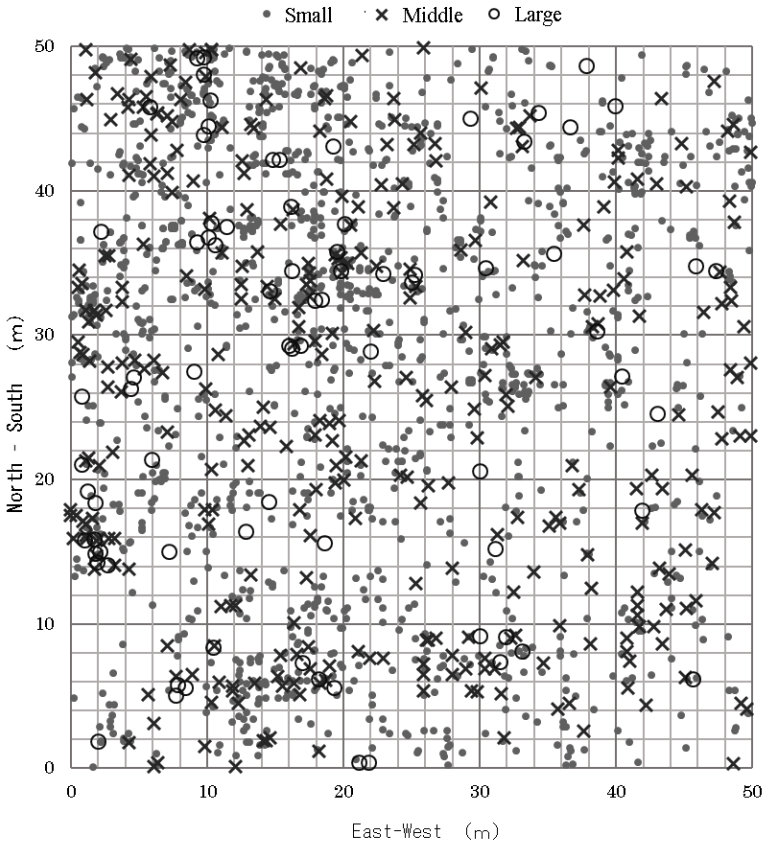

Figure 2. Distribution plot of RO (3rd crop, 2018)

3.2 Temporal Change of Spatial Dependence

Figure 3 shows the temporal change of spatial dependence (range) over the past 4 years. The a, b, c in the figure represent the harvest timing of each year, and the numerical values indicate the range values. Range increased from the first to the second crop, and decreased from the third to the first crop of following year. On the other hand, in the period of second to third crop, the both trend of increase and decrease was observed. The average value of the range from 2015 to 2018 was 3.51 and the standard deviation was 1.11, and it was found that the range was not constant but varied for each grass of each year (coefficient of variation = 0.316)

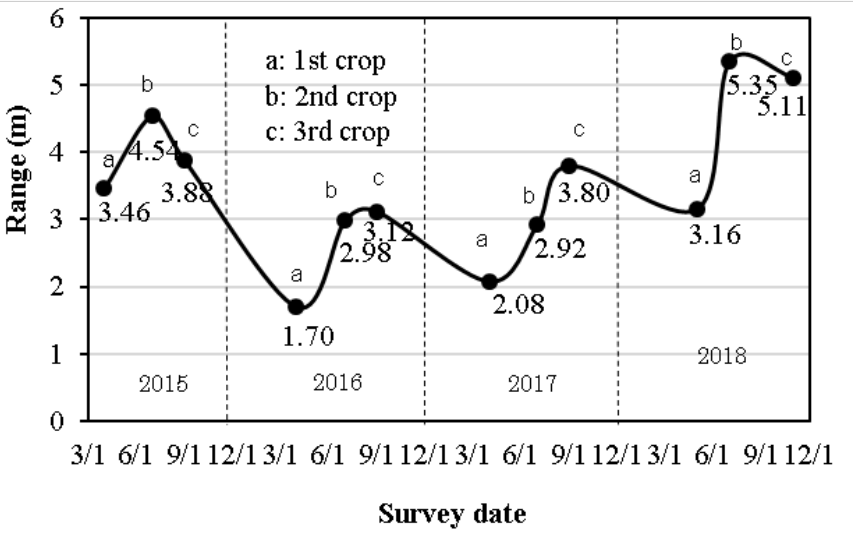

Figure 3. Temporal change of range value from 2015 to 2018

3.3 Statistic Test

Table 3 shows the results of first statistic test. As a result of t-test (significance level of 5%), the expected score of peripheral value showed the significant difference between within and outside the range in all score groups except for G1.

Table 3. Result of t-test (1)

Center	Peripheral range (m)	Mean	Degree of Freedom	t-value	p-value
G1	3	0.392	822	-1.77	0.0775
	10	0.567			
G2	3	0.460	683	4.88	$1.34\ e^{-06}$
	10	0.662			
G3	3	0.682	693	5.87	$6.76e^{-09}$
	10	0.535			

Table 4 shows the results of second statistic test. There were significant differences in the expected values among the central scores within the 3m range. Therefore, in within range, the smaller the central score, the smaller the peripheral score was observed, and vice versa, the larger the central score, the larger the peripheral score was observed. Therefore, the space dependence was confirmed within the range value.

Table 4. Result of t-test (2)

Center	Peripheral range (m)	Mean	Degree of Freedom	t-value	p-value
G1	3	0.392	922	-7.00	$5.05e^{-12}$
G2	10	0.567			
G1	3	0.567	983	-3.75	$1.84\ e^{-04}$
G3	10	0.682			
G2	3	0.392	862	-10.62	$7.51e^{-25}$
G3	10	0.682			

4. CONCLUSION

The temporal changes of the range value showed the increasing trend in the period which is from the first crop to the second crop, and the decreasing trend in the period which is from the third crop to the first crop of the following year regularity. The results of t-test showed that within the range where spatial dependency was observed, the total amount of RO tended to increase in the vicinity of the point where the amount of RO is large.

From these results, this study proposed the practical and effective strategy for weeding RO in grassland, that is, preferential spot weeding to large individual or the cluster controlling for the dense crowded area within the range of space dependency.

REFERENCES

Ayumi Nakatsubo, Katsuyuki Tanaka, Ayumu Mitani, Yoshinori Ishioka, Toshihiro Sugiura, Hideo Minagawa,Hiroshi Shimada(2013) Discrimination of Broad−Leaved Bock (*Rumex obtusifotius* L.) Biomass Using Aerial Remote Sensing in the Grassland, Jpn J Grassl Sci 59 :175−183

Poster Session | Postharvest/Food Technology and Process Engineering
[5-1130-P] Postharvest/Food Technology and Process Engineering (5th)
Thu. Sep 5, 2019 11:30 AM - 12:30 PM Poster Place (Entrance Hall)

[5-1130-P-13] RNA-Seq analysis of the transcriptome and genes expression profile during the browning of Lotus Root (*Nelumbo nucifera*)

*Kanjana Worarad[1], Haruka Norii[1], Yuya Muchizuki[1], Takashi Ishii[2], Keiko Shinohara[3], Takao Miyamoto [4], Eiichi Inoue [1] (1. Ibaraki University(Japan), 2. Ibaraki Agricultural Center, Horticultural Research Institute (Japan), 3. Tokushima Agriculture, Forestry and Fisheries Technology Support Center(Japan), 4. Renkon3kyodai Co.Ltd(Japan))

Keywords: Browning disorder, Metabolic pathways, RNA sequencing, Transcriptomics, Postharvest physiology

Lotus root (*Nelumbo nucifera*) has been widely cultivated in Japan. There is crisp texture, white color and enriched with a source of nutritional components. The consumption/production of fresh-cut lotus root has continuously increased as more consumers demand convenient and ready-to-eat foods. However, it is well known that the processing, storage and transportation of fresh-cut fruits and vegetables promotes a faster physiological deterioration, mainly browning and reduces the value of a product. This study aimed to clarify the functions of unigenes and browning associated metabolic pathway of intact lotus root during long-term storage using RNA-sequencing techniques. Lotus peel from the main cultivar in Ibaraki prefecture 'Kanasumi No.34' after harvest (AH), and unpacked (UP), and packed with water (PW) after storage under 5 ˚C for 6 hr. were collected. Over 200 million short single-end reads were mapped onto the *Nelumbo nucifera* consensus coding sequence set, and differences in the expression profiles between AH, UP, and PW tissues were assessed to identify candidate genes associated with internal browning in a tissue-specific manner. Based on Swiss-Prot, TrEMBL, KEGG mapping pathway and GO ontology databases, genes involved in phenylpropanoid biosynthesis, tyrosine metabolism, and lipid metabolism were significantly upregulated in the UP and PW when compared with AH. The expression levels of several of them will be confirmed using qRT-PCR. Additionally, the gene expression data presented in this study will help elucidate the molecular mechanism of browning development in lotus root at long-term storage. Base on this study, including phenylpropanoid biosynthesis-related genes, lipid-related genes (related to membrane alterations, and fatty acid degradation), for browning development in lotus root is proposed, which may be relevant for future studies towards improving the postharvest life of lotus root.

RNA-Seq analysis of the transcriptome and genes expression profile during the browning of Lotus Root (*Nelumbo nucifera*)

Kanjana Worarad[1] , Haruka Norii [1] , Yuya Muchizuki[1], Takashi Ishii [2], Keiko Shinohara [3], Takao Miyamoto [4] , Eiichi Inoue[1]*

[1] College of Agriculture, Ibaraki University, Japan
[2] Ibaraki Agricultural Center, Horticultural Research Institute, Japan
[3]Tokushima Agriculture, Forestry and Fisheries Technology Support Center, Japan
[4]Renkon3kyodai Co.Ltd, Japan

*Corresponding author: eiichi.inoue.a@vc.ibaraki.ac.jp

ABSTRACT

Lotus root (*Nelumbo nucifera*) has been widely cultivated in Japan. There is crisp texture, white color and enriched with a source of nutritional components. The consumption/production of fresh-cut lotus root has continuously increased as more consumers demand convenient and ready-to-eat foods. However, it is well known that the processing, storage and transportation of fresh-cut fruits and vegetables promotes a faster physiological deterioration, mainly browning and reduces the value of a product. This study aimed to clarify the functions of unigenes and browning associated metabolic pathway of intact lotus root during long-term storage using RNA-sequencing techniques. Lotus peel from main cultivar in Ibaraki prefecture 'Kanasumi No.34' after harvest (AH), and unpacked (UP), and packed with water (PW) after storage under 5 °C for 6 hr. were collected. Over 200 million short single-end reads were mapped onto the *Nelumbo nucifera* consensus coding sequence set, and differences in the expression profiles between AH, UP, and PW tissues were assessed to identify candidate genes associated with internal browning in a tissue-specific manner. Based on Swiss-Prot, TrEMBL, KEGG mapping pathway and GO ontology databases, genes involved in phenylpropanoid biosynthesis, tyrosine metabolism, and lipid metabolism were significantly upregulated in the UP and PW when compared with AH. The expression levels of several of them will be confirmed using qRT-PCR. Additionally, the gene expression data presented in this study will help elucidate the molecular mechanism of browning development in lotus root at long-term storage. Base on this study, including phenylpropanoid biosynthesis related genes, lipid-related genes (related to membrane alterations, and fatty acid degradation), for browning development in lotus root is proposed, which may be relevant for future studies towards improving the postharvest life of lotus root.

Keywords: Browning disorder, Metabolic pathways, RNA sequencing, Transcriptomics, Postharvest physiology

Poster Session | Food Quality

[5-1130-P] Food Quality (5th)

Thu. Sep 5, 2019 11:30 AM - 12:30 PM Poster Place (Entrance Hall)

[5-1130-P-15] Effect of Blending at Different Stages of Winemaking on the Quality of Mixed Fruit Wine

*Claire Solis Zubia[1], Erlinda Ignacio Dizon[1] (1. University of the Philippines Los Banos(Philippines))

11:30 AM - 12:30 PM

[5-1130-P-16] Pest Control of *Tetranychus urticae* by Branched Fatty Acids

*Mai Nagano[1], Akitaka Teshima[1], Toshinari Koda[2], Hiroshi Morita[1] (1. The University of Kitakyushu(Japan), 2. Nissan Chemical corporation(Japan))

11:30 AM - 12:30 PM

[5-1130-P-17] Evaluation of Quality and Structural Properties of Bread Containing Edible Cricket

*Kiko Kuroda[1], Tatsuya Oshima[1], Teppei Imaizumi[1] (1. Gifu Graduate School of Applied Biological Sciences and Faculty of Applied Biological Sciences(Japan))

11:30 AM - 12:30 PM

11:30 AM - 12:30 PM (Thu. Sep 5, 2019 11:30 AM - 12:30 PM Poster Place)

[5-1130-P-15] Effect of Blending at Different Stages of Winemaking on the Quality of Mixed Fruit Wine

*Claire Solis Zubia[1], Erlinda Ignacio Dizon[1] (1. University of the Philippines Los Banos(Philippines))
Keywords: blended fruit wine, carbonation, antioxidant, sensory

From a prior study on determination of best formulation for a multi-flavored fruit wine product, another study was conducted to determine the effect of blending at different stages of winemaking on the quality of mixed fruit wine. Using the optimized formulation of 50% mango, 25% pineapple and 25% passion fruit as components of the blend, three treatments were used: (1) blending of individually prepared mango, pineapple and passion fruit musts before fermentation, (2) blending of individually fermented mango, pineapple and passion fruit wines before aging, and (3) blending of individually aged mango, pineapple and passion fruit wines before bottling. Resulting products were evaluated and compared in terms of their physico-chemical and sensory properties. It was found out that blending of individually prepared mango, pineapple and passion fruit musts prior to fermentation, produced wine with the greatest alcohol content (13.37%) and total phenolic content (378 mg/mL GAE). It also achieved lowest acidity and highest pH level. By employing DPPH radical scavenging assay, the said sample was also observed to exhibit the highest antioxidant activity with 69% inhibition compared to samples from the two other treatments. The obtained wine products were carbonated and bottled and then subjected to sensory evaluation by quality scoring. Sample produced from blending of individually prepared musts scored highest in terms of bitterness, clarity and overall acceptability. It was also perceived to be the least sour and to have the most intense yellow color.

11:30 AM - 12:30 PM (Thu. Sep 5, 2019 11:30 AM - 12:30 PM Poster Place)

[5-1130-P-16] Pest Control of *Tetranychus urticae* by Branched Fatty Acids

*Mai Nagano[1], Akitaka Teshima[1], Toshinari Koda[2], Hiroshi Morita[1] (1. The University of Kitakyushu(Japan), 2. Nissan Chemical corporation(Japan))
Keywords: Pesticide, Spider mite, Fatty acid

Spider mite is one of the pests that infest many crops. Pesticides to prevent spider mites are less effective drugs due to the development of drug resistance by spider mites. Thus, new drugs are needed. The control of indoor environmental pollutants by fatty acid was examined for the purpose of creating a new safer control agent. In the process, it became clear that isopalmitic acid, which is a hyperbranched fatty acid, shows high acaricidal activity against house dust mite. Therefore, we decided to investigate the pest control effect of isopalmitic acid on the spider mites. The sample used isopalmitic acid (isoC16). As test ticks, the black spider mite (*Tetranychus urticae*) was used. It was fed with pea leaves. An acaricidal test was conducted against the spider mite. Pea leaves cut to a size of 2 cm × 2 cm were placed on damp filter paper. Ten female adults of *Tetranychus urticae* were placed on it. The sample was sprayed to 20 mg/cm^2 using a spray. After 24 h, lethality determination was performed under a stereomicroscope. The repellent effect was tested. Pea leaves were prepared in the same manner as the acaricidal test. Half of the leaf pieces were treated with the sample. One half was treated with ion-exchanged water to which 0.01% Tween 80 was added. Ten female adults of *Tetranychus urticae* were placed at the center of each disc. Under a microscope, the number of adult females was determined after 24 h and the number of eggs was determined after 72 h. The sustainability was tested. Pea leaf pieces were sprayed with the sample as in the acaricidal test. Sample Inoculation Five female

adults of *Tetranychus urticae* were inoculated on days 0, 1, 3 and 5 of sample inoculation. After 24 h, the lethality of adult females was determined under a microscope. As a result of the acaricidal test, it was found that when the concentration of isoC16 was 1%, the acaricidal effect was 50% or more. As a result of the repulsion test, no significant difference was observed in the population of the spider mite on the treated area and the non-treated area in isoC16. As a result of the sustainability test, isoC16 showed an adjusted mortality rate of 50% or less at 0-5 days after treatment. For this reason, it became clear that isoC16 is low in sustainability. The corrected mortality rate was less than 50% even after 0 days of sample processing. Therefore, it was shown that in order for isoC16 to exert its pest control effect, it is necessary for the drug to be in direct contact with *Tetranychus urticae.*

11:30 AM - 12:30 PM (Thu. Sep 5, 2019 11:30 AM - 12:30 PM Poster Place)

[5-1130-P-17] Evaluation of Quality and Structural Properties of Bread Containing Edible Cricket

*Kiko Kuroda[1], Tatsuya Oshima[1], Teppei Imaizumi[1] (1. Gifu Graduate School of Applied Biological Sciences and Faculty of Applied Biological Sciences(Japan))

Keywords: edible insect, cricket, bread, micro X-ray CT, structure

In the near future, it is predicated that we will be suffered from food shortage by climate change and population growth. Animal protein is estimated especially shortage, due to need more energy for production than any other nutrients. To overcome this problem, various solutions are suggested, and edible insects are one of the effective approaches. To reduce consumers' discomfort, insect should be mixed with processed food like bread. However, effects of insect addition on food quality have not been sufficiently clarified. In this study, we baked bread containing cricket powder, then evaluated physical and chemical quality.Bread sample ware baked using a bread machine (BK-B67, CCP Co., Ltd). After setting ingredients, the machine performs mixing, kneading, fermentation and baking automatically. In this study, normal bread (control) was made with 250 g of wheat flour and other ingredients (180 mL of water, 10 g of butter, 17 g of sugar, 5 g of salt, 6 g of skim milk and 2.8 g of dried east). For making bread containing cricket, 10 to 50 % of the flour weight was replaced with cricket powder, and named C10, C20, C30, C40 and C50, respectively.First, hardness of each bread was measured by AACC method with a little modification. The bread sample was cut into slices each having 25 mm thickness, then a slice obtained from middle part of the loaf was used. A cross section of the slice was compressed using a creep meter (TPU- 2DL, YAMADEN Co., Ltd) equipped with a disk-shaped plunger (20 mm diameter). The plunger was moved at 1 mm/sec. The compressive force at 25 % of deformation was defined as hardness. Second, structural properties of the bread sample (control, C10, C30) ware evaluated. Loaf volume of each bread was measured with the rapeseed replacement method. Additionally, the internal structure of the bread sample (control, C30) was analyzed by using an X-ray micro CT (SKYSCAN1172, Brucker Co., Ltd). A cube (10 mm) was obtained from central part of each bread. The flaming condition was X-ray power settings of 100 kV, 100 μA, four-flame averaging and a rotation step of 0.7 °. For image processing and analysis, the skyscan software, CT-Analyser was used and microstructural parameters ware obtained.Although the hardness of control was 0.488±0.0749 N, that of the cricket bread indicated higher values (0.565±0.182 - 6.12±1.27 N). The value increased with the amount of the cricket powder. Considering the actual use for bread making, hardness of the cricket bread should be similar to normal bread. Thus, in the subsequent experiments, we focused on the bread made with 30 % or less of cricket powder. Loaf volume of the bread was 1800.8, 1481.6 and 1255.3 mL for control, C10 and C30, respectively. It was implied bread rising was inhibited due to adding cricket powder and it contributed to increase hardness.According to the result of X-ray micro CT, structure separation of the cricket bread (C30)

was small (1363±212 um) while the value of control was large (906±39.6 μ m). In addition, object surface density of control (0.00548 ± 0.0000283 um^{-1}) was higher than C30 (0.00420 ± 0.000769 um^{-1}). These results shown that C30 constructed with larger pores in comparison with control.Aboutstructure thickness, C30 indicated large value (127±81.7 μ m) more than control (94.5±20.6 μ m), although the standard deviation was large. Therefore, C30 has partial thick structure in contrast to control, it agreed with the result of measuring volume or hardness experiments.

Poster Session | Food Safety

[5-1130-P] Food Safety (5th)

Thu. Sep 5, 2019 11:30 AM - 12:30 PM Poster Place (Entrance Hall)

[5-1130-P-18] Key Process Variables Affecting the Formation of Chlormequat Compounds During Baking of Cereal Products

*Adam Ekielski[1] （1. Warsaw University of Life Sciences(Poland)）

11:30 AM - 12:30 PM

[5-1130-P-19] Acaricidal effects of Linear fatty acids against *Tyrophagus putrescentiae*

*Kosuke Matsuoka[1], Toshinari Koda[2], Hiroshi Morita[1] （1. The University of Kitakyushu(Japan), 2. Nissan Chemical Corporation(Japan)）

11:30 AM - 12:30 PM

[5-1130-P-20] Improvement of the Cleanability of Milk Soil on a Highly Smooth Surface of Stainless Steel Tubing

*Ikko Ihara[1], Homi Takato[1], John K Schueller[2], Gen Yoshida[1], Kazutaka Umetsu[3], Hitomi Yamaguchi[2] （1. Kobe University(Japan), 2. University of Florida(United States of America), 3. Obihiro University of Agriculture and Veterinary Medicine(Japan)）

11:30 AM - 12:30 PM

11:30 AM - 12:30 PM (Thu. Sep 5, 2019 11:30 AM - 12:30 PM Poster Place)

[5-1130-P-18] Key Process Variables Affecting the Formation of Chlormequat Compounds During Baking of Cereal Products

*Adam Ekielski[1] (1. Warsaw University of Life Sciences(Poland))

Keywords: chlormequat formation, baking process, cereals

The aim of this work was to examine the effect of temperature and time chlormequat pesticides formation during the bread baking process. The flour and other dough addition used for the study were of the ecological type and verified by us to be free of any quaternary ammonium pesticides. Plant growth regulators are widely used in agricultural food production, mainly in the production of cereals, where they are used to shorten and strengthen the stem. Among the plant growth regulators, chlormequat is by far the most common. Residues of plant growth regulators must be expected in food products due to their extensive use. Permissible level of chlormequat is regulated at 0,02 mg/kg in citrus fruits up to 0,05 mg/kg in nuts. Chlormequat is not considered to pose any risk to human health so long as the residues are below the legal maximum residue levels. However, there is general concern that they may impair human fertility due to the detrimental effects of chlormequat on certain aspects of animal reproduction. Some reports clearly suggest that chlormequat may have serious adverse effects on animal reproduction, even at doses below the Acceptable Daily Intake for humans. Probably due these reasons, chlormequat is not approved for use in the UK. In previous studies, the possibility of formation of chlormequat compounds in brewing malt has been observed, and current studies have confirmed the possibility of formation of chlormequat compounds in the baking of cereal products. The paper presents the results of investigations of chlormequat content in baking products obtained in different production parameters. There are some published papers about mepiquat formation during food thermal processing. Considering the structural similarity chlormequat and mepiquat (Quarternary ammonium nature) and closer resemblance to methylating agents commonly found, it has been hypothesized with high probable that chlormequat formation can take similiar route. Mepiquat is generated under Maillard conditions via transmethylation reactions involving the nucleophile piperidine (formed by cyclisation of free lysine in the presence of reducing sugars) and a methyl donor (trigonelline, choline, glycine). Nevertheless, there is no obvious clue about the possible formation of chlormequat in such conditions. We have studied the effect of processing parameters (temperature and time, dought humidity etc.) and dough components share (type of flour, malt, dried milk), on the quantity of chlormeqat formed during the baking process. The experiment was prepared by using response surface and PCA (Principal Component Analysis) methods. It was found that the key factor determining the amount of the chloroquat compound produced during baking was temperature, which may suggest that the formation of chloromequat is correlated with Maillard's reactions. In our experiment, chlormequat was detected at temperatures above 165 ° C, but when the malt contain in the baking dough was reduced (from 4% to 1%), chlormequat was not observed in bakery products.

11:30 AM - 12:30 PM (Thu. Sep 5, 2019 11:30 AM - 12:30 PM Poster Place)

[5-1130-P-19] Acaricidal effects of Linear fatty acids against *Tyrophagus putrescentiae*

*Kosuke Matsuoka[1], Toshinari Koda[2], Hiroshi Morita[1] （1. The University of Kitakyushu(Japan), 2. Nissan Chemical Corporation(Japan)）
Keywords: Tyrophagus putrescentiae, linear fatty acid , acaricidal test

Tyrophagus putrescentiae is one of the cause of allergies and acariasis because they breed in various places in the room such as food, bedding and carpets. *Tyrophagus putrescentiae* also cause pollution of the food. Previous study has shown that 2-hexyldecanoic acid that is a branched higher fatty acid has an acaricidal effect against *Tyrophagus putrescentiae*. However, it is necessary to search for samples that has higher acaricidal effects. This study focused on linear fatty acids. We performed acaricidal test using hexadecanoic acid that has same number of carbons with 2-hexyldecanoic acid. After that, we performed same test using hexanoic acid, octanoic acid and decanoic acid that have carbons less than hexadecanoic acid. *Tyrophagus putrescentiae* were obtained from Earth Chemical Co., Ltd., and maintained in our laboratory without exposure to any acaricides. Hexanoic acid (C6), octanoic acid (C8), decanoic acid (C10) and hexadecanoic acid (C16) were used to the miticidal test as samples. They were obtained from FUJIFILM Wako Pure Chemical Corporation. Ethanol was used as the dilution solvent. In the acaricidal test, Tyrophagus putrescentiae was placed on a black cloth(45 mm × 45 mm) and samples were sprayed. The black cloth (45 mm×45 mm) was fixed on a petri dish with double sided tape, 30 adult mites were placed on the cloth. After that, samples of linear fatty acids (undiluted solution and 350mM) were dropped on the cloth and feed of insects were placed on the cloth. The petri dish was placed into a plastic container containing saturated saline solution. The temperature and humidity inside the container were kept at 25 ° C and 75 %. After 24 h, mortality was determined by observation using a microscope. As a result, the mortality of hexanoic acid, octanoic acid and decanoic acid were over 70 %. However, the mortality of hexadecenoic acid was 0 %. These results were suggested that the carbon number of linear fatty acids was related to the mortality of mites. As a problem, linear fatty acids have unpleasant smell. It is necessary to discover compounds that have miticidal effect and not smelling. In addition, it is thought that we remove the smell of linear fatty acids by masking agents as a possible solution.

11:30 AM - 12:30 PM (Thu. Sep 5, 2019 11:30 AM - 12:30 PM Poster Place)

[5-1130-P-20] Improvement of the Cleanability of Milk Soil on a Highly Smooth Surface of Stainless Steel Tubing

*Ikko Ihara[1], Homi Takato[1], John K Schueller[2], Gen Yoshida[1], Kazutaka Umetsu[3], Hitomi Yamaguchi[2] （1. Kobe University(Japan), 2. University of Florida(United States of America), 3. Obihiro University of Agriculture and Veterinary Medicine(Japan)）
Keywords: milk soil, surface roughness, cleanability

Stainless steel tubing is widely used for process equipment in milk processing industries. The presence of milk soils on internal surfaces of stainless steel tubing may cause deterioration in quality and food poisoning. Frequent cleaning of the equipment surface is needed to avoid contamination, however, it may cause an increase environmental impacts, linked to the consumption of water, detergent and energy. Surface roughness is one factor affecting the attachment and removal of food soils. EHEDG (European Hygienic Engineering &Design Group) recommends that large areas of food product contact surface should have a surface finish of 0.8 µm R_a. In this work, we studied cleanability of milk soil on a highly-smooth internal surface with 0.01 µm R_a of stainless tubing. The highly-smoothed stainless tube was prepared by magnetic abrasive finishing (MAF), which is an internal finishing process by the application of a magnetic field of permanent magnets. Three different levels of surface roughness of stainless steel tubings were tested to

evaluate the cleanability of milk soil. On the deposition test, whole milk at 44˚ C was circulated in a tested loops connected with the tested stainless tubings. After the deposition process, deionized water at different temperatures was flushed into the tested loops to clean milk deposition on the internal surface of stainless steel tubings. To evaluate the cleanability of the milk deposition in the tubings, we measured amounts of milk residues and residual proteins on the internal surface of the tubings. The data showed that the smoother surface had a tendency to improve the cleanability of milk soil and milk protein at 45˚ C of cleaning solution. When the temperature is raised from 20 to 45˚ C, the cleanability of milk soil was improved. However, when the temperature was raised from 45 to 50˚ C, almost no change was observed. At 35, 45, and 50˚ C, smoothing of the surface showed a tendency to improve detachment of milk soil. The cleaning solution temperature affected the removal of milk soil. The relationship between surface roughness and detachment of milk soil was clearly observed, when the cleaning solution temperature was at 45˚ C.

Poster Session | Others (including the category of JSAM and SASJ)

[5-1130-P] Other Categories (5th)

Thu. Sep 5, 2019 11:30 AM - 12:30 PM Poster Place (Entrance Hall)

[5-1130-P-21] Screening and Identification of Endophytic Bacteria from Thai Organic Rice for Plant Growth Promotion

*Somkid Deejing[1], Witchayaporn Pawong[1] (1. Program in biotechnology, Faculty of Science, Maejo University, Sansai, Chiang Mai(Thailand))

11:30 AM - 12:30 PM

[5-1130-P-22] Data Extraction for Pig Weight Prediction Model

*Khin Dagon Win[1], Kikuhito Kawasue[1], Hsu Lai Wai[1], Kumiko Yoshida[2] (1. University of Miyazaki(Japan), 2. KOYO Plant Service(Japan))

11:30 AM - 12:30 PM

[5-1130-P-23] Power Tiller's Wheel Structure and its Oscillatory Effects on Subsoiling Operation

*Oyetayo Olukorede Oyebode[1], Koichi Shoji[1] (1. Graduate School of Agricultural Science, Kobe University(Japan))

11:30 AM - 12:30 PM

[5-1130-P-24] Proposal of temperature control technology in pot cultivation for the citrus fruits

*Ryuta IBUKI[1], Yoshimichi Yamashita[2], Sachie Horii[2], Norihiro Hoshi[2], Madoka Chiba[1] (1. Miyagi University(Japan), 2. National Agriculture and Food Research Organization(Japan))

11:30 AM - 12:30 PM

[5-1130-P-25] Investigation by Driving Simulation of Tractor Overturning Accidents Caused by Steering Instability

*Masahisa Watanabe[1], Kenshi Sakai[1] (1. Tokyo University of Agriculture and Technology(Japan))

11:30 AM - 12:30 PM

[5-1130-P-26] Classification of Salinity Damaged Spring Potato (Solanum tuberosum) using Hyperspectral Imagery based on Decision Tree Classifier

*KyungSuk Kang[1], Sae Rom Jun[1], Si Hyeong Jang[1], Jun Woo Park[1], Hye Young Song[1], Ye Seong Kang[1], Chan Seok Ryu[1], Su Hwan Lee[2] (1. GNU(Korea), 2. RDA(Korea))

11:30 AM - 12:30 PM

[5-1130-P-27] Classification for Fire Blight Disease Infection Area using Vegetation Index and Background Segmentation based on Multispectral Image

*Jun-woo Park[1], Chan-seok Ryu[1], Ye-seong Kang[1], Sae-Rom Jean[1], Si-Hyeong Jang[1], Hye-Young Song[1], Kyung-Suk Kang[1] (1. GNU(Korea))

11:30 AM - 12:30 PM

[5-1130-P-28] The Static Load Test for Tractor Attached Three-Point Hitch Type Dynamometerd

*Hyo-Geol Kim[1], Sung-Bo Shim[2], Yeon-Soo Kim[1], Young-Joo Kim[1], Sang-Dae Lee[1] (1. Korea Institute of Industrial Technology(Korea), 2. Gyeongsang National University(Korea))

11:30 AM - 12:30 PM

[5-1130-P-29] **Isolation and Identification of Acetic Acid Bacteria from Philippine Fermented Rice Cake Batters by 16S rRNA Gene Sequence Analysis**

Audrey Mae Villamin Orillaza[1], Honey Bhabes R Iñigo[1], *Baby Richard Ragudo Navarro[1]
（1. Institute of Food Science and Technology, College of Agriculture and Food Science, University of the Philippines Los Baños(Philippines)）

11:30 AM - 12:30 PM

[5-1130-P-30] **Estimation of Greenhouse Gas Emissions from Poultry Farming Systems for a Broiler Meat Production and an Egg Production in Japan using a Life Cycle Assessment**

*Tatsuo Hishinuma[1], Tetsuya Hoshino[1], Atsuo Ikeguchi[1], （1.Utsunomiya Univ.(Japan)）

11:30 AM - 12:30 PM

Poster Session | Others (including the category of JSAM and SASJ)

[5-1130-P] Other Categories (5th)

Thu. Sep 5, 2019 11:30 AM - 12:30 PM Poster Place (Entrance Hall)

[5-1130-P-21] Screening and Identification of Endophytic Bacteria from Thai Organic Rice for Plant Growth Promotion

*Somkid Deejing[1], Witchayaporn Pawong[1] (1. Program in biotechnology, Faculty of Science, Maejo University, Sansai, Chiang Mai(Thailand))

Keywords: Endophytic bacteria, Indole acetic acid, Organic agriculture, Bacterial characteristics

Endophytic bacteria are able to colonize in plant tissues without causing harmfulness subsequently, sharing and exchanging beneficial metabolites to plant hosts. Plant growth can be promoted by these bacteria via their phytohormones i.e. indole acetic acid (IAA) and/or enhancement of nutrient availability. IAA is associated with plant cell division, cell elongation and lateral root formation. The population of endophytic bacteria are more diverse in crops planted following to organic practice. Thus, organic crops are interesting sources for endophytic isolation for further agricultural application as plant growth promoter. The aims of this present work were to isolate and identify promising endophytic bacteria from various part of rice with respect to their IAA production. Rice tissue samples were collected from five-year-old organic farm in Chiang Mai, Thailand. Bacteria were cultured on Plate count agar (PCA), Pikovskaya ' s medium (PVK), Tryptic soy agar (TSA) and International Streptomyces project (ISP_2). The results showed that 53 bacterial isolates were obtained and further screened for IAA production in medium containing 0.2 % tryptophan. The IAA producing bacteria were RRSPCA and LRSPCA2 which produced at 20.93 and 7.12 mg/L, respectively. They were identified as *Pseudomonas* sp. and *Chryseobacterium kwangyangense,* respectively, based on 16s rRNA gene sequencing at 100 % similarity. These endophytic bacteria in this study could be applied for enhancing a plant growth, resulted a plant yield. Moreover, their bioactive compounds could be used *for* biotechnological applications. Therefore, the endophytic bacteria will contribute to organic agriculture for more environmentally sustainable in the future.

Screening and Identification of Endophytic Bacteria from Thai Organic Rice for Plant Growth Promotion

Somkid Deejing[1*] and Witchayaporn Pawong[2]
[1,2] Program in Biotechnology, Faculty of Science, Maejo University, Thailand
*Corresponding author: kittydeejing@gmail.com, somkid_d@mju.ac.th

ABSTRACT

Endophytic bacteria are able to colonize in plant tissues without causing harmfulness subsequently, sharing and exchanging beneficial metabolites to plant hosts. Plant growth can be promoted by these bacteria via their phytohormones i.e. indole acetic acid (IAA) and/or enhancement of nutrient availability. IAA is associated with plant cell division, cell elongation and lateral root formation. The population of endophytic bacteria are more diverse in crops planted following to organic practice. Thus, organic crops are interesting sources for endophytic isolation for further agricultural application as plant growth promoter. The aims of this present work were to isolate and identify promising endophytic bacteria from various part of rice with respect to their IAA production. Rice tissue samples were collected from five-year-old organic farm in Chiang Mai, Thailand. Bacteria were cultured on Plate count agar (PCA), Pikovskaya 's medium (PVK), Tryptic soy agar (TSA) and International Streptomyces project (ISP_2). The results showed that 53 bacterial isolates were obtained and further screened for IAA production in medium containing 0.2 % tryptophan. The IAA producing bacteria were RRSPCA and LRSPCA2 which produced at 20.93 and 7.12 mg/L, respectively. They were identified as *Pseudomonas* sp. and *Chryseobacterium kwangyangense,* respectively, based on 16s rRNA gene sequencing at 100 % similarity. These endophytic bacteria in this study could be applied for enhancing a plant growth, resulted a plant yield. Moreover, their bioactive compounds could be used for biotechnological applications. Therefore, the endophytic bacteria will contribute to organic agriculture for more environmentally sustainable in the future.

Keywords: Endophytic bacteria, Indole acetic acid, Organic agriculture, Bacterial characteristics

1. INTRODUCTION

Thailand is one of major rice producer and exporter in the world. In 2011, export value of Thai Rice was 210,527 million baht (Nara et al., 2014). Organic rice derived from organic farming which uses fertilizers from organic substances and pesticides made from natural ingredients instead of chemical pesticides and chemical fertilizers. Therefore, organic rice is better for our health and environment safety make sustainable agriculture. Increasing environmental damage and human population pressure are two important problems indicating that global food production may soon become insufficient to feed all of the world's people (Etesami et al., 2015). Climate change, increases in temperatures, extreme temperatures, droughts, and rainfall intensity are abiotic stress that effected on rice production. The organic farming management system which application of endophytic bacteria offer a promising alternative and reduce health and environmental problems. Endophytic bacteria are bacteria that live within various parts of plants such as seeds, roots, stems, leaves result in benefit of their host plants by increasing nutrient uptake, producing biologically active phytohormones and suppressing pathogens by production of antibiotics, siderophores, and fungal cell wall-lysing enzymes including enhancement of the tolerance respond to abiotic stresses (Hameeda et al., 2008). Among these, indole acetic acid (IAA) is one of the most vital hormones which involed in lateral and adventitious root formation (Idris et al., 2007), increasing shoot growth, tillering and root elongation (Yang et al., 1993). IAA producing bacteria play a major role as plant growth promoter that were used as biofertilizer for enhancement of rice growth and yield (Etesami et al., 2015). The commonly found bacterial endophytic genera are *Pseudomonas, Bacillus, Burkholderia, Stenotrophomonas, Micrococcus, Pantoea* and *Microbacterium* etc. (Romero et al. 2014). Phetcharat and Duangpang (2012) found that the percentage of endophytic of IAA producing bacteria, ACC deaminase, and siderophore higher than rhizosphere bacteria (Prakamhan et al., 2009). Ji et al. (2014) isolated and characterized plant growth promoting endophytic bacteria from Korean rice. They obtained 576 isolates endophytic bacteria from the leaves, stems, and roots of 10 rice cultivars and identified

through 16S rDNA sequence analysis belong to *Penibacillus* sp., *Microbacterium* sp., *Bacillus* sp., and *Klebsiella* sp. Ten isolates have shown higher IAA producing activity, 6 isolates with high siderophore producing activity and 4 isolates high phosphate-solubilizing activity. Population density of endophytic diazotrophic bacteria (EDB) was highest in the rice landrace root tissues at nursery stage. Indole-3-acetic acid (IAA) production (0.85–16.66 μg/mL) was found in 21 strains tested. More than 80 % (18 isolates) of the isolates solubilized phosphate, while only 28.57 % (six isolates) of selected strains produced siderophore (Rangjaroen et al., 2014). Blanco and Lugtenberg (2014) reported the biotechnological applications of endophytic bacteria can promote plant growth, for example by the production of hormones or by making nutrients (such as nitrogen, phosphate and ferric ions) available to the plant. In addition, endophytes can also promote plant growth indirectly, for example by suppression of plant diseases, by inactivating environmental pollutants, and by alleviating stresses of the plant caused by excess of the hormone ethylene, by heavy metals, by draught and by salinated soil. Some endophytic bacteria can produce nanoparticles which have numerous applications. They concluded that endophytes are much more efficient in their application of active compounds and their metabolite.

The organic farming increases the crop productivity while sustaining the ecosystems. Health is also a consideration in organic farming practices. It is conceivable that the application of endophytic bacteria could be an advantage since they are present in a much more protected environment than rhizosphere bacteria and likely to be less vulnerable to changing environmental conditions. Therefore, the objectives of this study were to isolate, screening and identify of IAA producing endophytic bacteria from Thai organic red jasmine rice tissues in Sansai, Chiang Mai, Thailand for application to organic rice production system and help plant under climage change, including biotechnological application in the future.

2. MATERIALS AND METHODS

2.1 Isolation of endophytic bacteria from organic red jasmine rice tissue

Roots, stems, and leaves of rice were collected during growth stage from organic red jasmin rice farming in Sansai, Chiang Mai, Thailand. Tissue of rice samples were dipped in 70% ethanol for 2 min, then in 4% sodium hypochlorite for 15 min and finally rinsed eight times with sterile distilled water. After that, the sterilized pieces were put onto Plate count agar (PCA); (g/L) tryptone (5), yeast exratct (2.5), glucose (1.0), agar (15) and distilled water (1 L); Pikovskaya 's medium (PVK); (g/L) glucose (10), $Ca_3(PO_4)_2$ (5), $(NH_4)_2SO_4$ (0.5), KCl (0.2), $MgSO_4.7H_2O$ (0.1), agar (15) distilled water (1 L); Tryptic soy agar (TSA); (g/L) tryptone (15), soytone (5), NaCl (5), agar (15) and distilled water (1 L), and International Streptomyces project (ISP2); (g/L) malt extract (10), yeast extract (4), glucose (4) agar (15) and distilled water (1 L). Culture medium plate were incubated at 37 ºC for 24-48 h., while on ISP2 medium was incubated at 37 ºC for 7-14 days. Surface sterility test was performed for each of sample to ensure the elimination of surface microorganism. The soaking water from sterilized rice tissues were plated on Nutrient agar (NA) (g/L); beef extract (3), peptone (5), agar (15) and distilled water (1 L) by using pour plate technique. Endophytic bacterial strains growing on selective media plates were isolated, purified and were preserved on agar slants for further studies.

2.2 Preliminary screening of IAA producing endophytic bacteria

Preliminary screening of IAA production test was evaluated by growing the isolates bacteria in tryptone containing (g/L) tryptone (5) and distilled water (1 L) and then incubated by shaking 130 rpm at ambient temperature for 48 h. After incubation, Kovac's reagent was added to culture medium. Development of cherry red colour at the top layer in the form of ring indicated the positive test while its absence indicated the negative test. The isolates bacteria that positive test in primary screening test were selected for further study.

2.3 Quantitative analysis of IAA production of endophytic bacteria

Production of IAA was measured the quantitative analysis by culturing bacteria in Nutrient broth (NB) containing (g/L); beef extract (3), peptone (5) and distilled water (1 L) supplemented with 0.2 % L-tryptophan as precursor of IAA and then incubated 130 rpm on shaker at ambient temperature for 48 h. After incubation, the culture was centrifuged at 10,000 rpm for 20 min to collect the supernatant. Then, Salkowski coloring reagent (1 ml of 0.5 M $FeCl_3$ in 49 ml of 35% perchloric acid ($HClO_4$) and the supernatant were mixed and left in the dark for 25 min. After the reaction, the absorbance of the

mixtures was estimated at 530 nm. The IAA concentration in the culture was estimated based on the IAA standard curve. Endophytic bacteria which high IAA production was selected for identification.

2.4 Identification of selected endophytic bacteria

The selected bacteria was identified by studying the cultural, morphological and biochemical characteristics. Cultural characteristics of selected endophytic bacteria was streaked on Nutrient agar plates and then observed colonies such as shape, elevation, margin, colour and pigment after incubation at 37 °C for 24-48 h. Morphological characteristics was examined by Gram' s staining and observed under bright field microscope. Biochemical and physiological characteristics of endophytic bacteria were studied. Catalase test was done by adding 2% hydrogen peroxide solution to the culture on a slide. The release of free oxygen bubbles indicated a positive result. Oxidase test was determined by dipping the filter paper strip in 1% N, N, N.N-tetramethylene p-phenylene diamine dihydrochloride and then transferred the endophytic bacteria to filter paper strip. In a positive reaction, the reagent was oxidized to give intense blue violet colour within 5 min. Carbohydrate utilization test was also examined in culture broth with bromocresol purple as indicator and supplemented with different sources of carbohydrate (glucose, fructose, galactose, lactose, maltose, mannitol, xylitol and sucrose). Pure culture of selected endophytic bacteria was inoculated and incubated at 37 °C for 24 h. A positive test was represented by development of yellow colour due to acid production and bubbles trapped within the durham tube indicated the gas production

The identification of selected IAA producing endophytic bacteria was examined by using 16S rRNA gene sequencing. Amplification of the 16S rRNA gene was performed with 27F (5′-AGAGTTTGATCMTGGCTCAG-3′) universal primers. Sequencing of bases was undertaken by First BASE Laboratories, Malaysia. The sequence data were compared with NCBI GenBank and the similarities were determined by the Basic Local Alignment Search Tool (BLAST) software algorithm.

3. RESULTS AND DISCUSSION

3.1 Isolation of endophytic bacteria from organic red jasmine rice tissue

Endophytic bacteria were isolated from tissue of five-year-old organic red jasmine rice in Chiang Mai, Thailand on PCA, PVK, TSA and ISP2 medium. Total fifty-three isolates of endophytic bacteria of organic rice (isolates); roots (32); stems (9), and leaves (12) were obtained (Table 1). The results in this study found that endophytic bacteria was highest in roots. Our results are in agreement with Mano et al. (2008) found that the most number of endophytic bacteria was greatest in the rice roots. Ma et al. (2013) observed that the bacterial diversity in roots reed *Phragmites australis* was significantly higher than in the leaves. Petcharat and Duangpang (2012) isolated endophytic bacteria from various rice tissue of different three types of rice farm; 1 year, 3 years organic rice, and conventional rice farms in Thailand. They found that seventy-one isolates of endophytic bacteria were screened using PDA and TSA medium. The majority of strains isolated from root tissues were totally 26 isolates, exclusively collected from 3 years organic rice farm. Previous researches have reported that endophytic bacteria from root and stem of rice tissues of diverse varieties grown in different soil types (Stoltzfus et al., 1997). Huang (1986) described that endophytic have been considered to originate from the outside environment and enter the plant through stomata, lenticles, wounds, areas of emergence of lateral roots and germinating radicles. The capability of endophytic bacteria ascending migration from root to leaf of the rice seedlings was probably due to its ability in producing the plant-cell wall degrading enzymes endopolygalacturonase and endoglucanase. These enzymes play an important role in promoting colonization and ascending migration of endophytes from roots to leaves of the plant hosts. (Tharek et al., 2011). The root exudates produced by rice plants promote the interaction between endophytic bacteria and root tissues (Jiménez et al., 2003).

3.2 Screening of IAA producing endophytic bacteria

In this study, 53 isolates endophytic bacteria were screened among which two isolates showed positive test. Among all endophytic bacteria isolates, the isolates RRSPCA from roots and LRSPCA2 from leaves of organic red jasmine rice showed red color reaction with Kovac' s reagent indicating their ability to produce IAA. These isolates were selected for further investigated the quantitative of IAA production.

Table 1 Isolation of endophytic bacteria from organic rice on various kinds of culture media

Culture media	Number of endophytic bacteria (isolates)			
	Roots	Stems	Leaves	Total
PCA	5	1	5	11
PVK	7	1	0	8
TSA	11	4	6	21
ISP2	9	3	1	13
Total	32	9	12	53

3.3 Quantitative analysis of IAA production of endophytic bacteria

The result of quantitative analysis of IAA production of isolates RRSPCA and LRSPCA2 were 20.93 and 7.12 mg/L, respectively (Table 2). Among the endophytic bacteria, active isolates RRSPCA and LRSPCA2 showed positive reactions to Salkowski 's reagent with a pinkish or a deep red coloration (Fett et al. 1987). These positive reactions of test bacteria indicate their capacity of metabolizing L-tryptophane to IAA or some analogous compounds of IAA. Bacteria RRSPCA and LRSPCA2 could produce IAA 20.93 and 7.12 mg/L, respectively. Petcharat and Duangpang (2012) reported that endophytic bacteria *Bacillus* sp. which isolated from Thai organic rice produced IAA 14.58 µg/ml. Bandara et al. (2006) found that endophytic bacteria isolated from rice also produced IAA with variable quantity. Moreover, Hung et al. (2004) found that endophytic bacteria from soybean produced IAA over than 25 Pg/ml and endophytic bacteria R7 from rice could produce IAA 120.55 ppm (Sev et al., 2016). Therefore, in the present study bacteria RRSPCA and LRSPCA2 were further identified.

Table 2 IAA production of endophytic bacteria isolated from organic rice

Bacterial code	Source	IAA content (mg/L)
RRSPCA	Rice roots	20.93
LRSPCA2	Rice leaves	7.12

3.4 Identification of selected endophytic bacteria

Selected isolates endophytic bacteria RRSPCA and LRSPCA2 were examined cultural, morphological and biochemical characteristics. It was found that bacterial RRSPA had creamy white colony, circular, entire, flat colony and LRSPCA2 had yellow pigmented colony, circular, entire and raise colony on Nutrient agar. Bacteria RRSPCA and LRSPCA2 colonies were shown in Figure 1A and 1B, respectively. Both selected bacteria RRSPCA and LRSPCA2 were gram-negative, rods shape and appeared in single cell. Catalase and oxidase of both isolates were positive. The types of carbohydrates which are utilized by these bacteria can serve as a diagnostic tool for the identification of bacteria. Isolate RRSPCA fermented only glucose whereas LRSPCA2 not fermented various kinds of sugar in this test. The characteristic of those bacterium is given in Table 3.

In order to identify RRSPCA and LRSPCA2, these isolates were subjected to 16S rRNA amplification and sequencing. The sequence analyses revealed that two selected bacteria belong to *Pseudomonas* sp. and *Chryseobacterium kwangyangense* at 100 % similarity, respectively. The similarities with the closest type strain are shown in Table 4. Barrios et al. (2018) studied bacterial microbiota of rice roots by 16S rRNA-based taxonomic profiling of endophytic and rhizospheric diversity. They found that IAA producing endophytic bacteria from rice root were *Bacillus* sp., *Rhizobium* sp., *Delftia* sp., *Serratia* sp., *Aeromonas* sp. and *Pseudomonas* sp. *Pseudomonas* sp. has been reported to be among the most abundant members of the rice endophytic bacteria (Mano et al., 2008; Sessitsch et al., 2012.).

There are many application and benefit of endophytic bacteria such as promote plant and act as biocontrol agents producing a range of natural products that could be harnessed for potential use in medicine, agriculture or industry including biotechnological applications. Devi et al. (2017) found that endophytic *Pseudomonas aeruginosa* isolated from leaves of *Achyranthes aspera* had plant growth

Table 3 Characteristics of selected endophytic bacteria RRSPCA and LRSPCA2

Bacterial code	Cultural characteristic	Morpholo-gical characteristic	Biochemical and physiological characteristics									
			Cata-lase	Oxi-dase	F	S	M	G	Ga	X	L	M
RRSPCA	CC: creamy white CF: circular CM: entire CE: flat	Gram negative Rods, single	+	+	-	-	-	+	-	-	-	-
LRSPCA2	CC: yellow CF: circular CM: entire CE: raised	Gram negative Rods, single	+	+	-	-	-	-	-	-	-	-

Remark: CC = colony color, CF = colony form, CM = colony margin, CE = colony elevation, F = fructose, S = sucrose, M = maltose, G = glucose, Ga = galactose, X = xylitol, L = lactose, M = manitol

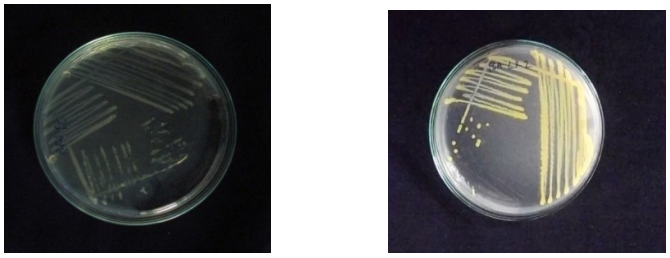

A) RRSPCA B) LRSPCA2

Figure 1 Colony of selected IAA producing endophytic bacteria on Nutrient agar for 24 h.

Table 4 Identification of selected endophytic bacteria by16S rRNA genes sequencing

Bacterial code	Bacteria	Accession number	Query Cover	Identities
RRSPCA	*Pseudomonas* sp.	abKU312801.1	100%	801/801 (100%)
LRSPCA2	*Chryseobacterium kwangyangense*	abEU169201.1	100%	800/800 (100%)

stimulating attributes including siderophore and indole acetic acid release, inorganic phosphate solubilization, along with nitrogenase, ammonification, and protease activities. It also exhibited anti-antifungal property against *Rhizoctonia solani*. The enzyme 1-aminocyclopropane-1-carboxylate (ACC) deaminase expressing endophyte *Pseudomonas* sp. enhances NaCl stress tolerance by reducing stress-related ethylene production, resulting in improved growth, photosynthetic performance, and ionic balance in tomato plants (Win et al., 2018). Susilowatia et al. (2018) found that IAA producing bacteria *Pseudomonas fragi, Bacillus cereus* and *Rhizobium* can promote plant height, while *Bacillus aerius, Pseudomonas fragi* and *Bacillus cereus* promote dry weight of rice grain, and *Bacillus amyloliquenfaciens* promote roots dry weight. *Pseudomonas putida* was found to promote root and shoot growth and protect the plants against the phytotoxic effects of phenanthrene which environmental contaminants such as polycyclic aromatic hydrocarbons (Khan et al., 2014). Joshi et al. (2018) reported endophytic bacteria *Enterobacter* sp., *Pseudomonas* sp. and *Azospirillium* sp. that isolated from *Ocimum sanctum* and *Aloe vera* roots could produced enzymes urease, pectinase, cellulase, catalase, lipase, casienase, gelatinase and chitinase. In recent years, co-inoculation of

endophytic microorganisms are playing key role for improving nutrient availability in sustainable agriculture production system. Jeong et al. (2016) suggested that the combination of several plant growth promoting bacteria could be more effective than individual strains as a horticultural product. Lally et al. (2017) reported application of endophytic *Pseudomonas fluorescens* and a bacterial consortium to *Brassica napus* can increase plant height and biomass under greenhouse and field conditions. They demonstrated that significant increases in crop height, stem/leaf, and pod biomass, particularly, in the case of the consortium inoculated treatment. Pragash et al. (2009) reported that *Chryseobacterium aquaticum* produces an antifungal protease, plant growth promoting enzymes such as ACC deaminase and phosphatase. Bacteria could be applied for plant growth promotion and biocontrol of fungal diseases. The synergistic interaction between ACC deaminase and both plant and IAA producing bacteria promoted plant growth, protect plants against flooding, drought, salt, flower wilting, metals, organic contaminants, and both bacterial and fungal pathogens (Glick, 2014). Radzki et al. (2013) reported that siderophores from strain *Chryseobacterium* sp. C138 are effective in supplying Fe to iron-starved tomato plants by the roots. Naik et al. (2009) found that colonization rates of endophytic microorganisms from rice *Oryza sativa* tissues were 40.3% in roots and 25.83% in leaves during winter season, 20.15% in roots and 8.66% in leaves during summer season. *Chaetomium globosum*, *P. chrysogenum* and *Streptomyces* sp. are suitable candidates for extraction biologically active compounds. Moreover, endophytic microorganisms have antagonistic properties against fungal pathogens. Domenech et al. (2006) reported the combination of bacteria *Bacillus subtilis* (a growth-promoting agent), *B. amyloliquefaciens* (an inducer of systemic resistance) and chitosan, *B. licheniformis*, *Pseudomonas fluorescens* and *Chryseobacterium balustinum* with BioControl LS213. They found that bacteria would have a synergistic effect on growth promotion and biocontrol on tomato and pepper against Fusarium wilt and Rhizoctonia damping off.

The combination of microorganisms gives better results probably due to the different mechanisms used. The selected IAA producing endophytic bacteria in this study might be use as environmentally friendly biofertilizers in microbial consortium and applied to organic agriculture for sustainable agriculture similar to previous report. There are many opinions on what an ideal agricultural system. Many would also agree that organic agriculture system should be maintained and improved human health, be economically and spiritually beneficial to both producers and consumers, actively preserve and protect the environment, be self-contained and regenerative, and produce enough food for world's population (Higa, 1991).

4. CONCLUSION

Fifty-three isolates of IAA endophytic bacteria were obtained. Two endophytic bacteria RRSPCA and LRSPCA2 produced IAA production in medium containing 0.2 % tryptophan at 20.93 and 7.12 mg/L, respectively. These endophytic bacteria identified as *Pseudomonas* sp. and *Chryseobacterium kwangyangense,* respectively, based on 16s rRNA gene sequencing. The results can be used selected IAA producing endophytic bacteria for production some bioactive compound which high value added of biotechnologically including has potentially lead to making organic farming more environmentally sustainable in the future.

ACKNOWLEDGMENT

Authors are grateful to Office of the National Research Council of Thailand (The Thailand Research, and the facility provided from Program in Biotechnology, Faculty of Science, Maejo University.

REFERENCES

Bandara, W.M.M., G. Seneviratne, and S.A. Kulasooriya. 2006. Interactions among endophytic bacteria and fungi: effectd and potentials. *Journal of Bioscience*, 31: 645-650.

Barrios, F.M., F. Gionechetti, A. Pallavicini, E. Marys, and V. Venturi. 2018. Bacterial microbiota of rice roots: 16S-based taxonomic profiling of endophytic and rhizospheric diversity, endophytes isolation and simplified endophytic community. *Microorganisms,* 6(1): 14.

Blanco, J.M. and B.J. Lugtenberg. 2014. Biotechnological applications of bacterial endophytes. *Current Biotechnology*, 3: 60-75.

Devi, K.A., G. Pandey, A.K.S. Rawat, G.D. Sharma, and P. Pandey. 2017. The endophytic symbiont *Pseudomonas aeruginosa* stimulates the antioxidant activity and growth of *Achyranthes aspera* L. *Frontiers in Microbiology*, 8: 1897.

Domenech, J., M.S. Reddy, J.W. Kloepper, B. Ramos and J.G. Manero. 2006. Combined application of the biological product LS213 with *Bacillus, Pseudomonas* or *Chryseobacterium* for growth promotion and biological control of soil-borne diseases in pepper and tomato. *Biological Control*, 51: 245–258.

Etesami, H., H.A. Alikhani, and H.M. Hosseini. 2015. Indole-3-acetic acid (IAA) production trait, a useful screening to select endophytic and rhizosphere competent bacteria for rice growth promoting agents. *MethodsX*, 2: 72–78.

Fett, W.F., S.F. Osman, and M.F. Dunn. 1987. Auxin production by plant-pathogenic Pseudomonads *Applied and Environmental Microbiology*, 53: 1839-1845.

Glick, B.R. 2014. Bacteria with ACC deaminase can promote plant growth and help to feed the world. *Microbiological Research*, 169(1): 30–39.

Hameeda, B., G. Harini, O.P. Rupela, S.P. Wani, and G. Reddy. 2008. Growth promotion of maize by phosphate solubilizing bacteria isolated from composts and macrofauna. *Microbiological Research,* 163: 234-42.

Higa, T. 1991. Effective microorganisms: A biotechnology for mankind. In *Proc. First International Conference on Kyusei Nature Farming. U.S. Department of Agriculture.,* eds. J.F. Parr, S.B. Hornick, and C.E. Whitman, 8-14. Washington, D.C. USA.

Huang, J.S. 1986. Ultrastructure of bacterial penetration in plants. *Annnual Review Phytopathology*, 24: 141-157.

Hung, P.Q. and K. Annapurna. 2004. Isolation and characterization of endophytic bacteria in soybean (*Glycine* sp.). *Omonrice*, 12: 92-101.

Idris, S.E., D.J. Iglesias, M. Talon, and R. Borriss. 2007. Tryptophan-dependent production of indole-3-acetic acid (IAA) affects level of plant growth promotion by *Bacillus amyloliquefaciens* FZB42. *Molecular Plant-Microbe Interactions*, 20: 619-626.

Jeong, J.J., H. Park, B. H. Park, M. Mannaa, M.K. Sang, I.G. Choi, and K.D. Kim. 2016. Draft genome sequence of a biocontrol Rhizobacterium, *Chryseobacterium kwangjuense* Strain KJ1R5, isolated from pepper (*Capsicum annuum*). Genome Announcement. 4(2): e00301-00316.

Ji, S.H.,M.A.Gururani, and S.C.Chun. 2014. Isolation and characterization of plant growth promoting endophytic diazotrophic bacteria from Korean rice cultivars. *Microbiological Research*, 169: (1): 83-98.

Jiménez, M, A.S Flores, V.E. Zapata, P.E. Campos, S. Bouquelet, and E. Zenteno. 2003. Chemical characterization of root exudates from rice (*Oryza sativa*) and their effects on the chemotactic response of endophytic bacteria. *Plant Soil*, 249: 271-277.

Joshi, S. , A.V. Singh, and B. Prasad. 2018. .Enzymatic activity and plant growth promoting potential of endophytic bacteria isolated from *Ocimum sanctum* and *Aloe vera. International Journal of Current Microbiology and Applied Sciences*, 7(6): 2314-2326.

Khan, Z.A., D.M. Román, and S.L. Doty. 2014. Degradation, phytoprotection and phytoremediation of phenanthrene by endophyte *Pseudomonas putida*, PD1. *Environmental Science and Technology,* 48(20): 12221-12228.

Lally, R.D., P. Galbally., A.S. Moreira , J. Spink, D. Ryan, K.J. Germaine, and D.N. Dowling. 2017. Application of endophytic *Pseudomonas fluorescens* and a bacterial consortium to *Brassica napus*ncan increase plant height and biomass under greenhouse and field conditions. *Frontiers in Plant Science,* 8: 2193.

Ma, B., L. Xiaofei, A. Warren, and J. Gong. 2013. Shifts in diversity and community structure of endophytic bacteria and archaea across root, stem and leaf tissues in the common reed, *Phragmites australis*, along a salinity gradient in a marine tidal wetland of northern China. *Antonie van Leeuwenhoek*, 104: 759–768.

Mano, H and H. Morisaki. 2008. Endophytic bacteria in the rice plant. *Microbes and Environments*, 23(2): 109-117.

Naik, B.S., J. Shashikala, and Y.L.Krishnamurthy. 2009. Study on the diversity of endophytic communities from rice (*Oryza sativa* L.) and their antagonistic activities *in vitro. Microbiological Research*, 164(3): 290-296.

Nara, P., G.G. Maob, and, T.B. Yen. 2014. Climate change impacts on agricultural products in Thailand: A case study of Thai rice at the Chao Phraya river basin. *Asia-Pacific Chemical, Biological and Environmental Engineering Society Procedia 8*, 136-140.

Phetcharat, P. and A. Duangpaeng. 2012. Screening of endophytic bacteria from organic rice tissue for indole acetic acid production. *Procedia Engineering*, 32: 177-183.

Pragash, G.M., K.B. Narayanan, P.R. Naik, and N. Sakthivel. 2009. Characterization of *Chryseobacterium aquaticum* strain PUPC1 producing a novel antifungal protease from rice rhizosphere soil. *Journal of Microbiology and Biotechnology*, 19(1): 99-107.

Prakamhang, J, K. Minamisawa, K. Teamtaisong, N. Boonkerd, and N. Teaumroong. 2009) The communities of endophytic diazotrophic bacteria in cultivated rice (*Oryza sativa* L.). *Applied Soil Ecology*, 42: 141-149.

Radzki, W., F.J.G.Manero, E. Algar, J.A.L.Garc, A.G. Villaraco, and B.R. Solano. 2013. Bacterial siderophores efficiently provide iron to iron-starved tomato plants in hydroponics culture. *Antonie van Leeuwenhoek*, 104: 321-330.

Rangjaroen, C, B. Rerkasem, N. Teaumroong, R. Sungthong, and S. Lumyong. 2014. Comparative study of endophytic and endophytic diazotrophic bacterial communities across rice landraces grown in the highlands of Northern Thailand. *Archives of Microbiology*, 196: 35-49

Romero, F.M., M. Marina, and F.L. Pieckenstain. 2014. The communities of tomato (*Solanum lycopersicum*L.) leaf endophytic bacteria, analyzed by16S ribosomal RNAgene pyro sequencing. *FEMS Microbiology.Letters*, 351: 187-194.

Sessitsch, A., P. Hardoim, J. Döring, A. Weilharter, A. Krause, T. Woyke, B. Mitter, L.L. Hauberg, F. Friedrich, M. Rahalkar, T. Hurek, A. Sarkar, L. Bodrossy, L. van Overbeek, D. Brar, J.D. van Elsas, and R.B. Hurek. 2012. Functional characteristics of an endophyte community colonizing rice roots as revealed by metagenomic analysis. *Molecular Plant-Microbe Interactions Journal,* 25: 28-36.

Sev, T.M. A. A. Khai, A. Aung, and S. San Y. 2016. Evaluation of endophytic bacteria from some rice varieties for plant growth promoting activities . *Journal of Scientific and Innovative Research*, 5(4): 144-148.

Stoltzfus, J.R., R. So, P.P. Malarvithi, J.K. Ladha, and F.J. de Bruijn. 1997. Isolation of endophytic bacteria from rice and assessment of thier potential for supplying rice with biologically fixed nitrogen. *Plant and Soil*, 194: 25-36.

Susilowatia, D.N., E.I. Riyanti, M. Setyowati, and K. Mulya. 2018. Indole-3-acetic acid producing bacteriaand its application on the growth of rice. In *Proc. AIP Conference*, 020016. New York, 15-18 August.

Tharek, M.,K. Dzulaikha,S. Salwani, H.G. Amir, and N. Najimudin. 2011. Ascending endophytic migration of locally isolated diazotroph, *Enterobacter* sp. strain USML2 in rice. *Biotechnology*, 10(6): 521-527.

Win, K.T., F.Tanaka, K. Okazaki, and Y. Ohwaki. 2018. The ACC deaminase expressing endophyte *Pseudomonas* spp. enhances NaCl stress tolerance by reducing stress-related ethylene production, resulting in improved growth, photosynthetic performance, and ionic balance in tomato plants. *Plant Physiology and Biochemistry*, 127: 599-607.

Yang, T., D.M. Law, and P.J. Davies. 1993. Magnitude and kinetics of stemelongation in duced by exogenous indole-3-acetic acid in intact light grown pea seedling. *Plant Physiology*, 102: 717-724.

11:30 AM - 12:30 PM (Thu. Sep 5, 2019 11:30 AM - 12:30 PM Poster Place)

[5-1130-P-22] Data Extraction for Pig Weight Prediction Model

*Khin Dagon Win[1], Kikuhito Kawasue[1], Hsu Lai Wai[1], Kumiko Yoshida[2] (1. University of Miyazaki(Japan), 2. KOYO Plant Service(Japan))

Keywords: Weight estimation, Machine learning, 3D information, Random Forest, Multiple slits

Recently, automatic pig sorting systems have been popular to manage pigs in some pig farms. This systems automatically select pigs with appropriate weight for delivery. Normally, the pigs with over 115 kg are delivered in Japan. Therefore, this weight estimation system is essential to determine the maturity of pigs for shipment. A load cell is generally used in automatic sorting systems. However, it takes over 20 seconds to measure weight to detect stable weight. Sawdust is often used in pig house, but it can be attached to load cell and can lead to mechanic errors. Therefore, the use of load cell becomes big challenges to apply in actual pig farms.To overcome problems of load cell, we have developed an automatic pig weight measurement system using a camera. This system is composed on a camera, multiple slits and random dots projector. The camera with band-pass filter captures the pig image which enters into the system without influence on external luminous. Random dots and multiple slits are simultaneously projected to the pig body. Random dots projector is used to detect the location of pigs in the system and multiple slits projector is used to measure 3-dimensional shapes of pig body. Random dots projector is simultaneously projected to cover the whole surface of multiple slits. This measurement device is set up at the top of the system to detect back shape of pig body because the back shape can hold the definite growth conditions of pigs without being influenced by their daily nourishment levels. The image processing based weight estimation system consists of 3 steps: Extraction of pig from capture image, Quantitative analysis of the pig size from extracted image, Weight estimation from pig size using machine learning algorithm. Sawdust is often used in pig house. Moreover, those sawdust can be attached to a pig body. These attached sawdust can be influenced on extraction process of pig from captured images. In our system, Fast Fourier Transform (FFT) is applied to extract the pigs without being influenced by the surface situations of pig body. FFT detects the displacement of random dots to judge of existence of pigs in measurement area. 2-dimensional pig size information can be established with silhouette pig image. Furthermore, 3-dimensional pig size information is also considered to observe more specific growth conditions of pigs. For 3-dimensional information, it is needed to process slits image which are projected on pig body. Each slit location is detected to perform in the triangulations and 3D information such as length, girth and height are calculated. The adequate selection from 2D&3D information to estimate the pig weight is important and difficult process for our system. Therefore, Random Forest algorithm is utilized in our system. Random Forest randomly selects the samples from datasets and splits the data into several trees according to their features importance. The estimated weights are resulted by majority voting of its several trees. This method is adequate for pig weight estimation on practical conditions. The experimental results show the usefulness of our pig weight estimation system for automatic sorting system.

Poster Session | Others (including the category of JSAM and SASJ)
[5-1130-P] Other Categories (5th)
Thu. Sep 5, 2019 11:30 AM - 12:30 PM Poster Place (Entrance Hall)

[5-1130-P-23] Power Tiller’ s Wheel Structure and its Oscillatory Effects on Subsoiling Operation

*Oyetayo Olukorede Oyebode[1], Koichi Shoji[1] （1. Graduate School of Agricultural Science, Kobe University(Japan)）

Keywords: Power tiller, Hexagonal Wheel, Subsoiler, Oscillatory motion

The path followed by a subsoiler attached to a hexagonal wheeled power tiller was studied. Many researchers have reported a significant reduction in draft force and an improved tillage quality when the performance of oscillated tillage tools was compared with rigidly fixed tillage tools. However, these improvements usually come with drastically increased engine power use and fuel consumption. Developing the oscillatory motion without significantly increasing the engine power use is therefore the focus of this research. A model subsoiler was fabricated and attached to a power tiller. The tiller wheels were replaced with 200 mm regular hexagonal wheels made of perforated steel and having a width of 200 mm. To have an understanding of the workings of the subsoiler, the path followed by the tip of the subsoiler was measured at two speeds of 0.037 m/s and 0.140 m/s. An ultrasonic sensor which was rigidly fixed above but independent of the power tiller was used to measure the vertical displacements made by the subsoiler as it travels in the soil bin. A graph of the height of the subsoiler versus time was thus plotted. The results show that the path followed by the subsoiler as it travels laterally at both speeds was sinusoidal or oscillatory in the vertical direction. The amplitudes for both speeds were approximately the same, but the frequency increased with increase in speed. It was also observed that the tip of the subsoiler moved downward through uncut soil suggesting that the effort at reducing power consumption with the investigated wheel configuration may not be as successful as expected.

Power Tiller's Wheel Structure and its Oscillatory Effects on Subsoiling Operation

Oyetayo Oyebode[1] and Koichi Shoji[1*]

[1]Graduate School of Agricultural Science, Kobe University
[*]Corresponding Author: shojik@kobe-u.ac.jp

ABSTRACT

The path followed by a subsoiler attached to a hexagonal wheeled power tiller was studied. Many researchers have reported a significant reduction in draft force and an improved tillage quality when the performance of oscillated tillage tools was compared with rigidly fixed tillage tools. However, these improvements usually come with drastically increased engine power use and fuel consumption. Developing the oscillatory motion without significantly increasing the engine power use is therefore the focus of this research. A model subsoiler was fabricated and attached to a power tiller. The tiller wheels were replaced with 200 mm regular hexagonal wheels made of perforated steel and having a width of 200 mm. To have an understanding of the workings of the subsoiler, the path followed by the tip of the subsoiler was measured at two speeds of 0.037 m/s and 0.140 m/s. An ultrasonic sensor which was rigidly fixed above but independent of the power tiller was used to measure the vertical displacements made by the subsoiler as it travels in the soil bin. A graph of the height of the subsoiler versus time was thus plotted. The results show that the path followed by the subsoiler as it travels laterally at both speeds was sinusoidal or oscillatory in the vertical direction. The amplitudes for both speeds were approximately the same, but the frequency increased with increase in speed. It was also observed that the tip of the subsoiler moved downward through uncut soil suggesting that the effort at reducing power consumption with the investigated wheel configuration may not be as successful as expected.

Key Words: Power tiller, Hexagonal wheel, Subsoiler, Oscillatory motion

Poster Session | Others (including the category of JSAM and SASJ)
[5-1130-P] Other Categories (5th)
Thu. Sep 5, 2019 11:30 AM - 12:30 PM Poster Place (Entrance Hall)

[5-1130-P-24] Proposal of temperature control technology in pot cultivation for the citrus fruits

*Ryuta IBUKI[1], Yoshimichi Yamashita[2], Sachie Horii[2], Norihiro Hoshi[2], Madoka Chiba[1] (1. Miyagi University(Japan), 2. National Agriculture and Food Research Organization(Japan))

Keywords: pot cultivation, thermal management

Disaster area of Fukushima restarted farming mainly by the large-scale rice production corporation by farmland accumulation and the flower farmer using pipe house, which have little concern about reputational damage. For effective use of pipe house, there is a need for new crops that can be grown in pipe house at times other than floriculture and rice seedlings. With this situation as the background, we focused on pot cultivation. It has been considered to cultivate 'citrus fruits', which is cultivated in warmer regions under meteorological conditions by cultivation using pots, outdoors in summer and in a pipe house in winter. In addition to alleviating the northern limit of temperature-based cultivation, we are exploring new thermal management techniques for the pot cultivation environment. A difference was observed in the condition depending on the presence or absence of the whole covering sheet on the 'citrus fruits' (e.g. 'Citrus sphaerocarpa', etc.) in pot placed in the pipe house from 2017 to 2018, and the plant growth was good at the tree with the covering. Then, from 2018 to 2019, we investigated the thermal effect of the covering. 'Citrus sudachi' grown in pots (diameter 385 mm, depth 310 mm, black soil and pumice in the bottom of pots) was wintered, and the temperature and heat transfer conditions in the cultivation environment were compared for the presence or absence of the covering. The leaf surface temperature with an infrared radiation thermometer and the 10 cm depth soil temperature with a T-type thermocouple were examined during the winter (February 4 to March 4, 2019). The lowest, average and the highest (T_{min},T_a, T_{max}) were surveyed, with leaf temperatures of (-7 ˚C, 7 ˚C, 38 ˚C) in the covering tree, (-6 ˚C, 8 ˚C, 41 ˚C) in the control area, with the soil temperature (1 ˚C, 11 ˚C, 29 ˚C) under the covering tree, and (1 ˚C, 12 ˚C, 33 ˚C) in the control. From this, it was found that the cover texture contributes to the suppression of the high temperature of 3 to 4 ˚C during the day rather than the heat retention effect at night. In addition, we also investigated the time-dependent change of the temperature distribution of the soil in the pot placed in the pipe house from February 4 to February 26, 2019. The soil temperatures in pot at the inner side of the south sidewall, the center and the inner side of the north wall were measured at intervals of 10 minutes using a T-type thermocouple for a depth of 2 cm, 10 cm and 20 cm. The inner side of the south wall surface is the hottest and the maximum value on a fine day is extremely high, showing 50 to 60 ˚C. On the other hand, the daily maximum value of the pot center 10 cm deep showed a value 20 to 30 ˚C lower than that of the south side wall surface. Also, the time to reach the maximum temperature at the point showed a delay of about 3 hours as compared with the wall surface. During the period, the soil temperature changes at the center of the pot is delayed while the air temperature goes up with the sunrise during the daytime. According to Konakahara(1975), due to strong winds and physiological changes in the tree, low land temperatures in the land-planted 'Citrus Unshiu' inhibit water supply from the roots, and the amount of transpiration exceeds water supply, resulting in poor water balance in the tree. The balance tends to occur, the decrease of the water content in the leaves becomes remarkable, and quantitatively the effect starts to be seen at the soil temperature of 10 ˚C or less, and the effect becomes remarkable at that of 5 ˚C or less. In the measurement, the time when the central soil temperature exceeded 5 ˚ C was after 11:00, and the time exceeding 10 ˚ C was after noon. On the other hand, the temperature difference between the air and the center of the pot was

maximum in the morning and was 20 to 30 ˚C. This is consistent with the case of Konakahara, and suggests the need to manage the ground temperature and temperature difference, taking into consideration the high temperature of the daytime inside the house even in winter. Based on these results, we considered that more sophisticated control of temperature distribution and heat transfer in the pot throughout the year will contribute to the improvement of productivity in pot cultivation. For example, the water content of the soil, which affects the thermal conductivity, is considered to have a large effect, and measurements were performed to understand the change in the water content in the pot. This work was conducted under "A Scheme to Revitalize Agriculture and Fisheries in Disaster Area through Deploying Highly Advanced Technology" by the Ministry of Agriculture, Forestry and Fisheries, Japan.

Proceedings of the 2019 International Joint Conference on JSAM and SASJ, and 13th CIGR VI Technical Symposium
joining FWFNWG and FSWG Workshops

Proposal of Temperature Control Technology in Pot Cultivation for the Citrus Fruits

Ryuta Ibuki[1*], Yoshimichi Yamashita[2], Sachie Horii[3], Norihiro Hoshi[2], Madoka Chiba[1]

[1]School of Food Industrial Science, Miyagi University, Japan
[2]Fukushima Research Station, National Agriculture and Food Research Organization, Japan
[3] Institute of Fruit Tree and Tea Science, National Agriculture and Food Research Organization, Japan

*ibuki@myu.ac.jp

ABSTRACT

In this study we investigated thermal environment condition of the pot cultivation in pipe house during winter for future development of novel thermal management system on pot cultivation. Disaster area of Fukushima restarted farming and the flower farmer using pipe house, which have little concern about reputational damage. For effective use of pipe house, there is a need for new crops that can be grown in pipe house. Cultivation using pots was planned and effective thermal management was start to be considered. A whole covering that is used as a simple method to protect plants from cold damage was evaluated its heat retention effect by temperature measurement of leaf and cultivating soil of 'Citrus sudachi' in the winter during 2018 to 2019. The lowest, average and the highest (T_{min}, T_a, T_{max}) were surveyed, with leaf temperatures of (-7 °C, 7 °C, 38 °C) in the covering tree, (-6 °C, 8 °C, 41 °C) in the control area, with the soil temperature (1 °C, 11 °C, 29 °C) under the covering tree, and (1 °C, 12 °C, 33 °C) in the control. Also, temperature, heat flux, net radiation and moisture distribution in and around pot soil was measured. Temperature difference of cold soil and hot air in the pipe house of early morning was observed and warried about water balance in plant. Heat flux decreasing in soil near south wall was observed and it was considered to be influenced by moisture content of soil. Although plastic pots are lighter and more durable than pottery pots, we consider it necessary to devise thermal management. In the winter months, it is necessary to warm the soil in the morning to maintain a healthy water balance of the plants. Oppositely, it is necessary to have a device that does not overheat the soil during winter daytime or summer season.

Keywords: Pot cultivation, Thermal management

1. INTRODUCTION

Disaster area of Fukushima restarted farming mainly by the large-scale rice production corporation by farmland accumulation and the flower farmer using pipe house, which have little concern about reputational damage. For effective use of pipe house, there is a need for new crops that can be grown in pipe house at times other than floriculture and rice seedlings. With this situation as the background, we focused on pot cultivation. It has been considered to cultivate 'citrus fruits', which is cultivated in warmer regions under meteorological conditions by cultivation using pots, outdoors in summer and in a pipe house in winter. In addition to alleviating the northern limit of temperature-based cultivation, we are exploring new thermal management techniques for the pot cultivation environment.

In this study we investigated thermal environment condition of the pot cultivation in pipe house during winter for future development of novel thermal management system on pot cultivation.

2. MATERIALS AND METHODS

Firstly measurement of heat retention effect of the whole covering on pot cultivating 'Citrus sudachi' was carried out. Then measurement of pot soil circumstances, temperature and water distribution was carried out to grasp heat transfer in pot.

書式変更: フォントの色 : 自動
書式変更: フォントの色 : 自動
書式変更: フォントの色 : 自動
書式変更: フォントの色 : 自動
書式変更: フォント : 11 pt, フォントの色 : 自動
削除: Start from here. (11 point, No space with heading. The body of the abstract should be limited up to 500 words. Include importance of the work, overall objectives, brief description of materials and methods, major results, and implication of your work) .
書式変更: フォント : Times New Roman
書式変更: フォント : Times New Roman
削除: List up to 7 words or phrases (left margin), normal style, CAP only first letter of each keyword. Separate with one space.
書式変更: フォント : Times New Roman
書式変更: フォントの色 : 自動
削除: Start from here. (11 point, normal style. No space with heading) .
書式変更: フォント : 太字 (なし)
書式変更: フォント : 太字 (なし)

2.1 Experiment on Heat Retention Effect of Covering

From 2017 to 2018, we considered optimizing the cultivation environment of 'citrus fruits' (e.g. 'Citrus sphaerocarpa', etc.) in the pipe house by using a whole covering that is used as a simple method to protect plants from cold damage. Breathable polypropylene sheet is generally used as the covering. A difference was observed in the condition depending on the presence or absence of the whole covering sheet on the 'citrus fruits' in pot placed in the pipe house, and the plant growth was good at the tree with the covering.

Then, from 2018 to 2019, we investigated the thermal effect of the covering. 'Citrus sudachi' grown in pots (diameter 385 mm, depth 310 mm, black soil and pumice in the bottom of pots) was wintered, and the temperature and heat transfer conditions in the cultivation environment were compared for the presence or absence of the covering. The leaf surface temperature with an infrared radiation thermometer and the 10 cm depth soil temperature with a T-type thermocouple were examined during the winter during February 4 to March 4 in 2019. Air temperature was measured with forced convection

2.2 Experiment on Temperature and Water Distribution in Pot Soil

Because the temperature distribution in the pot is affected by solar radiation, the change in temperature due to the azimuth is not uniform. Jizuka (1956) was measured the time-dependent change of temperature distribution about the soil in the some types of pottery pot. Since pottery pots are heavy in workability, we tested using a practical plastic pot. Okamoto and Yanagawa (2013) told that unlike ground planting, roots grow in a limited space, we must be aware of the growth conditions such as nutrients, moisture, and temperature, which are the environment of the rhizosphere. They measured soil temperature under flowers cultivated condition with some types of pot including plastic pot and reported about directional soil temperature difference near pot surface. The pot wall surface and the soil surface is irradiated with solar radiation and the amount of evaporation of water is larger than that in the deep part. The thermal conductivity of water is higher than the thermal conductivity of air, and the dried soil with reduced water content has lower thermal conductivity (Datta, 2002). Since the thermal conductivity of the soil is related to the warming of the soil and the heat retention at night, it is important information in temperature control of the pot to grasp the state.

2.2.1 Pot Soil Temperature Measurement

The temporal change of the temperature distribution of black soil in the plastic pots in the pipe house was also investigated from February 4 to February 26, 2019. Figure 1 show the measurement setup. The temperatures at the inner side of the south sidewall (TC3, 6 and 9), the center (TC2, 5 and 8) and the inner side of the north wall (TC1, 4 and 7) were measured at intervals of 10 minutes using a T-type thermocouple for a depth of 2 cm, 10 cm and 20 cm.

書式変更: フォントの色 : 自動

書式変更: フォントの色 : 自動

コメントの追加 [幸江1]: Condition というよりも、カンキツの生育が良かったの方がいいのかなと思いました。The plant growth とか？

書式変更: フォントの色 : 自動

削除: Nishiuchi

削除: of unglazed pottery

削除: unglazed

書式変更: フォントの色 : 自動

書式変更: フォントの色 : 自動

削除: It is thought that t

削除: surface of the

書式変更: フォントの色 : 自動

削除: Reference

書式変更: フォントの色 : 自動

削除:

削除: .

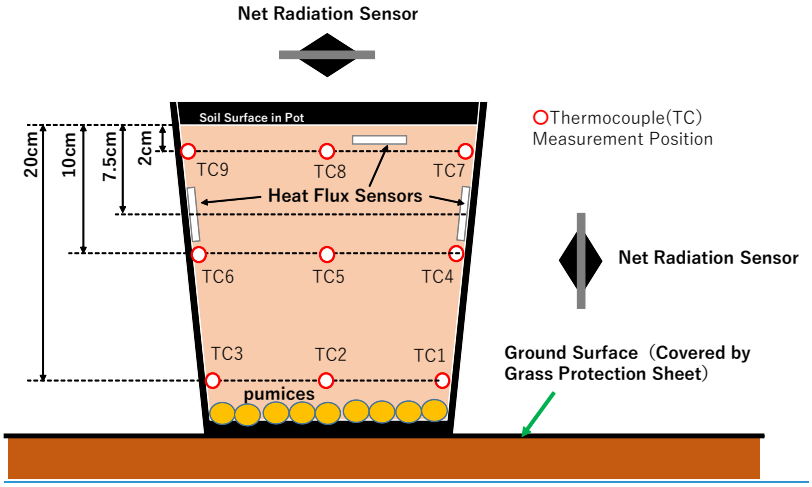

Figure. 1 Measurement setup of soil temperature and heat flux in pot

2.2.2 Measurement on Heat Flux and Net Radiation

Two net radiation sensors (CPR-NR-LITE, Kipp & Zonen) were placed on soil surface and southern side of the pot wall and also three heat flux sensor were placed in the pot soil as shown in fig. 1. Pyranometer (PCM-01N, PLEDE) was used to measure solar irradiation.

2.2.3 Measurement on Water Content Distribution and Time Dependent Variation

The water content of the soil affects the thermal conductivity,was assumed to have a large effect in our experiment and measurements were carried out to understand the water content distribution in the pot and its time dependent change. Several pots of soil were placed in the pipe house. The each pots were collected different few days and the moisture content was measured by vertical layer and location. Also, black soil with different water content was prepared in a beaker, and thermal conductivity was measured for each soil by the thermal probe method. Thermal properties analyzer, DECAGON KD-2, was used for measurement. We compared water content and thermal conductivity then we considered about heat transfer in pot.

3. RESULTS AND DISCUSSION

Heat retention effect of covering was considered from results of leaf temperatures and soil temperatures. Soil temperatures were more influenced than leaf temperatures. Then thermal circumstances of pot soil was measured in detail.

3.1 Test of Covering on Heat Retention Effect

Figure. 2 shows the average temperature, the minimum temperature, and the maximum temperature obtained from the time-dependent change data of leaf surface temperature and soil temperature in the pot which had grown "Citrus sudachi" from 2018 to 2019 over winter. The lowest, average and the highest (T_{min}, T_a, T_{max}) were surveyed, with leaf temperatures of (-7 °C, 7 °C, 38 °C) in the covering tree, (-6 °C, 8 °C, 41 °C) in the control area, with the soil temperature (1 °C, 11 °C, 29 °C) under the covering tree, and (1 °C, 12 °C, 33 °C) in the control. From this, it was found that the cover texture contributes to the suppression of the high temperature of 3 to 4 °C during the day rather than the heat retention effect at night.

書式変更: フォント : 11 pt
書式変更: フォント : 11 pt
書式変更: 1 行の文字数を指定時に右のインデント幅を自動調整しない, グリッドへ配置しない
削除: 1
削除: 2
削除: Sub-Subheading
書式変更: フォント : 11 pt, フォントの色 : 自動
書式変更: 左揃え, 1 行の文字数を指定時に右のインデント幅を自動調整する, グリッドへ配置
削除: Start from here. (11 point, normal style. No space with heading)
書式変更: フォントの色 : 自動
書式変更: フォント : 11 pt, フォントの色 : 自動
書式変更: フォントの色 : 自動
書式変更: フォント : 11 pt, フォントの色 : 自動
書式変更: フォントの色 : 自動
書式変更: フォント : 11 pt, フォントの色 : 自動
削除: .
書式変更: フォント : 太字 (なし) , フォントの色 : 自動
削除: (Numbered, 11 point, bold, left margin, all CAPS, separate with one space between the last paragraph of MATERIALS AND METHODS) .
Start from here. (11 point, normal style. No space with heading) .
書式変更: フォントの色 : 自動
削除: Subheading (Similar with the MATERIALS AND METHODS)
書式変更: フォントの色 : 自動
書式変更: フォントの色 : 自動

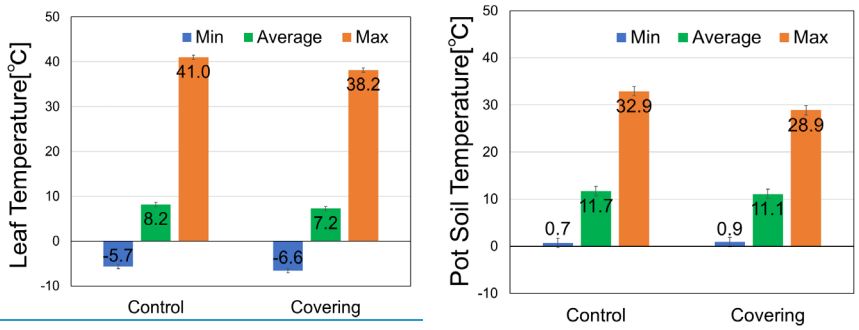

Figure.2 Leaf temperature of "Citrus sudachi" and growing Pot soil temperature of minimum, average and maximum in the measurement period from February 4 to March 4, 2019, which compares the presence or absence of a covering.

3.2 Test of Pot Soil Circumstance

Circumstance of the pot soil, temperature distribution, heat flux, net radiation and water content were measured.

3.2.1 Soil Temperature Variation

Figure 3 shows the change over time in the temperature distribution of middle depth when only the soil was put in the pot for the entire measurement period. The inner side of the south wall surface is the hottest and the maximum value on a fine day is extremely high, showing 50 to 60 °C. It is concerned that such high temperatures near the walls would affect root damage. Figure. 4 shows representative day data of temperatures when only soil was put in the pot and the time-dependent change in temperature distribution was measured. South side wall had maximum temperature in the pot. Okamoto et al. reported the higher temperature trend at the south wall and west wall. The daily maximum value of the pot center 10 cm deep showed a value 20 to 30 °C lower than that of the south side wall surface. Also, the time to reach the maximum temperature at the point showed a delay of about 3 hours as compared with the wall surface. During the period, the soil temperature changes at the center of the pot is delayed while the air temperature goes up with the sunrise during the daytime. According to Konakahara (1975), due to strong winds and physiological changes in the tree, low land temperatures in the land-planted 'Citrus Unshiu' inhibit water supply from the roots, and the amount of transpiration exceeds water supply, resulting in poor water balance in the tree. The balance tends to occur, the decrease of the water content in the leaves becomes remarkable, and quantitatively the effect starts to be seen at the soil temperature of 10 °C or less, and the effect becomes remarkable at that of 5 °C or less. In the measurement, the time when the central soil temperature exceeded 5 ° C was after 11:00, and the time exceeding 10 ° C was after noon. On the other hand, the temperature difference between the air and the center of the pot was maximum in the morning and was 20 to 30 °C. This is consistent with the case of Konakahara, and suggests the need to manage the ground temperature and temperature difference, taking into consideration the high temperature of the daytime inside the house even in winter. Based on these results, we considered that more sophisticated control of temperature distribution and heat transfer in the pot throughout the year will contribute to the improvement of productivity in pot cultivation.

削除:
書式変更: フォントの色 : 自動
書式変更: フォントの色 : 自動
削除: Start from here. (11 point, normal style. No space with subheading) .
書式変更: フォントの色 : 自動
削除: 1
削除: ub-Subheading (Similar with subheadings)
書式変更: フォントの色 : 自動
書式変更: フォント : 11 pt, フォントの色 : 自動
書式変更: 両端揃え
書式変更: フォント : 11 pt
書式変更: フォント : 11 pt, フォントの色 : 自動
書式変更: フォント : 11 pt
書式変更: フォント : 11 pt
書式変更: フォント : 11 pt

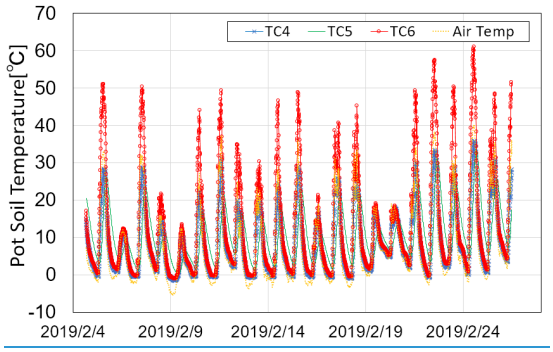

Figure. 3 Time dependent change data of temperature in the middle depth of the pot soil

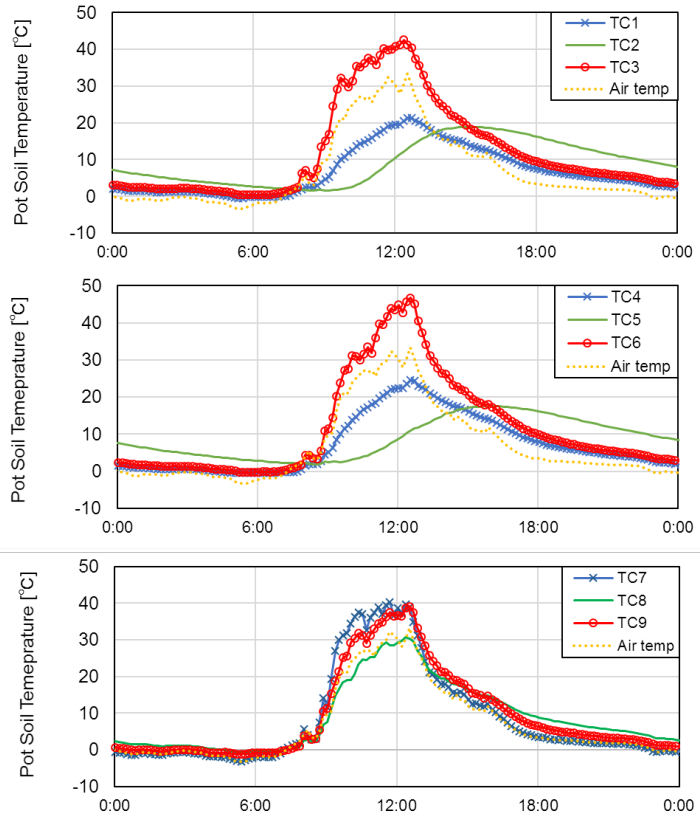

Figure. 4 Time dependent change in temperatures distribution when only soil was put in the pot on Feb 14, 2019.

書式変更: 中央揃え

書式変更: 両端揃え

削除:

書式変更: フォントの色：自動

削除: Start from here. (11 point, normal style. No space with heading)

3.2.2 Heat Flux and Net Radiation around Pot

Figure 5 shows time dependent change data of solar irradiation and heat flux in pot soil at three points, soil surface, south wall and north wall. Compared to time dependent change of solar irradiation, that of heat flux at south wall showed tendency to degrease day by day. It could be assumed that soil touching with south wall was dried and thermal conductivity near south wall was degreased compared to that near north wall and that near soil surface, because south wall had extremely heated as show in figure 4.

Figure 6 shows time dependent change data of net radiation around pot. Intensity of net radiation of pot side was 25% smaller at daytime of fine day and 75% larger at night than that of pot top.

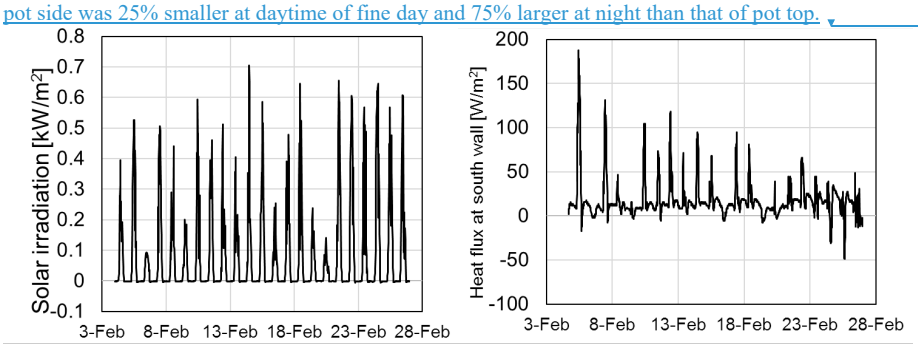

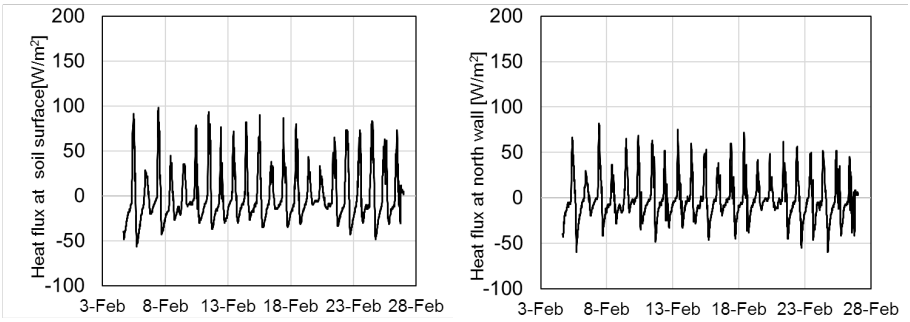

Figure. 5 Time dependent change data of solar irradiation and heat flux in pot soil from Feb.4 to Mar. 4 in 2019.

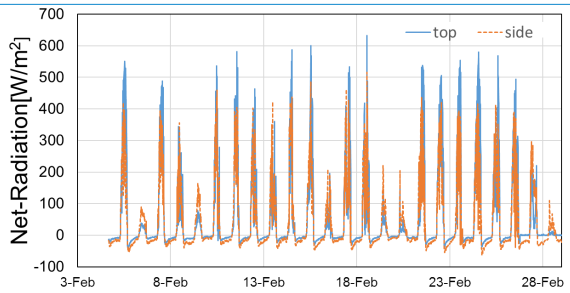

Figure. 6 Time dependent change data of net radiation around pot from Feb.4 to Mar. 4 in 2019.

削除: 1
削除: Sub-Subheading
書式変更: フォント : 11 pt, フォントの色 : 自動
書式変更: フォントの色 : 自動
書式変更: フォント : 11 pt, フォントの色 : 自動
書式変更: フォントの色 : 自動
削除: Start from here. (11 point, normal style. No space with heading) .
書式変更: インデント : 最初の行 : 0 mm
削除:

3.2.3 Moisture Content in Pot Soil

Figure 7 shows time dependent water content in pot soil. Uniform water content in pot was measured before Feb. 13. Figure 8 shows water content vs thermal conductivity of black soil between 5% and 35% of water content. Large difference of thermal conductivity was measured between 25% and 30% of water content. Compared to Figure 6, significant change of thermal conductivity relating on heat transfer might be happen after Feb. 18. However, heat flux at south wall showed significant decrease on Feb. 7. Therefore, the water content of soil we measured was not directly influenced the heat flux at south wall in Fig. 5. We considered that pot soil was dried by inner wall surface of the pot and thermal resistance on this boundary was increased on early stage of the measurement. Although plastic pots are lighter and more durable than pottery pots, we consider it necessary to devise thermal management. In the winter months, it is necessary to warm the soil in the morning to maintain a healthy water balance of the plants. Oppositely, it is necessary to have a device that does not overheat the soil during winter daytime or summer season.

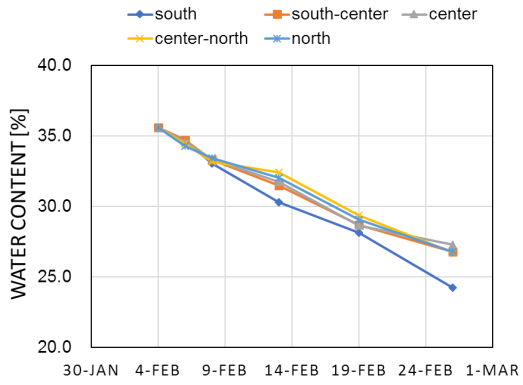

Figure 7 Time dependent change of water content distribution in middle layer of pot soil

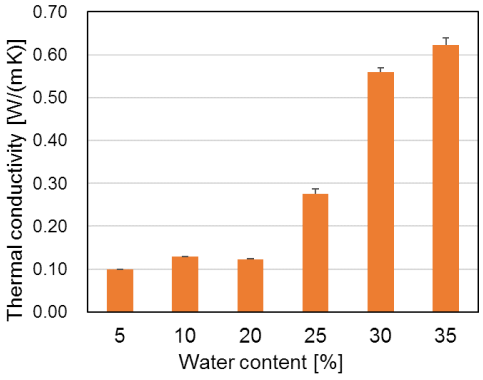

Figure 8 Water content vs thermal conductivity of black soil

4. CONCLUSION

Initial test measurements were carried out on the thermal management of citrus grown in pots.

書式変更: フォントの色：自動
削除:
書式変更: 中央揃え
削除:
書式変更: 中央揃え
書式変更: インデント：最初の行： 7 字
削除:
削除:

The effect of the whole covering on pot cultivated 'citrus fruits' in pipe house had an effect on suppressing temperature rise during the daytime. Temperature difference between pot soil and air, lower temperature of soil and higher temperature of air, was observed in winter morning which causes unbalance of transpiration and water supply from roots was concerned.

ACKNOWLEDGMENT

This work was conducted under "A Scheme to Revitalize Agriculture and Fisheries in Disaster Area through Deploying Highly Advanced Technology" by the Ministry of Agriculture, Forestry and Fisheries, Japan.

REFERENCES

Datta, A. K., 2002, Biological and Bioenvironmental Heat and Mass Transfer, New York: Marcel Dekker, Inc.

Iizuka, I. and Konami, M., 1956, On the Changes of Flower-Pot Temperature (1) The Temperature in Various Kinds of Pots and the Changes of Pot Temperature after Watering, Journal of Agricultural Meteorology, 13-1.pp.25-29.

Konakahara, M., 1975, Experimental Studies on the Mechanisms of Cold Damage and Its Protection Methods in Citrus Trees, Special Bulletin No.3 of The Shizuoka Prefectural Citrus Experiment Station (In Japanese).

Okamoto K. and Yanagawa, T., 2013, Studies on Pots and Soil Temperature in Pot Cultures - Effects of Materials and Size of Culturing Pots on Soil Temperature in Chrysanthemum Pot Cultures -, Annual report of researches in environmental education, Kyoto University of Education, 21, pp.91-100, (In Japanese).

書式変更

削除: (Numbered, 11 point, bold, left margin, all CAPS, separate with one space between the last paragraph of Results and Discussion) .
Start from here. (11 point, normal style. No space with heading) .

書式変更

書式変更: フォント : 11 pt

書式変更: 両端揃え

削除: (If needed) (Not numbered, 11 point, **bold**, left margin, all CAPS, separate with one space between before paragraph) .
Start from here. (11 point, normal style. No space with heading) .

削除: (Not numbered, 11 point, bold, left margin, all CAPS, separate with one space between the last paragraph of Conclusion)

書式変更

書式変更: フォント : 11 pt

書式変更: 改ページ時 1 行残して段落を区切る, 日本語と英字の間隔を自動調整しない, 日本語と数字の間隔を自動調整しない, グリッドへ配置

書式変更

書式変更: フォント : 太字 (なし)

書式変更: フォント : (英) Times New Roman

書式変更: 改ページ時 1 行残して段落を区切る, 日本語と英字の間隔を自動調整しない, 日本語と数字の間隔を自動調整しない, グリッドへ配置

書式変更

書式変更: フォント : 太字

削除: List alphabetically by first author's last name from here. (See details in "Author Guideline of CIGR Journal (http://www.cigrjournal.org/index.php/Ejounral/about/submissions#authorGuidelines)" .
In text refer to as (Wang, 2005) or (Wang et al., 2005) or if in a sentence Wang et al. (2005) reported that. Please see example references in Example of CIGR Publication.

Poster Session | Others (including the category of JSAM and SASJ)

[5-1130-P] Other Categories (5th)

Thu. Sep 5, 2019 11:30 AM - 12:30 PM Poster Place (Entrance Hall)

[5-1130-P-25] Investigation by Driving Simulation of Tractor Overturning Accidents Caused by Steering Instability

*Masahisa Watanabe[1], Kenshi Sakai[1] (1. Tokyo University of Agriculture and Technology(Japan))

Keywords: Tractor, Farm accident, Driving simulator, Overturning, Lateral slippage

Overturning tractors are the leading cause of fatalities on farms. Steering instability contributes significantly to the tractor overturning. This study investigated tractor overturning accidents caused by the steering instability using a driving simulator. The general commercial driving simulator CarSim® (Mechanical Simulation Cooperation, MI, USA) was used. Tractor operations on steep passage slopes were simulated to mimic conditions present for a real accident case reported in Japan. Simulations were performed on roads with and without slopes. The tractor overturned only when on the road with the steep slope. The decrease in the vertical force on the front wheel caused the steering instability and the tractor to overturn. The steering instability caused understeer which prevents the operator from being able to control the tractor properly. Subsequently, the tractor overturned in the simulation. The tractor driving simulator was capable of reproducing the steering instability which can lead to the overturning accident.

Investigation by Driving Simulation of Tractor Overturning Accidents Caused by Steering Instability

Masahisa Watanabe [1*], Kenshi Sakai [2]

[1] Department of Food and Energy Systems Science, Graduate School of Bio-Applications and Systems Engineering, Tokyo University of Agriculture and Technology, Japan
[2] Division of Environmental and Agricultural Engineering, Institute of Agriculture, Tokyo University of Agriculture and Technology, Japan

*Corresponding author: s160479z@st.go.tuat.ac.jp

ABSTRACT

Overturning tractors are the leading cause of fatalities on farms. Steering instability contributes significantly to the tractor overturning. This study investigated tractor overturning accidents caused by the steering instability using a driving simulator. The general commercial driving simulator CarSim® (Mechanical Simulation Cooperation, MI, USA) was used. Tractor operations on steep passage slopes were simulated to mimic conditions present for a real accident case reported in Japan. Simulations were performed on roads with and without slopes. The tractor overturned only when on the road with the steep slope. The decrease in the vertical force on the front wheel caused the steering instability and the tractor to overturn. The steering instability caused understeer which prevents the operator from being able to control the tractor properly. Subsequently, the tractor overturned in the simulation. The tractor driving simulator was capable of reproducing the steering instability which can lead to the overturning accident.

Keywords: Tractor Farm accident Driving simulator Overturning Steering instability

1. INTRODUCTION

There are approximately 400 fatal farm accidents each year in Japan. Accidents involving agricultural tractors are a major contributor to farm fatalities. In 2016, 115 of the total 312 fatal farm accidents were tractor-related (Ministry of Agriculture, Fishery, and Forestry, 2018). More specifically, the tractor overturning is the leading cause of fatalities with 53 cases in 2016.

In Japan, small tractors specially designed for paddy fields are used in harsh environments such as rough farm roads, steep passage slopes, and narrow inclined side paths. This dangerous terrain can lead to a decrease in the vertical force on the front wheel. In some cases, this can result in separation of the front wheel from the underlying ground. This phenomenon causes vertical bouncing and lateral slippage of the tractor, both of which can lead to steering instability and overturning. The impact dynamics induced by the bouncing dramatically deteriorate tractor stability (Sakai, 1999; Sakai et al, 2000; Watanabe & Sakai, 2019a). If in addition to the bouncing slippage of the wheels occurs, the operator will not be able to maintain full control of the tractor. Consequently, the quality of the tractor posture dramatically decreases.

Several studies have contributed to the development of the tractor driving simulator and its application to farm safety and automation research (Gonzalez et al., 2017; Han et al., 2019; Watanabe & Sakai, 2019b). The tractor driving simulator is a strong platform for accident prevention research. The aim of the present paper is to apply the tractor driving simulator to investigation of overturning accidents induced by steering instability. A general driving simulator called CarSim® (Mechanical Simulation Cooperation, MI, USA) was used as a platform for the tractor driving simulator. Simulations of tractor operation on steep passage slopes were conducted. A real accident case reported in Japan was used as the basis for these simulations.

2. MATERIALS AND METHODS

The configuration of the tractor driving simulator is presented. CarSim® 2016 version was employed for the driving simulator. Vehicle and road configuration can be input by the user. Table 1 shows the tractor parameters used.

Table 1 Tractor parameter specification.

Parameters	**Value**	**Unit**
Mass of tractor body	788	kg
Mass of wheels	200	kg
Pitch moment of inertia	700	kg m^2
Distance between center of gravity of tractor body and front wheel	0.7	m
Distance between center of gravity of tractor body and rear wheel	0.64	m

The road surface of the steep passage slope (on which the real accident case occurred) was recreated in the tractor driving simulator. According to the survey conducted by the Japanese Association of Rural Medicine, the tractor overturning accident happened on a steep passage slope of 19° gradient and 0.7 m in height (JARM, 2013). The tractor moved onto the passage slope from the farm field to the farm road and tried to turn right on the road to move into another farm field. However, the tractor was not able to turn and fell from the road. The road surface and scenario were configured in the driving simulator. To investigate the influence of the steep slope on the steering instability, two different types of the road surface were compared. Namely, with slope and without slope. Figure 1a and b shows the road surface with slope and without slope, respectively.

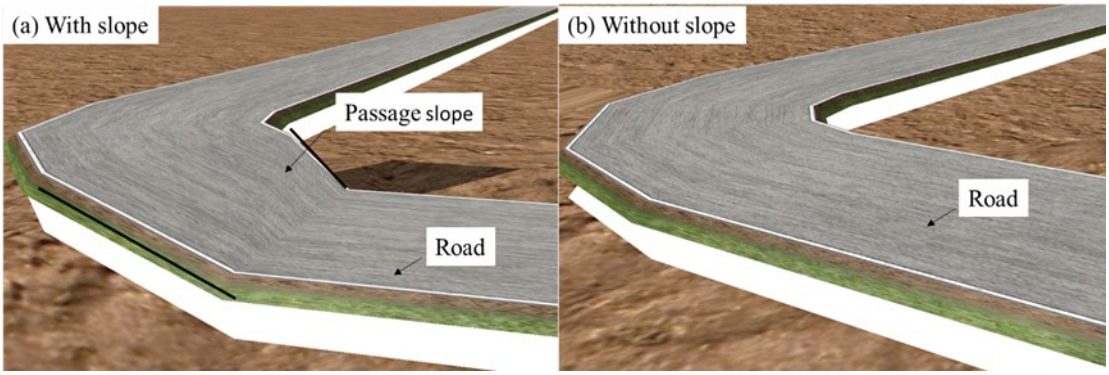

Figure 1 (a) Road surface with a slope; (b) Road surface without a slope.

Figure 2 shows the road profile of the slope.

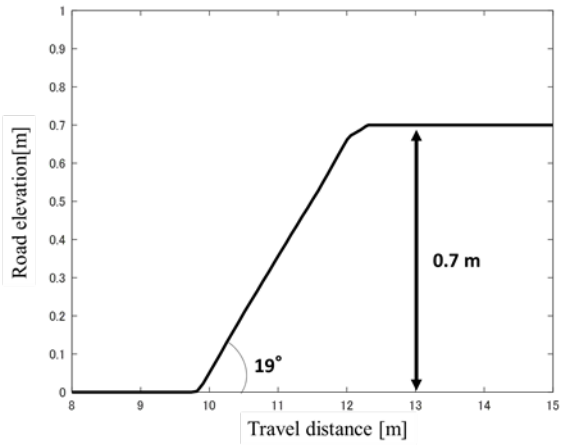

Figure 2 Profile of the slope. The gradient is 19° and the height is 0.7 m.

3. RESULTS AND DISCUSSION

The velocity of the tractor was set to 4.3 m/s in the simulation. The tractor was ran on the road with slope and without slope. Figure 3 shows the tractor trajectories on the road in each simulation.

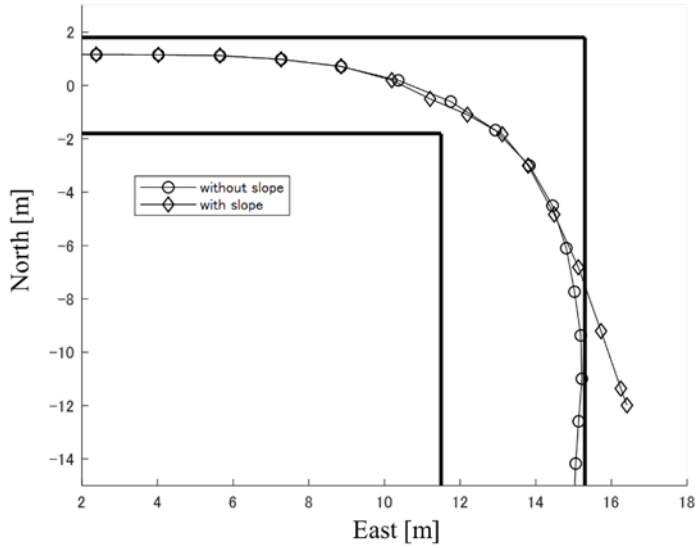

Figure 3 Tractor trajectories of each simulation.

The tractor remained in contact with the road during the whole simulation when the tractor ran on the road without slope. In contrast, the tractor ran off the road and then overturned when the tractor ran on

the road with slope. To visualize the numerical results, Figure 4 and 5 show the animation of the driving simulation for the simulation without slope and with slope, respectively.

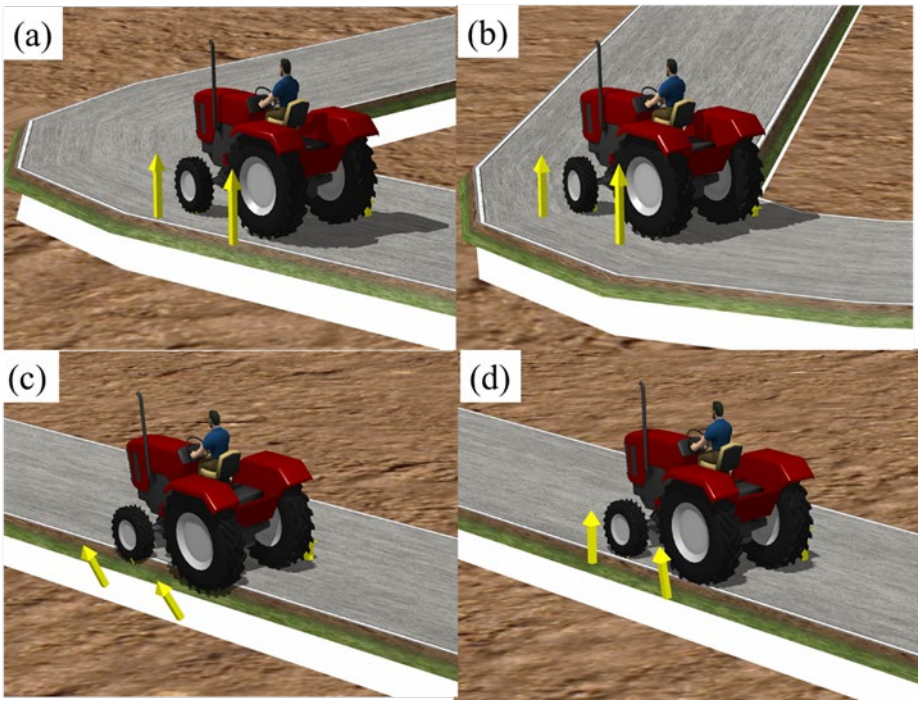

Figure 4 Animation of the tractor operation on the road without slope. (a) Tractor moved onto the corner; (b) Tractor ran on the corner; (c) Tractor was on the edge of the road; (d) Tractor continued to run without overturning.

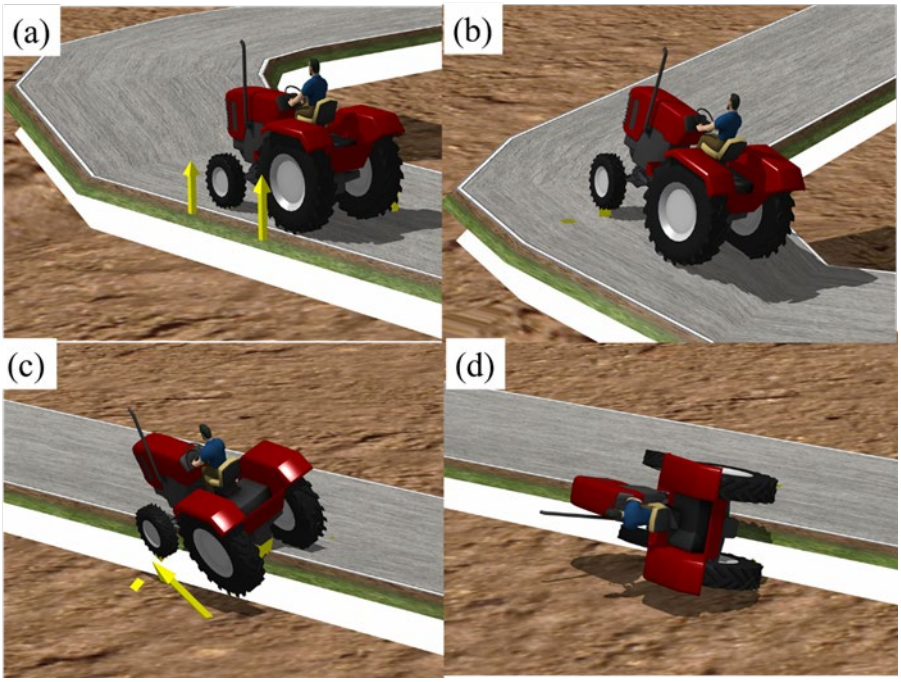

Figure 5 Animation of the tractor operation on the road with slope. (a) Tractor moved onto the slope; (b) Tractor ran on the slope; (c) The wheels went off the road; (d) Tractor overturning occurred.

Figure 6a and b show the vertical force on the front wheel and the cornering force on the front wheel, and the road elevation and the steering angle of the operator, respectively.

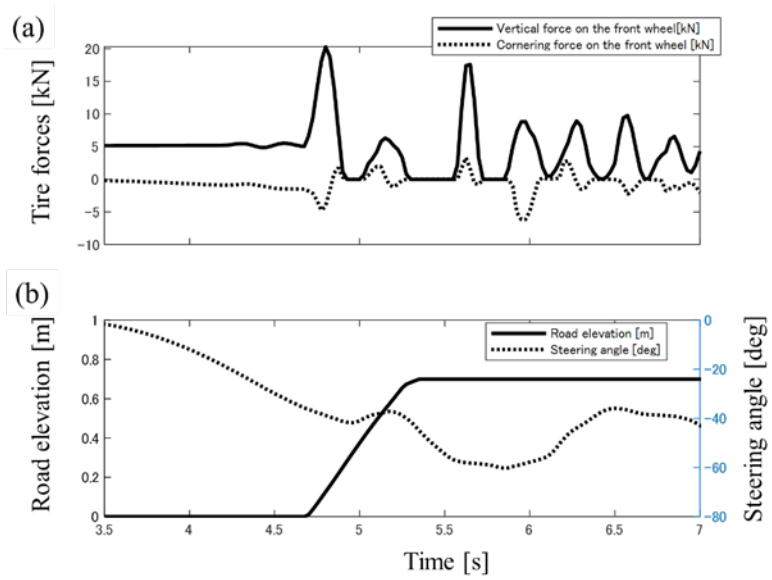

Figure 6 (a) The vertical force and the cornering force on the front wheel; (b) Road elevation and the steering angle of the operator.

When the front wheel of the tractor moved onto the slope, vibrations were induced and the vertical force on the front wheel decreased to zero as the road elevation increased. This caused the cornering force to be zero. Consequently, the operator cannot maintain control of the tractor and steering instability occurred. The steering instability caused understeer of the tractor and overturning. The results indicated that the tractor driving simulator could reproduce the steering instability which can lead to overturning.

4. CONCLUSION

The simulations of the tractor operations on the steep passage slope were conducted using the tractor driving simulator. Tractor overturning occurred in the simulation due to the steering instability. Future research will investigate how to avoid overturning by steering and develop accident prevention control for the overturning.

ACKNOWLEDGMENT

We thank Prof. Shrini Upadhyaya and Prof. Heinz Bernhardt for their kind support. This work was supported by JSPS Grant-in-Aid No. 19J11183 and 19H00959.

REFERENCES

Gonzalez, D. O., Martin-Gorriz, B., Berrocal, I. I., Morales, A. M., Salcedo, G. A., & Hernandez, B. M. (2017). Development and assessment of a tractor driving simulator with immersive virtual reality for training to avoid occupational hazards. Computers and Electronics in Agriculture, 143, 111-118.
Han, X., Kim, H. J., Jeon, C. W., Moon, H. C., Kim, J. H., & Yi, S. Y. (2019). Application of a 3D tractor-driving simulator for slip estimation-based path-tracking control of auto-guided tillage operation. Biosystems Engineering, 178, 70-85.
Ministry of Agriculture, Fishery and Forestry, (2018 February 13). Report on fatal farm accidents that happened in 2016 (in Japanese).
Retrieved from: http://www.maff.go.jp/j/press/seisan/sizai/180213.html.

SAKAI, K. (1999). Theoretical analysis of nonlinear dynamics and chaos in bouncing tractor. JOURNAL of the JAPANESE SOCIETY of AGRICULTURAL MACHINERY, 61(6), 65-71.
SAKAI, K., SASAO, A., SHIBUSAWA, S., & BUKTA, A. (2000). Experimental analysis of nonlinear dynamics and chaos in bouncing tractor. Journal of the Japanese society of agricultural machinery, 62(4), 63-70.
The Japanese Association of Rural Medicine, Case study of farm accidents. (2013 March). Case study of farm accidents in Japan II (in Japanese).
Retrieved from: http://www. maff.go.jp/j/seisan/sien/sizai/s_kikaika/anzen/23taimen. html#houkoku2.
Watanabe, M., & Sakai, K. (2019a). Impact dynamics model for a nonlinear bouncing tractor during inclined passage. Biosystems Engineering, 182, 84-94.
Watanabe, M., & Sakai, K. (2019b). Numerical Analysis of Tractor Accidents using Driving Simulator for Autonomous Driving Tractor. In Proceedings of the 5th International Conference on Mechatronics and Robotics Engineering (pp. 65-68). ACM.

Poster Session | Others (including the category of JSAM and SASJ)
[5-1130-P] Other Categories (5th)
Thu. Sep 5, 2019 11:30 AM - 12:30 PM Poster Place (Entrance Hall)

[5-1130-P-26] Classification of Salinity Damaged Spring Potato (Solanum tuberosum) using Hyperspectral Imagery based on Decision Tree Classifier

*KyungSuk Kang[1], Sae Rom Jun[1], Si Hyeong Jang[1], Jun Woo Park[1], Hye Young Song[1], Ye Seong Kang[1], Chan Seok Ryu[1], Su Hwan Lee[2] (1. GNU(Korea), 2. RDA(Korea))

Keywords: Hyperspectral imagery, Potato, Salinity, Decision tree, Classification accuracy

Salinity which is detected on reclaimed land is a major obstacle factor to crop growth. Currently, salinity is determined by experts directly examining the salinity of water and soil on farmland suspected of salinity. However, if salinity can be identified in real time and non-destructive way on the vast landfills, it can quickly respond to salinity to ensure stable cultivation. Accordingly, the objective of this paper is to verify the possibility of saline determination of non-destructively spring potatoes (Solanum tuberosum) through decision tree classifier using hyperspectral imagery of spring potatoes. In each vegetative period (VP), root formative period (RFP) and root growing period (RGP), the potatoes deal with treatment of normal watering, no-watering(drought) and salinity watering. The hyperspectral imagery of the treated potatoes was acquired at every midday. Individual potatoes canopies in hyperspectral imagery were extracted by a spectral imagery processing software (ENVI 4.7, Exeils Visual Information Solution Inc., USA). Reflectance data in the extracted canopies areas was used to classify each treatment. Calculated classification accuracy was evaluated by overall accuracy (OA) and kappa coefficient (KC). As a result, in all growth stage and treatment, the Rpart shows the highest classification accuracy. In particular, the classification accuracy was the highest between treatments OA 93.3% and KC 87.3% in the RFP that highly absorbs the moisture, and the lowest below OA 90.5% and KC 82.7% in the VP. As a classification of normal, drought and salinity using hypersepctral imagery, it showed that the possibility of salinity is different with spring potatoes in all the growth stage and it is also judged that these results can be applied as important basic results for further research to qualify and quantify salinity.

Classification of Salinity Damaged Spring Potato (*Solanum tuberosum*) using Hyperspectral Imagery based on Decision Tree Classifier

Kyung Suk Kang[1, 2], Sae Rom Jun[1, 2], Si Hyeong Jang[1, 2], Jun Woo Park[1, 2], Hye Young Song[1, 2], Ye Seong Kang[1, 2], Chan Seok Ryu[1, 2*], Su Hwan Lee[3]

[1]Division of Bio-system Engineering, Gyeongsang National Universuty, Jinju 52828, Republic of Korea
[2]Institute of Agriculture & Life Science, Gyeongsang National Universuty, Jinju 52828, Republic of Korea
[3]National Institute of Crop Science, Rural Development Administration, 54875, Jeonju, Republic of Korea

*Corresponding author: ryucs@gnu.ac.kr

ABSTRACT

Salinity which is detected on reclaimed land is a major obstacle factor to crop growth. Currently, salinity is determined by experts directly examining the salinity of water and soil on farmland suspected of salinity. However, if salinity can be identified in real time and non-destructive way on the vast landfills, it can quickly respond to salinity to ensure stable cultivation. Accordingly, the objective of this paper is to verify the possibility of saline determination of non-destructively spring potatoes (*Solanum tuberosum*) through decision tree classifier using hyperspectral imagery of spring potatoes. In each vegetative period (VP), root formative period (RFP) and root growing period (RGP), the potatoes deal with treatment of normal watering, no-watering(drought) and salinity watering. The hyperspectral imagery of the treated potatoes was acquired at every midday. Individual potatoes canopies in hyperspectral imagery were extracted by a spectral imagery processing software (ENVI 4.7, Exeils Visual Information Solution Inc., USA). Reflectance data in the extracted canopies areas was used to classify each treatment. Calculated classification accuracy was evaluated by overall accuracy (OA) and kappa coefficient (KC). As a result, in all growth stage and treatment, the Rpart shows the highest classification accuracy. In particular, the classification accuracy was the highest between treatments OA 93.3% and KC 87.3% in the RFP that highly absorbs the moisture, and the lowest below OA 90.5% and KC 82.7% in the VP. As a classification of normal, drought and salinity using hypersepctral imagery, it showed that the possibility of salinity is different with spring potatoes in all the growth stage and it is also judged that these results can be applied as important basic results for further research to qualify and quantify salinity.

Keywords: Hyperspectral imagery, Potato, Salinity, Decision tree, Classification accuracy

ACKNOWLEDGMENT

This work was performed with the support of "Development of salinity prediction technique and automatic water management by using ICT technology in reclaimed upland" (Project title: Development of salinity hazard prediction techniques for crop by using hyperspectral technology, Project No.: PJ013884042019), Rural Development Administration, Republic of Korea.

Poster Session | Others (including the category of JSAM and SASJ)
[5-1130-P] Other Categories (5th)
Thu. Sep 5, 2019 11:30 AM - 12:30 PM Poster Place (Entrance Hall)

[5-1130-P-27] Classification for Fire Blight Disease Infection Area using Vegetation Index and Background Segmentation based on Multispectral Image

*Jun-woo Park[1], Chan-seok Ryu[1], Ye-seong Kang[1], Sae-Rom Jean[1], Si-Hyeong Jang[1], Hye-Young Song[1], Kyung-Suk Kang[1] (1. GNU(Korea))

Keywords: Multispectral image, Point Cloud, Fire Blight, Vegetation index, Pear tree

Fire Blight (FB) is a bacterial virus called erwinia amylovora. The disease enters the flower or wounded area of the fruit tree, turning leaves and branches brown or black, and dies within one year. Leaves and branches dead by natural wind or pruning also fall into the orchard soil and become brown, similar to FB infection. In the aerial image for the FB discrimination of a wide orchard, there are naturally cut leaf and branches in addition to the desired FB area, which interferes with the FB discrimination.
In this study, we used the digital surface model (DSM) and vegetation index to remove unwanted areas and try to classify the FB infection area. The study area will be located on orchard A at Dokjeong-ri, Ipjang-myeon Cheonan-si, Chungcheongnam-do, Republic of Korea (36˚92'42.0224"N, 127˚22'70.6734"E) on June 7, 2018, and on June 20, it will be an orchard B at the National Institute of Horticultural &Herbal Science Pear Research Institute, Naju, Jeollanam-do, Republic of Korea (35˚01'27.9912"N, 126˚44'53.0412"E). Study equipment Unmanned aerial vehicles (UAVs) equipped with multispectral image sensors were used to acquire pear infection and non-infection multispectral images from two orchards. The acquired images were removed by using DSM generated by using the point cloud technique of Drone mapping software (Pix4D 4.3.31, Pix4D SA, Swiss) and GIS software (ArcGIS 10.5.1, Esri, USA), and the images were matched. The images were classified by FB area using vegetation index maps converted to spectral image software (ENVI 5.3, Exelis Visual Information, USA). Drone mapping software and GIS software were used to remove the background height of 100cm from the surface considering the FB area. As a result, an area of about 2,780 m² has been reduced to about 778 m². The area of the FB-infected area was estimated using the histogram and reflection values for the FB-infected and non-infected areas in the background-removed image. When histograms were used, the area of expected FB infection area was 142m² when Otsu's method was used at the NIR wavelength. When using the reflection values, a significant difference was found in the histograms of the red-red edge region and the red-NIR region, and only the overlapping regions were extracted by dividing the regions by Otsu's method. As a result, the estimated area of FB infection was reduced to 71m². As a result, removing the 100-cm-high background and then slinging certain areas of the reflection value could reduce the area of the FB-infected area the most.

Classification for Fire Blight Disease Infection Area using Vegetation Index and Background Segmentation based on Multispectral Image

Jun-Woo Park[1], Chan-Seok Ryu[1*], Ye-Seong Kang[1], Sae-Rom Jean[1], Si-Hyeong Jang[1], Hye-Young Song[1], Kyung-Suk Kang[1]

[1]Department of Bio-systems Engineering, GyeongSang National University (Instirute of Agriculture & Life Science), Jinju, Republic of Korea

*Corresponding author: ryuce@gnu.ac.kr

ABSTRACT

Fire Blight (FB) is a bacterial virus called erwinia amylovora. The disease enters the flower or wounded area of the fruit tree, turning leaves and branches brown or black, and dies within one year. Leaves and branches dead by natural wind or pruning also fall into the orchard soil and become brown, similar to FB infection. In the aerial image for the FB discrimination of a wide orchard, there are naturally cut leaf and branches in addition to the desired FB area, which interferes with the FB discrimination.

In this study, we used the digital surface model (DSM) and vegetation index to remove unwanted areas and try to classify the FB infection area. The study area will be located on orchard A at Dokjeong-ri, Ipjang-myeon Cheonan-si, Chungcheongnam-do, Republic of Korea (36°92'42.0224"N, 127°22'70.6734"E) on June 7, 2018, and on June 20, it will be an orchard B at the National Institute of Horticultural & Herbal Science Pear Research Institute, Naju, Jeollanam-do, Republic of Korea (35°01'27.9912"N, 126°44'53.0412"E). Study equipment Unmanned aerial vehicles (UAVs) equipped with multispectral image sensors were used to acquire pear infection and non-infection multispectral images from two orchards. The acquired images were removed by using DSM generated by using the point cloud technique of Drone mapping software (Pix4D 4.3.31, Pix4D SA, Swiss) and GIS software (ArcGIS 10.5.1, Esri, USA), and the images were matched. The images were classified by FB area using vegetation index maps converted to spectral image software (ENVI 5.3, Exelis Visual Information, USA). Drone mapping software and GIS software were used to remove the background height of 100cm from the surface considering the FB area. As a result, an area of about 2,780 m² has been reduced to about 778 m². The area of the FB-infected area was estimated using the histogram and reflection values for the FB-infected and non-infected areas in the background-removed image. When histograms were used, the area of expected FB infection area was 142m² when Otsu's method was used at the NIR wavelength. When using the reflection values, a significant difference was found in the histograms of the red-red edge region and the red-NIR region, and only the overlapping regions were extracted by dividing the regions by Otsu's method. As a result, the estimated area of FB infection was reduced to 71m². As a result, removing the 100-cm-high background and then slinging certain areas of the reflection value could reduce the area of the FB-infected area the most.

Keywords: Multispectral image, Point Cloud, Fire Blight, Vegetation index, Pear tree

ACKNOWLEDGMENT

This work was performed with the support of “Development of Image-based Precision Forecasting Technology for Fire Blight” (Project title: Development of a UAV-based remote sensing technology for monitoring the growth of major upland crop, Project No.: PJ012776032019), Rural Development Administration, Republic of Korea.

Poster Session | Others (including the category of JSAM and SASJ)
[5-1130-P] Other Categories (5th)
Thu. Sep 5, 2019 11:30 AM - 12:30 PM Poster Place (Entrance Hall)

[5-1130-P-28] The Static Load Test for Tractor Attached Three-Point Hitch Type Dynamometerd

*Hyo-Geol Kim[1], Sung-Bo Shim[2], Yeon-Soo Kim[1], Young-Joo Kim[1], Sang-Dae Lee[1] （1. Korea Institute of Industrial Technology(Korea), 2. Gyeongsang National University(Korea)）

Keywords: Static load test, Three-point hitch, Tractor dynamometer, Traction force, Six-component force

Due to the mechanization of agriculture and the aging of the countryside, the use of tractors and tractor machines is increasing. The tractor generates a force between the tractor and the implement, which depends on the soil properties and moisture content. The tractor travels and generates traction force, generates vertical force for maintains the position of the implement, and creates lateral forces by rolling and soil surfaces. It also interacts with the soil and causes moment in the same direction. These forces act as stresses on the tractor and the implement, causing fatigue damage and fatigue failure on the frames and components. Accurately measuring the force generated during tractor operation can predict vulnerable parts and residual life of the tractor and machine. In this study, we developed a three-point hitch type dynamometer that can accurately measure these forces, and formulated a formula for calculating the force with the geometry of the load cell attached to the three-point hitch type dynamometer. The developed dynamometer measures six components force with a single axis load cell combination and measures the PTO torque with a strain gage and telemetry system. In addition, a static load test was conducted to verify the validity of the dynamometer. Static load tests showed an accuracy of 97% or more over the entire range, from 98.9% in the traction force direction, 99.2% in the vertical force direction and 97.4% in the lateral force direction. The accuracy of the traction direction moment was 98.2%, the vertical direction moment was 97.3%, and the lateral direction moment was 96.8%, which is more than 96% accurate in all moment sections. Therefore, the formula used in the experiment is more than 96% accurate, and the reliability of the dynamometer is more than 96%. In future studies, we will establish and verify the improved formula considering the transportation pitch caused by the three-point hitch moving.

The Static Load Test for Tractor Attached Three-Point Hitch Type Dynamometer

Hyo-Geol Kim[1], Sung-Bo Shim[2], Yeon-Soo Kim[1], Young-Joo Kim[1], Sang-Dae Lee[1*]

[1]Convergence Agricultural Machinery Group, Korea Institute of Industrial Technology, Republic of Korea
[2]Dept. of Biosystems Engineering, Gyeongsang National University, Republic of Korea

*Corresponding author: sdlee96@kitech.re.kr

ABSTRACT

Due to the mechanization of agriculture and the aging of the countryside, the use of tractors and tractor machines is increasing. The tractor generates a force between the tractor and the implement, which depends on the soil properties and moisture content. The tractor travels and generates traction force, generates vertical force for maintains the position of the implement, and creates lateral forces by rolling and soil surfaces. It also interacts with the soil and causes moment in the same direction. These forces act as stresses on the tractor and the implement, causing fatigue damage and fatigue failure on the frames and components. Accurately measuring the force generated during tractor operation can predict vulnerable parts and residual life of the tractor and machine. In this study, we developed a three-point hitch type dynamometer that can accurately measure these forces, and formulated a formula for calculating the force with the geometry of the load cell attached to the three-point hitch type dynamometer. The developed dynamometer measures six components force with a single axis load cell combination and measures the PTO torque with a strain gage and telemetry system. In addition, a static load test was conducted to verify the validity of the dynamometer. Static load tests showed an accuracy of 97% or more over the entire range, from 98.9% in the traction force direction, 99.2% in the vertical force direction and 97.4% in the lateral force direction. The accuracy of the traction direction moment was 98.2%, the vertical direction moment was 97.3%, and the lateral direction moment was 96.8%, which is more than 96% accurate in all moment sections. Therefore, the formula used in the experiment is more than 96% accurate, and the reliability of the dynamometer is more than 96%. In future studies, we will establish and verify the improved formula considering the transportation pitch caused by the three-point hitch moving.

Keywords: Static load test, Three-point hitch, Tractor dynamometer, Traction force, Six-component force

1. INTRODUCTION

Recently, as agriculture becomes mechanized and agriculture workforce ages, the use of tractors and tractor attaching implement is increasing. When a tractor is working, a force is generated between the tractor and the implement, and this force acts as a stress on the tractor and the implement. Therefore, these forces affect the fatigue and residual life of the tractor and the implement parts, and the reliability and durability of the tractor and the implement can be evaluated if these forces can be accurately measured. The Wismer-Luth et al. (1974) and Brixius (1987) model are used to predict the traction force and are the ASABE standard test method, but only the traction force is calculated and no other forces are obtained. Because it is also a predictive model, it is more inaccurate than the measured value. Therefore, the most accurate value can be obtained by directly attaching the dynamometer. Al-Jalil et al. (2001) developed an inverted U-shaped dynamometer mounted on a three-point hitch using a strain gauge. Kim

et al. (2017) performed a static load test of a dynamometer, and predicted the residual life of the combined implement. However, only two directions force and one direction moment among six directions were tested and no static load test was performed for three directions. By using a three-point hitch-mounted dynamometer, you can get the most realistic data. However, because the dynamometer is made up of six single-axis load cells, you can get more inaccurate data if the formula is not accurate or the calibration is not accurate. In this study, we formulated a formula to derive three directional forces and moments using the geometric elements of the load cell combination. In addition, a static load test was carried out using a hydraulic actuator and a surface plate to apply force to six directions and confirm that they match the formula.

2. MATERIALS AND METHODS

2.1 Three-Point Hitch Type Dynamometer

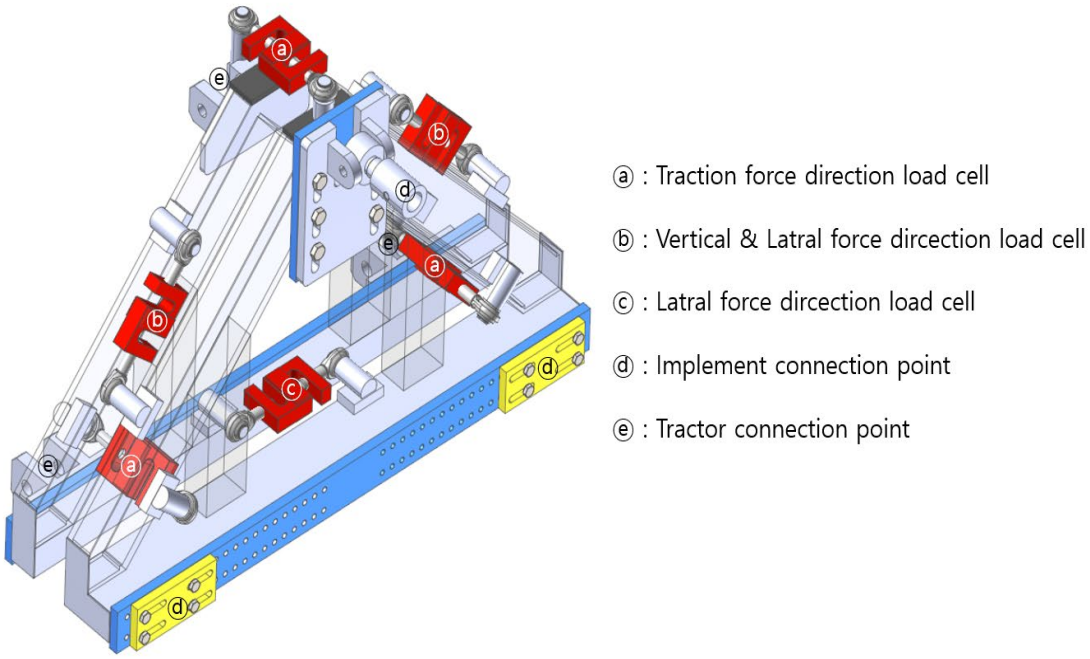

Figure 1. Dynamometer 3D Modeling.

The dynamometer is based on the Category I tractor specified in ISO Standard 730-1. Three tractor connection points are hard points, and three implement connection points are soft points. The dynamometer is connected via six single-axis load cells, and the load cell is connected to the rod end with limited spherical joint constraints at both ends. The upper hitch point connection of the implement can be adjusted by the up and down hinge hole and the lower hitch point connection is adjustable by the left-right hinge hole. The center of the dynamometer has a space for the universal joint for power connection. The dynamometer configuration is shown in Fig. 1 and the load cell specifications used in dynamometer configuration are shown in Table 1.

Table 1. Specification of Load Cell.

Model name	CAS S-Beam Type
Rated capacity (kgf)	2000
Accuracy rating	D3 / C3
Combined error (%)	≤0.03 / ≤0.02
Creep (half hour, %)	≤0.03 / ≤0.017

Proper input voltage (V)	10
Maximum input voltage (V)	15
Temperature compensation range (℃)	-10 ~ 40
Allowable temperature range (℃)	-30 ~ 80
Materials and Painting	Nickle plated steel

The three-point hitch-type dynamometer is equipped with a telemetry system using a strain gauge and a wireless transmit-receive. The strain measured at the strain gage is transmitted at the transmitter in the form of strain ratio, and the receiver interlocks with the DAQ (Data Acquisition) system and converts it into torque. The strain gage and transmitter are attached to the universal joint for power connection of the tractor and the implement. The system can measure the torque of implement that is operating with PTO (Power Take Off) power.

2.2 Dynamometer Component Force-Moment Equation

2.2.1 Component Force Equation

The force components in three directions are defined as shown in Fig 2. The traction force is defined as the sum of the pulling force direction load cell Fa, Fb, Fc. The vertical force is defined as the sum of the vertical component force of Fd and Fe. The lateral force is defined as the sum of the lateral component of Fd and Fe and Ff. The six load cells mounted on the dynamometer measure the force in each direction. Fa, Fb, and Fc detect only force in the traction direction, and Fd and Fe detect both vertical and lateral forces. Ff detects only lateral force. The angle θ that determines the vertical-lateral force is determined by the load cell mounting angle.

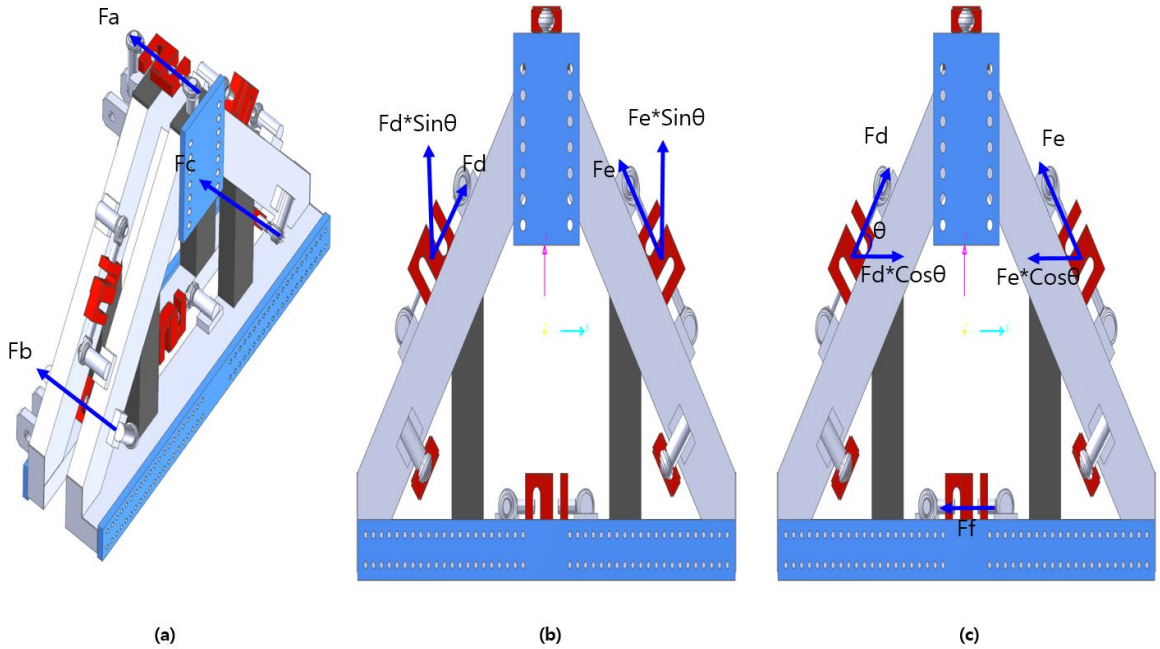

Figure 2. Force Diagram of Dynamometer
(a) : Traction Force, (b) : Vertical Force, (c) : Lateral Force.

Therefore, when the center of a triangle is defined as a reference coordinate, the force in three directions is as shown in eq. (1), (2), (3).

$$\text{Traction Force } P_T = F_a + F_b + F_c \quad (1)$$

$$\text{Vertical Force } P_V = F_d \sin\theta + F_e \sin\theta \quad (2)$$

$$\text{Lateral Force } P_H = F_d \cos\theta - F_e \cos\theta - F_f \quad (3)$$

2.2.2 Moment Force Equation

The Moment forces in three directions are defined as shown in Fig 3. The moment force is calculated by the moment balance equation when looking at the dynamometer in the 3-axis direction. The traction direction moment is calculated as the moment balance equation when viewed from the front view of the dynamometer. The vertical force moment is calculated as the moment balance equation when viewed from the top view. The lateral force moment is calculated as the moment balance equation when viewed from the side view.

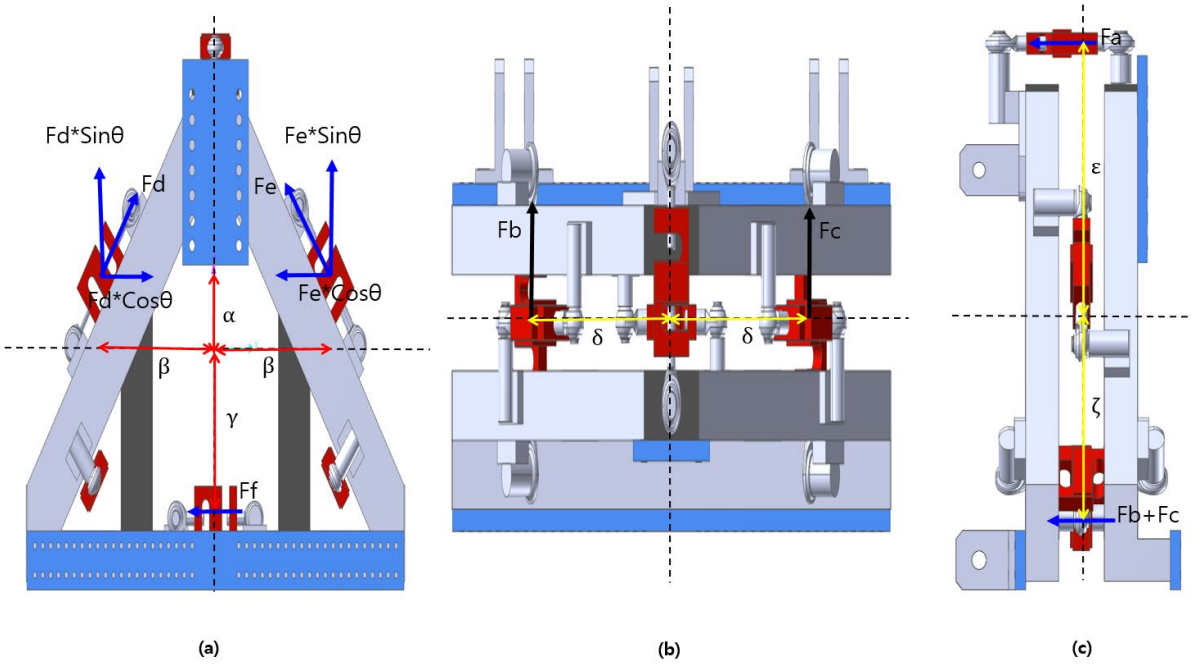

Figure 3. Moment Force Diagram of Dynamometer
(a) : Traction Moment, (b) : Vertical Moment, (c) : Lateral Moment.

The length of the moment arm is determined by the geometry of the dynamometer. The beta value is the same on both sides, and the delta value is also the same. Moment balance equation formulated using force and moment arm length is shown in Eq. (4), (5) and (6). The moment force is positive in the clockwise direction and negative in the counterclockwise direction.

$$\text{Traction Moment } M_T = (F_d \sin\theta\,\beta) + (F_d \cos\theta\,\alpha) - (F_e \sin\theta\,\beta) - (F_e \cos\theta\,\alpha) + (F_f\gamma) \quad (4)$$

$$\text{Vertical Moment } M_V = (F_b\delta) - (F_c\delta) \quad (5)$$

$$\text{Lateral Moment } M_H = \zeta(F_b + F_c) - (F_a\varepsilon) \quad (6)$$

2.3 Data Collection System

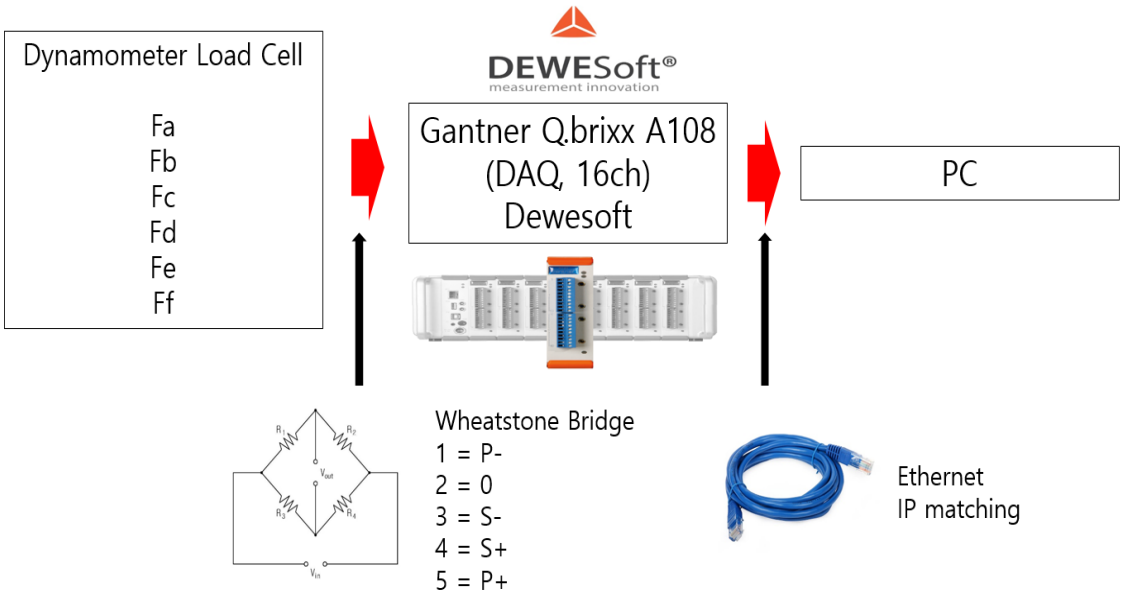

Figure 4. Data Collection Diagram of Six Load Cells.

Fig 4 shows the data collection diagram of six load cells. Six load cells are connected to the data acquisition device through the Wheatstone bridge, and the data acquisition device matches the IP with the PC and Ethernet cable and collects the data.

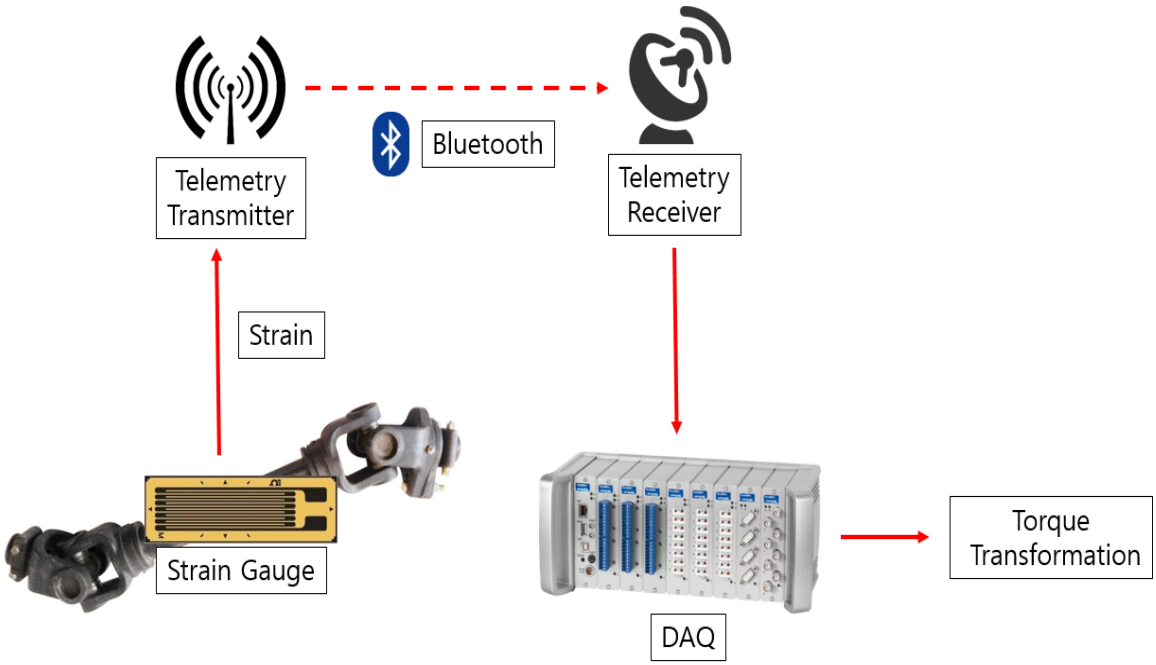

Figure 5. Data Collection Diagram of PTO Torque Telemetry.

Fig 5 shows the data collection diagram of PTO torque telemetry. The strain gauge is connected to the telemetry transmitter through the normal wire, and the transmitter and the receiver are connected by BLUETOOTH. The receiver is connected to the DAQ by the I/O cable, and finally the strain is converted to torque in the program.

2.4 Test Method

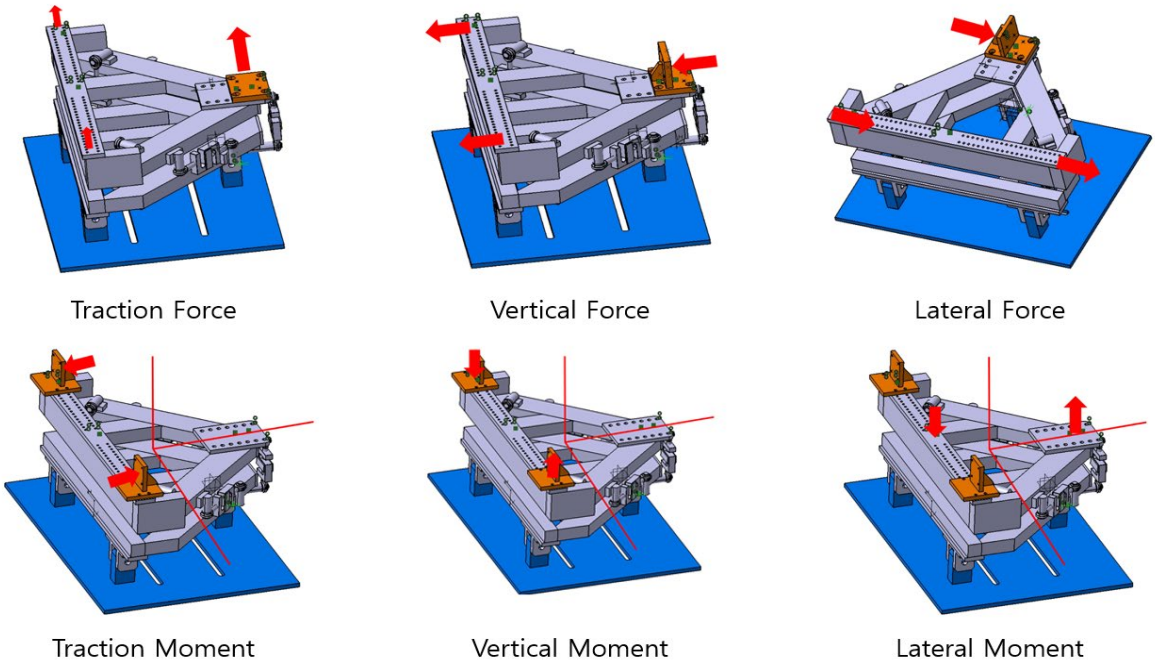

Figure 6. Hydraulic Actuator Power Direction.

1. Fix the dynamometer hard point (tractor connection side) to the jig and place it on the surface plate.
2. Apply force as shown in Table 2. At this time, the force is set to be a peak at 90 seconds.
3. Each value calculated by the formula is measured and compared with the value calculated by the actual force.

Table 2. Hydraulic Actuator Force Magnitude

	Applied Force (kgf)			
	Top	Bottom Left	Bottom Right	Sum
Traction Force	500	500	500	1500
Vertical Force	500	250	250	1000
Lateral Force	250	125	125	500
Traction Moment		500	-500	0
Vertical Moment		500	-500	0
Lateral Moment	500	-500		0

3. RESULTS AND DISCUSSION

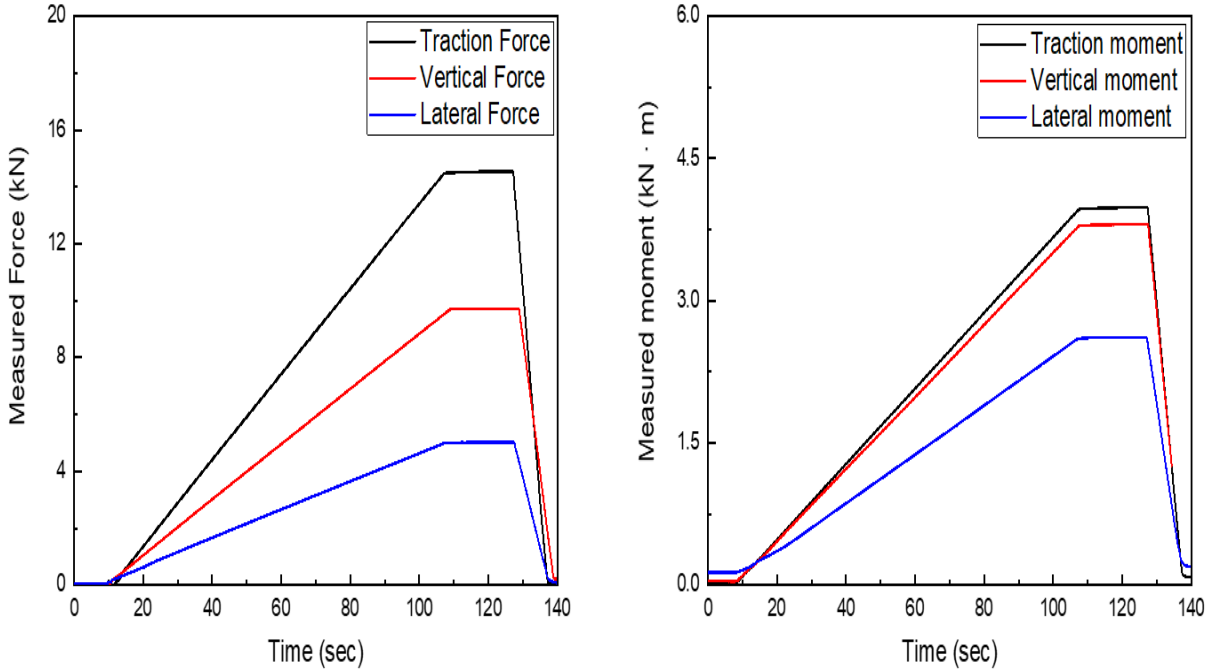

Figure 7. Measured Force and Moment.

Figure 6 and Table 3 show the measured forces when the force of Table 2 is applied. The force is multiplied by the gravity acceleration g to represent the Newton unit system. The moment force is calculated by multiplying the vertical distance between the hydraulic actuator and the center of the dynamometer.

Table 3. Applied Force and Measured Force.

	Applied Force (kN)	Measured Force (kN)	Accuarcy (%)
Traction Force	14.709	14.551	98.9
Vertical Force	9.806	9.732	99.2
Lateral Force	4.903	5.032	97.4
Traction Moment	3.912	3.983	98.2
Vertical Moment	3.912	3.807	97.3
Lateral Moment	2.535	2.619	96.8

As a result of the experiment, the accuracy of 96% or more was obtained in all the sections and satisfactory reliability was secured. The small errors in the component force tests are expected to be due to manufacturing error and misalignment when joining the surface plates. The small error of the moment force test is expected to be the measurement error of the manufacturing error and the moment arm length. The maximum accuracy of 99.2% and the minimum accuracy of 96.8% were calculated for the whole test period, and the dynamometer is considered reliable even considering the error rate.

4. CONCLUSION

This study was conducted to verify the reliability of three-point hitch type dynamometer and static test was conducted to verify reliability. The conclusion of this study is as follows.

1) Since the dynamometer is composed of a single axis load cell combination, the three direction force of traction force - vertical force - lateral force is calculated by the component force equation.

2) Likewise, the traction moment - vertical moment - lateral moment is also calculated by the moment balance equation.
3) The forces calculated by the component force equation are compared with the forces actually applied by the hydraulic actuator. As a result, the accuracy of 99.2% and 96.8% was obtained.
4) A small amount of error is expected to be due to manufacturing errors, surface plate mounting error, moment arm length measurement error, and the dynamometer is considered reliable.

ACKNOWLEDGMENT

This work was supported by the Technology Innovation Program (or Industrial Strategic Technology Development Program (KM190022, Development of an autonomous sprayer suitable for atypical road surface of an actual orchard) funded By the Ministry of Trade, Industry & Energy (MOTIE, Korea)

REFERENCES

1. Wismer. R. D., H. J. Luth. (1974). Off-road traction prediction for wheeled vehicles: *Transactions of the ASAE,* 17(1), 8-14. https://doi.org/10.13031/2013.36772
2. Brixius, W. W. (1987). Traction prediction equations for bias ply tires: *Transactions of the ASAE*, 87-1622.
3. Al-Jalil. H. F., Khdair. A., Mukahal. W. (2001). Design and performance of an adjustable three-point hitch dynamometer: *Soil and Tillage Research., 62*(3), 153-156. https://doi.org/10.1016/S01671987(01)00219-7
4. Kim. Y. K., Moon. S. G., OH. C. M., Han. J. W. (2017). Working Load Measurement using 6-Component Load Cell and Fatigue Damage Analysis of Composite Working Implement: *Journal of Agricultural, Life and Environmental Sciences*., *29*(3), 225-236. https://doi.org/10.12972/jales.20170021
5. Koo. Y. M., Hong. J. G., Han. J. W., Ha. Y. S. (2018). Operating Power and Draft Performance of an Integrated Tractor Implement for Flat Ridge Preparation: *Journal of Agriculture & Life Science*., *52*(4), 137-150. https://doi.org/10.14397/jals.2018.52.4.137
6. ISO Standards. (2009). ISO 730-1: Agricultural wheeled tractors — Rear-mounted three-point linkage — Categories 1N, 1, 2N, 2, 3N, 3, 4N and 4.

Poster Session | Others (including the category of JSAM and SASJ)
[5-1130-P] Other Categories (5th)
Thu. Sep 5, 2019 11:30 AM - 12:30 PM Poster Place (Entrance Hall)

[5-1130-P-29] Isolation and Identification of Acetic Acid Bacteria from Philippine Fermented Rice Cake Batters by 16S rRNA Gene Sequence Analysis

Audrey Mae Villamin Orillaza[1], Honey Bhabes R Iñigo[1], *Baby Richard Ragudo Navarro[1] (1. Institute of Food Science and Technology, College of Agriculture and Food Science, University of the Philippines Los Bañ os(Philippines))

Keywords: Acetic acid bacteria, fermented rice cake, 16S rRNA sequence analysis, phylogenetics

As part of our work to study the microflora of Philippine traditional fermented foods, batters from fermented rice cakes, or *puto* in the vernacular, from different parts of the Philippines were sampled and used for the isolation, screening and purification of acetic acid bacteria (AAB) by culture-based methods. Pure AAB isolates were then identified by DNA-based methods [i.e., cetyl trimethylammonium bromide (CTAB) DNA extraction, polymerase chain reaction (PCR), and 16S rRNA gene sequence analysis], DNA base composition determination, phenotypic characterization, and phylogenetic analysis. Six isolates were obtained from three types of rice cake batter: *puto* Calasiao, *puto* Lanson, and *puto* Boac batters. The AAB isolates were identified to belong to the genera *Acetobacter* at 94-99% homology with DNA base compositions ranging from 54.40-55.74 mol% GC content. The isolates were Gram-negative, catalase-positive rods that oxidize ethanol to acetic acid and grow in mannitol agar and in most sugars. None of them were cellulose producer or motile. 02CPPu1-2 produced a water-soluble brown pigment in glucose-yeast extract-peptone (GYP) medium and 24BMTa2-3 yielded γ-pyrones from D-glucose. From the phylogenetic tree deduced from the 16S rRNA gene sequence analysis results, the isolates clearly formed an independent clade distinct from the type strains of other genera of acetic acid bacteria. The *puto* Lanson and *puto* Boac batter isolates were closely related to *A. pasteurianus* and *A. lovaniensis*, respectively. On the other hand, the *puto* Calasiao isolates were associated with none of the type species of AAB. Overall, our data suggest that the fermented rice cake batter isolates comprise a possibly newspecies of acetic acid bacteria under the genus Acetobacter. This is very interesting considering that all the isolates were sourced from batters of only traditionally fermented rice cakes. DNA-DNA hybridization and detailed phenotypic characterization are recommended to verify this new species possibility, which may be linked the difference in geographical location, raw material and processing technique employed in traditional rice cake making in the Philippines.

Isolation and Identification of Acetic Acid Bacteria Isolates from Philippine Fermented Rice Cake Batters by 16S rRNA Gene Sequence Analysis

Audrey Mae V. Orillaza,* Honey Bhabes R. Iñigo, and Baby Richard R. Navarro

Institute of Food Science and Technology, College of Agriculture and Food Science, University of the Philippines Los Baños, Philippines

*Corresponding author: avorillaza@up.edu.ph

ABSTRACT

As part of our work to study the microflora of Philippine traditional fermented foods, batters from fermented rice cakes, or *puto* in the vernacular, from different parts of the Philippines were sampled and used for the isolation, screening and purification of acetic acid bacteria (AAB) by culture-based methods. Pure AAB isolates were then identified by DNA-based methods [i.e., cetyl trimethylammonium bromide (CTAB) DNA extraction, polymerase chain reaction (PCR), and 16S rRNA gene sequence analysis], DNA base composition determination, phenotypic characterization, and phylogenetic analysis. Six isolates were obtained from three types of rice cake batter: *puto* Calasiao, *puto* Lanson, and *puto* Boac batters. The AAB isolates were identified to belong to the genera *Acetobacter* at 94-99% homology with DNA base compositions ranging from 54.40-55.74 mol% GC content. The isolates were Gram-negative, catalase-positive rods that oxidize ethanol to acetic acid and grow in mannitol agar and in most sugars. None of them were cellulose producer or motile. 02CPPu1-2 produced a water-soluble brown pigment in glucose-yeast extract-peptone (GYP) medium and 24BMTa2-3 yielded γ-pyrones from D-glucose. From the phylogenetic tree deduced from the 16S rRNA gene sequence analysis results, the isolates clearly formed an independent clade distinct from the type strains of other genera of acetic acid bacteria. The *puto* Lanson and *puto* Boac batter isolates were closely related to *A. pasteurianus* and *A. lovaniensis*, respectively. On the other hand, the *puto* Calasiao isolates were associated with none of the type species of AAB. Overall, our data suggest that the fermented rice cake batter isolates comprise a possibly newspecies of acetic acid bacteria under the genus Acetobacter. This is very interesting considering that all the isolates were sourced from batters of only traditionally fermented rice cakes. DNA-DNA hybridization and detailed phenotypic characterization are recommended to verify this new species possibility, which may be linked the difference in geographical location, raw material and processing technique employed in traditional rice cake making in the Philippines.

Keywords: Acetic acid bacteria, fermented rice cake, puto, 16S rRNA sequence analysis, CTAB method, DNA extraction, phylogenetics

1. INTRODUCTION

The Philippines, a tropical country in Southeast Asia, is recognized as one of the centers of microbial diversity. This is in part due to the various traditional methods of food preservation in the country. An archipelago of 7107 islands, it has different food preservation methods that vary among islands, and hence a wide array of fermented foods (Sanchez, 2008) consumed throughout the archipelago, which are part and parcel of our culture (Banaay et al., 2013). However, it is common knowledge that the market of traditional Philippine fermented foods has always remained local, for instance, domestic for *bagoong*, *patis*, *alamang*, and *suka*, regional for some such as *buro* and *tuba*, and even provincial for some such as *etag, pindang*, *bahalina*, and native *longanisa* (i.e., *longanisang* Vigan and Lucban). In fact, a few of our traditional fermented foods such as *sabeng* and *tengba* never reach the market, their production only linked to festivities that celebrate the richness or sanctity of our indigenous cultures.

This is unfortunate considering that the top 5 most consumed food items in the US are all fermented foods, namely, beer, bread, cheese, wine and fermented meat in descending order. Moreover, with the trend in globalization, a few Asian fermented food products have already seeped through the changing Western culinary landscape, with soy sauce now considered the most used condiment not only in Asia but also in the world, while a few such as *kimchi* and fish sauce are slowly finding their niche in international cuisines. Thus said, there is clearly an explosive market that awaits other fermented foods in the future with the increasing population and intensifying food insecurity across the globe. It is therefore vital that active up-to-date research on traditional Philippine fermented foods be carefully carried out with the purpose of making them at par, in terms of quality and product image and design, with fermented foods of other countries that have reached global commercialization. Note that, in recent years, traditional fermented foods have become increasingly relevant not only because of their guaranteed safety, high nutritional quality or unique sensory profile, but also because of their potential huge market contribution, as proved by the global probiotic market projected to reach USD 46.6 billion by 2020, with Europe as the largest and Asia-Pacific region as the fastest-growing markets (Elegado et al., 2016).

Currently, there is a dearth of solid statistics concerning our traditional fermented foods, most likely linked to the limited market and consumer research on them. Nonetheless, it is unequivocal that our traditional fermented foods can stand up to those of other countries in terms of flavor, nutritional value and health benefits. It is only the lack of consistent quality and use of non-standardized and unhygienic manufacturing processes that have relegated our food products to their local status and inferior image. In addition, since most of the traditional food fermentation industries in the Philippines are rural, seasonal, labor-intensive, informal, and capital-deficient, their supply remains much too limited to establish a huge market such that their market and ultimately their consumption remain confined only to places where they are produced. Also, most producers of our traditional fermented foods are local farmers, fisherfolks, and housewives who are poor and capital-deficient, which logically dictates the choice of the least expensive methods of production (even if these methods are non-GMP-compliant and non-HACCP-certified) as well as understandably highlight the need for easy money turn-over (vending “unripe” products), which often result in compromised product qualities and products that do not reach their full bloom. Lastly, there is extremely limited scientific and technological knowledge about our traditional fermented food products, particularly about their microbial and biochemical aspects because of the lack of research institutes passionate for, dedicated to, and fully equipped for research and development of our traditional fermented food products. (Only large private food industries are technologically equipped for food science research, most of which however neither prioritize nor sense the importance of our traditional food products.) This is in large contrast to the comprehensive research knowledge on wine and cheese in France, on balsamic vinegar in Italy, on soy sauce in Japan, and on *kimchi i*n Korea, which perhaps explain why these fermented food products, unlike ours, command global respect, as these products are continuously being researched and polished to perfection. These might as well be the reasons behind the meager research on Philippine traditional fermented food products, as well as behind the insignificant contribution of the fermentation food industry to our gross domestic products compared with that of the agricultural industry. But the crux of the matter is this: without research on our fermented foods, there will be no improvement in them; without improvement, there will be no increase in their market share; without an increase in market share, there will be no research attention on them. Therefore, it is crucial that extensive research on Philippine fermented foods be carefully performed if such food products are to infiltrate the global food market. This could be started through the use of genotypic methods side by side with biomolecular analyses in conducting an in-depth accurate analysis of the fermenting microflora (including unculturable microorganisms) of these fermented foods.

Thus, as part of our comprehensive research on Philippine fermented foods, in this study, we isolated, screened, purified and identified acetic acid bacteria (AAB) from batters of traditionally fermented rice cakes by culture-based methods and molecular methods. We focused on acetic acid bacteria since in previous works, lactic acid bacteria (e.g., *Leuconostoc mesenteroides*, *Streptococcus faecalis*, and *Lactobacillus plantarum*) and yeasts (e.g. *Saccharomyces cerevisiae*) have already been isolated from fermented rice cake batters; these microorganisms are expected as they are commonly associated with cereal fermentation (Kelly, Asmundson, Harrison, & Huang, 1995; Sanchez, 1999; Tamang et al., 2016; Uchimura, Garcia, & Flores, 1984). We consider it interesting to determine the proliferation of

other fermentative microorganisms such as acetic acid bacteria (AAB) in rice cake fermentation. Our objectives were to isolate, identify and characterize AAB from different Philippine traditional fermented rice cakes.

2. MATERIALS AND METHODS

2.1 Sampling

Fermenting batters from local fermented rice cakes were obtained on site or purchased from local producers and processed for AAB isolation by inoculating a loopful of each batter onto glucose-yeast extract-peptone (GYP) slants within 12 h of collection and incubating it at room temperature. The slants were kept in an ice box once growth had been observed.

2.2 Isolation, screening, purification, and storage

In the laboratory, 5 mL of sterile physiological saline solution (PSS) was added to each GYP slant with growth, and the cell culture was suspended by aseptically scraping it using a wire loop and then vortexing the mixture. Appropriate dilutions of the suspension were then spread-plated on GYP agar plates with $CaCO_3$ and then incubated at 30°C for 18-48 h. Colonies that formed a zone of clearing on the GYP agar plates were then individually transferred onto GYP slants and incubated as described above. The cultures were again suspended in PSS, and appropriate dilutions of the suspension were then streaked on GYP agar plates with $CaCO_3$ as acid production indicator. The plates were then incubated at 30°C for 18-48 h. After incubation, colonies with a zone of clearing were picked up and again transferred onto GYP slants. Resuspension and replating were repeated several times until visual and microscopic examinations of colonies and cells of each isolate showed homogenous morphological characteristics. The pure isolates were then subjected to Gram staining by the Hucker method (Hucker & Conn, 1923) and to catalase test using the method of MacFaddin (2000). Only pure isolates from GYP agar that were Gram-negative and catalase-positive were presumed to be AAB and stored in glycerol solution.

2.3. DNA extraction

DNA was extracted from each AAB isolate using a modified cetyl trimethylammonium bromide (CTAB) DNA extraction protocol (Wilson, 1987). 5 mL of 24-h GYP broth culture at 30ºC was centrifuged at 12,000 rpm for 45 s at room temperature. The cell pellet obtained was suspended in 200 µL of Tris-EDTA (TE) buffer (pH 8), to which 25 µL of 10% sodium dodecyl sulfate (SDS) and 5 µL of 25 mg mL^{-1} proteinase K were added. The mixture was then incubated with gentle shaking at 37ºC for 1 h. The resulting viscous lysate was added with 45 µL of 5 M sodium chloride (NaCl) and 40 µL of CTAB solution (10% CTAB in 0.7 M NaCl), and then with an equal volume of chloroform:isoamyl alcohol (24:1); this was left to stand for 10 min, centrifuged at 12,000 rpm for 10 min at room temperature, added with an equal volume of cold isopropanol, and mixed gently. The resulting mixture was centrifuged at 8,000 rpm for 5 min at 4ºC, and the supernatant was decanted to obtain a DNA pellet, which was then washed with 1 mL of 70% ethanol by centrifugation at 12,000 rpm for 5 min at 4ºC. The supernatant was discarded, and the remaining precipitate was air-dried for 5-10 min and redissolved in 100 µL of TE buffer. This DNA solution was subjected to spectrophotometry and agarose gel electrophoresis to confirm its purity and quality, respectively.

2.4. Polymerase chain reaction (PCR) amplification

PCR amplification was done based on the optimized protocol of Dalmacio et al. (2011), in which the V1-V8 region of the 16S rRNA gene was amplified using universal primers: 8F (5' AGAGTTTGATCCTGGCTCAG 3') and 1492R (5' GGTTACCTTGTTACGACTT 3'). The PCR reaction mixture (1x TE buffer, 0.5 U Taq polymerase, 0.3 µM each of the bacterial 8f and 1492r primers, 1.5 mM $MgCl_2$, 0.2 mM dNTP, ≥ 30 ng/µL template DNA, and nanopure water) was subjected to an optimized amplification program as follows: initial denaturation at 94ºC for 5 min, 35 cycles of denaturation at 94ºC for 1 min, annealing at 53ºC for 1 min, and elongation at 72ºC for 1.75 min, and final elongation at 72ºC for 5 min. The PCR products were subjected to electrophoresis on 1.0% (w/v) agarose gel with 0.5x Tris-acetate EDTA (TAE) buffer and visualized using ethidium bromide for confirmation of the desired length of 1.5 kb.

2.5. 16S rRNA gene sequencing

The amplified DNAs of the AAB isolates were sent to First Base Laboratories in Malaysia for 16S rRNA gene sequencing using the same primers mentioned above and determined of their identity

and % homology to type strains of different species of acetic acid bacteria using the Basic Local Alignment Search Tool (BLAST) (https://blast.ncbi.nlm.nih.gov/Blast.cgi).

2.6. Determination of DNA base composition

DNA base composition expressed as mol% GC content was determined using an online GC calculator (http://www.endmemo.com/bio/gc.php).

2.7. Phenotypic characterization

Cell form was determined by growing AAB isolates on GYP agar. Unless otherwise stated, the isolates were incubated at 30ºC for 18-48 h. The oxidation of ethanol to acetic acid as indicated by a zone of clearing after 2-3 days of incubation, and catalase production as indicated by evolution of gas were tested in GYP agar with $CaCO_3$. Motility was also determined by growing the isolates in soft GYP agar stabs. The formation of cellulose and a water-soluble brown pigment was examined by visual observation in GYP broth and agar cultures, respectively. The production of dark brown γ-pyrones from D-glucose and D-fructose was determined by adding $FeCl_3$ to 11-day broth cultures. Growth in mannitol agar and various sugars (i.e., D-glucose, D-fructose, D-xylose, D-sucrose, D-galactose, D-sorbitol, D-maltose, and D-starch) in broth cultures was also determined.

2.8. Phylogenetic analysis

DNA sequences of the AAB isolates and type species of the 14 valid AAB genera (i.e., *Acetobacter, Glunocobacter, Gluconoacetobacter, Ameyamaea, Tanticharoenia, Asaia, Swaminathania, Kozakia, Neoasaia, Granulibacter, Acidimonas, Komagataeibacter, Saccharibacter*, and *Neokomagataea*) (Mamlouk & Gullo, 2013) were subjected to multiple sequence alignment using CLUSTAL W and the neighbor-joining method (Saitou & Nei, 1987) with 1000 bootstrapping replicates (Felsenstein, 1985) to construct the phylogenetic tree (Nei & Kumar, 2000) using Mega X software (Kumar, Stecher, Li, Knyaz, & Tamura 2018).

3. RESULTS AND DISCUSSION

3.1. Sampling and isolation, screening and purification of AAB isolates

Samples of batter from four types of local fermented rice cakes (i.e., *puto Calasiao* from Calasiao, Pangasinan; *puto* Lumban from Lumban, Laguna; *puto* Lanson from Irosin, Sorsogon; and *puto* Boac from Boac, Marinduque) procured from their towns of production were used in AAB isolation. Initially, seven isolates with acid production ability in GYP agar were isolated. This number was whittled down to six aerobic, acid-producing, Gram-negative, catalase-positive, ellipsoidal to rod-shaped isolates after preliminary characterization and purification. The six isolates were sourced from *puto* Calasiao, *puto* Lanson, and *puto* Boac batters; no isolates were obtained from the *puto* Lumban batter.

The predominant microorganisms in fermented rice cakes include LAB and yeasts such as *Leuconostoc mesentoides, Streptococcus faecalis*, *Lactobacillus delbrueckii*, *Lactobacillus fermenti*, *Lactobacillus lactis*, *Pediococcus cerevisiae*, *Geotrichum candidum*, *Torulopsi holmii*, *Torulopsi candida* and *Trichospora pibulans*, which have been isolated from *idli*, *dosa* and *dhokla*, varieties of steamed blend of rice and black gram (*Phaseolus mungo*) in India (Blandino et al., 2003), as well as *Lactobacillus casei*, *Lactobacillus brevis*, *Leuconostoc mesenteroides* and *Saccharomyces cerevisiae*, which are found in *jeung-pyun*, a sponge-like bread in Korea (Park et al., 2017). However, AAB have been shown to be in symbiotic relationship with LAB and yeasts in *jiaozi*, a traditional steamed bread in China. Li et al. (2016) have identified *Acetobacter tropicalis* (22.8%), together with *Saccharomyces cerevisiae* (42.9%), *Pediococcus pentosaceus* (38.6%), *Wicherhamomyces anomalus* (27.0%), *Lactobacillus plantarum* (24.3%), *Saccharmomycopsis fibuligera* (22.2%), *Torulaspora delbrueckii* (7.9%), *Enterococcus durans* (5.7%), *Bacillus cereus* (2.9%), and *Enterococcus faecium* (1.4%) in *jiaozi* by combined culture-based method and PCR-DGGE analysis. One possible reason for AAB seemingly being the minor microflora in fermented rice cakes is their late proliferation in the fermenting batter, growing only after yeasts and LAB have already taken hold during fermentation. Thus, their growth is hindered by the predominance of these earlier colonizers of the fermenting batter, such that they only exist in very small numbers. At such small numbers, they are not generally isolated by traditional culture-based methods using common growth media, being classified as 'VBNC'. Another possible reason for the low AAB load in *puto* batter is linked to the inherent nature of AAB. AAB generally thrive in the natural environment (e.g., soil, herbs, fruit, and flowers) and a wide variety of fermentation substrates (Crotti et al., 2010) that are good sources of simple sugars, not

starch.

3.2. Molecular identification of AAB isolates

Through the alignment of their DNA nucleotide sequences to sequences in the BLAST database, the six potential AAB isolates were all confirmed to share 94-99% nucleotide sequence homologies to known species of acetic acid bacteria belonging to the genus *Acetobacter*. The four isolates of *puto* Calasiao showed >94% homologies with the following AAB species indicated: 02CPPu1-2 with *Acetobacter orientalis* (at 94% homology), 02CPPu2-1 with *Acetobacter persici* (at 95%) and both 02CPPu2-2 and 02CPPu3-1 with *Acetobacter malorum* (at 98 and 99%, respectively). The isolates from *puto* Lanson (12ISPu1-1) and *putong* Boac, on the other hand, were found to have 97 and 99% homologies with *Acetobacter pasteurianus* and *Acetobacter lovaniensis*, respectively.

The DNA base contents of the six AAB isolates ranged from 54.40 to 55.74 mol% GC content (Table 1), which fit the DNA base content range of the genus *Acetobacter*.

Table 1. Phenotypic characteristics and DNA base composition of AAB isolates from local fermented cake batter.

Test	Isolate Code					
	02CPPu1-2	02CPPu2-1	02CPPu2-2	02CPPu3-1	12ISPu1-1	24BMTa2-3
A. Cell form	short rods	short rods	ellipsoidal to rods	ellipsoidal to rods	rods	rods
B. Oxidation of ethanol to acetic acid	+	+	+	+	+	+
C. Catalase test	+	+	(+)	+	+	+
D. Cellulose production	-	-	-	-	-	-
E. Formation of brown soluble pigment	+	-	-	-	-	-
F. Motility test	-	-	-	-	-	-
G. Γ-pyrones from sugars						
D-glucose	-	-	-	-	-	+
D-fructose	-	-	-	-	-	-
H. Growth in MYPA	+	+	+	+	+	+
I. Growth in sugars						
D-glucose	+	+	+	+	+	+
D-fructose	+	+	-	+	+	+
D-xylose	+	+	-	-	+	+
D-sucrose	+	+	+	+	+	-
D-galactose	-	-	+	+	+	(+)
D-sorbitol	+	+	+	(+)	+	+
D-maltose	+	+	+	-	+	(+)
D-starch	+	+	+	+	+	+
J. G+C content (mol%)	55.03	55.45	55.74	55.33	55.84	54.40

Positive, +; negative, -, weak, (+)

In this study, the AAB isolates from the batters of three of the rice cakes sampled, namely, *puto* Calasiao, *puto* Lanson, and *puto* Boac, were found to belong to the genus *Acetobacter*, differently from those of the *puto* Lumban batter. According to Raspor and Goranovic (2008), *Acetobacter* strains

prefer alcohol-enriched environments, which explain the presence of *Acetobacter* in the fermented rice cake batter samples. Note that all the batter samples were obtained in the late fermentation stage prior to steaming or baking, and hence fermentation by yeasts and/or lactic acid bacteria is almost complete, making the conditions in the fermenting batter supportive of AAB growth, that is, rich in alcohol as a result of the alcoholic fermentation by yeasts and with a slightly acidic pH of approximately 5.0 as a result the addition of lye, sugar and other flavoring ingredients, which bumped up the low batter pH of approximately 3.5 caused by lactic acid production by LAB. Furthermore, *Acetobacter* species have an optimum growth pH range of 5-6.5 (although they can grow even as low as pH 3-4) at 28-30 ºC (Mamlouk & Gullo, 2013), the very same conditions present in local fermented rice cake batter.

3.3. Phylogenetic relationship among AAB isolates

From the phylogenetic tree (Fig. 1) constructed based on the alignment of 905 bp 16S rRNA gene sequences, all the AAB isolates from the local fermented rice cake batter samples distinctly clustered with the type strains of all known *Acetobacter* species, separate from the other type species of other AAB genera. Moreover, our isolates formed an independent clade together with *A. pasteurianus* and *A. lovaniensis*. 12ISPu1-1 and 24BMTa2-3 from *puto* Lanson and *puto* Boac batters corroborated their BLAST database homologies to *A. pasteurianus* and *A. lovaniensis*, respectively. On the other hand, all four isolates from *puto* Calasiao batter interestingly formed a tight-knit clade not associated with the AAB species to which they had high % homologies based on BLAST alignment results.

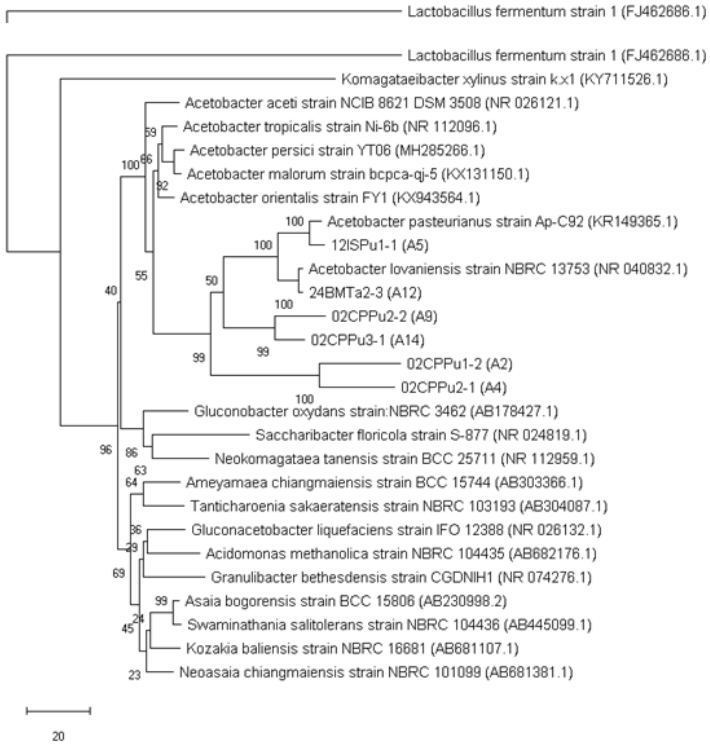

Fig. 1. Phylogenetic relationships of AAB isolates from 16S rRNA gene sequence clustering. The tree was made based on an alignment of 905 bp of 16S rRNA gene sequences and constructed by neighbor-joining method. Numbers indicate the bootstrap percentage values derived from 1000 replications. Sequences used in this study are represented in sample codes. *Lactobacillus fermentum* strain 1 (GenBank accession number FJ462686.1) is used as an outgroup.

Interestingly, despite the differences in preparation method, ingredients and geographic location of *puto* Calasiao, *puto* Lanson, and *puto* Boac, all the AAB species isolated from all three fermented rice cakes were of the same genus, *Acetobacter.* This suggests that similar microorganisms are at work in the fermentation of our local fermented rice cakes, regardless of type. This is evident in in the deduced phylogenetic tree of the six isolates together with the type strains of all valid *Acetobacter* species and the type species of the other 13 valid AAB genera. Despite the homology data obtained from the nucleotide sequence alignment with the BLAST database suggesting the wide variety of species (i.e., *A. malorum*, *A. persici*, *A. tropicalis*, *A. pasteurianus*, and *A. lovaniensis*) responsible in rice cake

fermentation, results of the phylogenetic analysis indicate otherwise. All our six isolates formed a highly distinct clade, with the four isolates from *puto* Calasiao forming a clade that is entirely separate from all known valid *Acetobacter* species. Therefore, this strongly suggests that the four aforementioned isolates constitute a new species in the genus *Acetobacter*. Thus, it is important that DNA-DNA hybridization of the *puto* Calasiao isolates with all valid *Acetobacter* species as well as quinone analysis be conducted to confirm this possibility. If confirmed, it will be highly interesting to study why a highly specific AAB microflora is associated with Philippine rice cake fermentation. This could likely lead to hitherto unknown fermentation mechanisms by AAB that utilizes starch as substrate.

3.4. Phenotypic characteristics relevant to the acetification by AAB species

As shown in Table 1, all the AAB isolates are Gram-negative, catalase-positive rods. They oxidize ethanol to acetic acid. They also grow in mannitol agar and in most of the sugar sources, particularly starch. None of them are cellulose producer or motile. 02CPPu1-2 produces a brown water-soluble pigment in GYP medium and 24BMTa2-3 yields γ-pyrones from D-glucose.

Majority of the phenotypic characteristics of the isolates were reflective of the species indicated in the BLAST homology search. Their growth in mannitol agar confirmed their identity as *Acetobacter* utilizing mannitol as an energy source. 02CPPu1-2 was noted to produce a brown water-soluble pigment, similarly to a few *Acetobacter* species such as *A. polyoxogenes* isolated from vinegar broth (Entani et al., 1985) and *A. aurantius* now under genus *Frateuria* isolated from golden-rayed lily (*Lilium auratum* Lindl.) (Swings et al., 1980), as well as to *Gluconacetobacter liquefaciens* (Navarro and Komagata, 1997). 12ISPu1-1 was observed to ferment all representative sugars in the study but its homologous species *A. pasteurianus* prefers only glucose, mannitol and ethanol as carbon sources (Konig et al., 2009). 24BMTa2-3 produced γ pyrones from D-glucose. It was also the only isolate that did not ferment D-sucrose, exactly the same as its homologous species *A. lovaniensis* (Konig et al. 2009), unequivocally confirming its identity. Furthermore, note that all the isolates fermented D-starch, the major component of rice-based products. This characteristic is not typical of *Acetobacter* species (Sievers & Swings, 2015), a possible indication of the unique fermentation mechanism conducted by these rice cake batter isolates. More importantly, this ability to grow on starch provides a strong support to the possibility not just of a new species but perhaps also of a new genus.

AAB isolates are generally associated with dough acidification, which favors LAB growth, as well as with the production of enzymes and exopolysaccharides (such as levan) resulting in the hydrolysis of biochemical compounds and in the formation of the structural network of bread in the absence of gluten proteins in rice flour, respectively (Korakli et al., 2001; Tieking et al., 2003). However, the exact role of our isolates in fermented rice cake fermentation remains to be elucidated, what with the yet to be confirmed identity of the *puto* Calasiao. Further analyses (e.g., DNA-DNA hybridization, as mentioned earlier, and detailed phenotypic characterization). Likewise, microbial succession analysis using PCR-DGGE must be conducted to determine the fermentation mechanism wherein the VBNC state of AAB can also be resolved.

4. CONCLUSION

From this study, the similarity in the fermenting microflora isolated from batters of various Philippine fermented rice cakes in Luzon was highlighted. Although a wide variety of AAB species were identified by BLAST search analysis, namely, *A. malorum, A. orientalis, A. persici*, *A. pasteurianus* and *A. lovaninensis* from fermented rice cake batters from Pangasinan, Sorsogon, and Marinduque, results of phylogenetic analysis, indicated otherwise. The deduced phylogenetic tree showed that the isolates from the *puto* Calasiao batter formed a tight-knit clade completely separate from all known species of *Acetobacter* and the other 13 genera of AAB. This points to a hitherto undiscovered group of starch-fermenting *Acetobacter* strains that may perhaps constitute a new *Acetobacter* species, at least, if not an altogether novel genus in the family Acetobacteraceae.

ACKNOWLEDGMENT

We thank the UP OVPAA *Balik* Scientist Program for the financial support, and the UPLB Institute of Animal Science for granting us access to the equipment and facility used in the study.

REFERENCES

Banaay, C.B., Balolong, M.P. and Elegado, F.B. 2013. Chapter 4: Lactic acid bacteria in Philippine traditional fermented foods. In: R&D for food, health and livestock purposes. InTech. pp. 571-584.

Blandino, A., Al-Aseeri, M.E., Pandiella, S.S., Cantero, D., & Webb, C. (2003). Cereal-based fermented foods and beverages. *Food Research International, 36*, 527-543.

Dalmacio, L. M. M., Angeles, A. K. J., Larcia, L. L. H., Balolong, M. P., & Estacio, R. C. (2011). Assessment of bacterial diversity in selected Philippine fermented food products through PCR-DGGE. *Beneficial Microbe, 2(4),* 273–281.

Department of Environment and Natural Resources- CALABARZON-. (2018). Physical and Socio-Economic Profile. Retrieved from http://calabarzon.denr.gov.ph/index.php/about-us/regional-profile/reg-profile-physical-socio-eco

Endmemo. (2017). DNA/RNA GC Content Calculator. Retrieved from http://www.endmemo.com/bio/gc.php

Elegado, F.B., Colegio, S.T., Lim, V.T., Gervasio, A.R., Perez, M.M., Balolong, M.P., Banaay, C.B. and Mendoza, B.C. 2016. Ethnic fermented foods of the Philippines with reference to lactic acid bacteria and yeasts. Springer, India. p. 325.

Entani, E., Ohmori, S., Masai, H., & Suzuki, K. (1985). *Acetobacter polyoxogenes* sp. nov., a new species of an acetic acid bacterium useful for producing vinegar with high acidity. *Journal of General and Applied Microbiology, 31,* 475-490.

Felsenstein, J. (1985). Confidence limits on phylogenies: An approach using the bootstrap. *Evolution, 39*, 783-791.

Haruta, S., Ueno, S., Egawa, I., Hashiguchi, K., Fujii, A., Nagano, M., Ishii, M., … Igarashi, Y. (2006). Succession of bacterial and fungal communities during a traditional pot fermentation of rice vinegar assessed by PCR-mediated denaturing gradient gel electrophoresis. *International Journal of Food Microbiology, 109,* 79–87.

Hashimoto, M., Obara, K., Furuyashiki, M., Ikeda, T., Suda, Y., Fukase, K., Fujimoto, Y., … Shigehisa, H. (2013). Separation and characterization of the immunostimulatory components in unpolished rice black vinegar (*kurozu*). *Journal of Bioscience and Engineering, 116 (6),* 688-696.

Hommel, R. K. (2014). Acetobacter. *Encyclopedia of Food Microbiology, 1,* 3-10.

Hucker, G. J. & Conn, H. J. (1923). Methods of Gram Staining. New York City: State Agr Expt Sta Tech Bull. p.129.

Kelly, W. J., Asmundson, R. V., Harrison, G. L., & Huang, C. M. (1995). Differentiation of dextran-producing *Leuconostoc* strains from fermented rice cake (*puto*) using pulse-field gel electrophoresis. *International Journal of Food Microbiology, 26,* 345-352.

Konig, H., Unden, G., & Fröhlich, J. (Eds.). (2009). Biology of Microorganisms on Grapes, in Must, and in Wine. Berlin Heidelberg: Springer-Verlag.

Korakli, M., Rossmann, A., Gänzle, M. G., & Vogel, R. F., (2001). Sucrose metabolism and exopolysaccharide production in wheat and rye sourdoughs by *Lactobacillus sanfranciscensis*. *Journal of Agricultural Food Chemistry, 49,* 5194-5200.

Kumar, S., Stecher, G., Li, M., Knyaz, C., & Tamura, K. (2018). MEGA X: Molecular Evolutionary Genetics Analysis across computing platforms. Molecular Biology and Evolution. Retrieved from https://doi.org/10.1093/molbev/msy096

Li, Z., Li, H., & Bian, K. (2016). Microbiological characterization of traditional dough fermentation starter (*Jiaozi*) for steamed bread making by culture-dependent and culture-independent methods. *International Journal of Food Microbiology, 234,* 9–14.

Mamlouk, D. & Gullo, M. (2013). Acetic Acid Bacteria: Physiology and Carbon Sources Oxidation. *Indian Journal of Microbiology, 53(4),* 377–384.

MacFaddin J. F. (2000). Catalase-Peroxidase Tests. Biochemical Tests for Identification of Medical Bacteria. (3rd ed.). Philadelphia: Lippincott Williams and Wilkins. pp. 78-97.

Nanda, K., Taniguchi, M., Ujike, S., Ishihara, N., Mori, H., Ono, H., and Murooka, Y. (2001). Characterization of Acetic Acid Bacteria in Traditional Acetic Acid Fermentation of Rice Vinegar (*Komesu*) and Unpolished Rice Vinegar (*Kurosu*) Produced in Japan. *Applied and Environmental Microbiology, 67 (2),* 986-990.

National Center for Biotechnology Information, U.S. National Library of Medicine. (n.d.) Basic Local Alignment Search Tool. Retrieved from https://blast.ncbi.nlm.nih.gov/Blast.cgi

National Economic and Development Authority- MIMAROPA. (2013). Marinduque: Location, Geography and Climate. Retrieved from http://mimaropa.neda.gov.ph/marinduque/

Navarro R.R. and Komagata, K. (1997). Differentiation of *Gluconacetobacter liquefaciens* and *Gluconacetobacter xylinus* on the basis of DNA base composition, DNA relatedness and oxidation products from glucose. J. Gen. Appl. Microbiol. 45:7-15.

Nei M. & Kumar S. (2000). Molecular Evolution and Phylogenetics. New York: Oxford University Press.

Park, J., Seo, J., Kim, S., Shin, S., Park, J., & Han, N. (2017). Microbial Diversity of Commercial *Makgeolli* and Its Influence on the Organoleptic Characteristics of Korean Rice Sourdough, *Jeung-pyun*. *Journal of Microbiology and Biotechnology, 27(10),* 1736-1743.

Pothakos, V., Illeghems, K., Laureys, D., Spitaels, F., Vandamme, P., & De Vuyst, L. (2016). Acetic acid bacteria in fermented food and beverage ecosystems. In Matsushita, K., Toyama, H., Tonouchi, N., & Kainuma, N. (Eds). *Acetic Acid Bacteria: Ecology and Physiology* (pp. 73-99). New York: Springer.

Philippine Statistics Authority. NSCB Bicol Region. (2014). Sorsogon: Overview of the Region. Retrieved from http://nap.psa.gov.ph/ru5/overview/geography.html

Philippines Travel and Hotel Guide. (2018). Pangasinan: Best of the Islands Philippines. Retrieved from http://info.philtravelcenter.com/pangasinan-info1.php

Sanchez, P. C. (2008). Philippine fermented foods: Principles and technology. Diliman: The University of the Philippines Press.

Saitou, N. & Nei, M. (1987). The neighbor-joining method: A new method for reconstructing phylogenetic trees. *Molecular Biology and Evolution, 4,* 406-425.
Sanchez, P.C. (1999). Microorganisms and technology of Philippine Fermented Foods. *Japanese Journal of Lactic Acid Bacteria, 10(1),* 19-28.

Sievers, M. & Swings, J. (2015). *Acetobacteraceae*. In Bergey's Manual of Systematics of Archaea and Bacteria. John Wiley & Sons, Inc.

Swings, J., Gillis, M., Kersters, K., De Vos, P., Gossele, F., & De Ley, J. (1980). *Frateuria*, a new genus for "*Acetobacter aurantius*". UK: International Journal of Systematic Bacteriology. pp. 547-556.

Tamang, J. P., Watanabe, K, & Holzapfel, W. H. (2016). Review: Diversity of Microorganisms in Global Fermented Foods and Beverages. *Frontiers in Microbiology, 7,* 377.

Tieking, M., Korakli, M., Ehrmann, M. A., Ganzle, M. G., & Vogel, R. F., (2003). *In situ* production of exopolysaccharides during sourdough fermentation by cereal and intestinal isolates of lactic acid bacteria. *Applied Environmental Microbiology, 69,* 945-952.

Uchimura, T., Garcia, V. V., & Flores, D. M. (1984). Microbiological Studies on Fermented Rice Cake, *"Puto*" and the Application to *Puto* Making using Cassava Flour. Japan: Tropical Root Crops: Postharvest Physiology and Processing. pp. 273-283.

Wilson, K. (1987). Preparation of genomic DNA from bacteria. In: Ausubel, F. M., Brent, R., Kingston, R. E., Moore, D. D., Seidman, J. G., Smith, J. A., & Struhl, K., (Eds). *Current Protocols in Molecular Biology* (pp. 241–245). New York: John Wiley & Sons.

11:30 AM - 12:30 PM (Thu. Sep 5, 2019 11:30 AM - 12:30 PM Poster Place)

[5-1130-P-30] Estimation of Greenhouse Gas Emissions from Poultry Farming Systems for a Broiler Meat Production and an Egg Production in Japan using a Life Cycle Assessment

*Tatsuo Hishinuma[1], Tetsuya Hoshino[1], Atsuo Ikeguchi[1], （1.Utsunomiya Univ.(Japan)）

Keywords: broiler production, layer, egg production, LCA

The increase of greenhouse gas is a cause of global warming, and the possible contributing to cause climate change locally and globally. The reduction of greenhouse gas emissions is an issue to be solved worldwide. In Japan, the aim of reducing greenhouse gas emissions was 26% by 2030 comparison with 2013. In 2015, agriculture contributed 34.8 Mt-CO2e (2.5%) of Japan’ s greenhouse gas emissions. Contributions for greenhouse gas emissions from agriculture are from livestock, soil and manure sources (methane and nitrous oxide). Furthermore, CO2 emission from energy and material use at agricultural practices was contributed environmental impact. Furthermore, CO2 emission from energy and material used at agricultural practices is contributed to environmental impact. Therefore, the evaluation of environmental aspects of agricultural production systems by life cycle thinking was required to reveal direct impacts as well as indirect impacts for considering mitigation measures. Several studies have been reported GHG emissions from beef production systems and pork production systems by the LCA in Japan. However, life cycle GHG emissions from broiler meat production systems and egg production systems have not been reported. The aim of this study was to assess life cycle GHG emissions from poultry farming systems of a broiler meat production system and an egg production system.

The system boundary and process model of poultry farming system of broiler meat and egg production include the feed production process, livestock management process and manure treatment process. The functional unit was defined as 1 kg of broiler meat and 1kg of an egg at the evaluation of broiler meat and egg production system respectively.

The amount of agricultural material consumption data of the process model of the poultry farming system for life cycle inventory analysis were collected from statistical based data and reports. Most of the background data, such as GHG emission from fuel combustion and indirect GHG emission at agricultural materials, for inventory analysis were used the values from the database of the IDEA ver.2.2, which mostly represents Japanese production. The indirect GHG emissions associated with animal husbandry equipment, machinery, and poultry houses production processes were excluded from the system boundary. The GHG emissions were evaluated using GWP100 (CO2:1, CH4:34, N2O: 298). The objective broiler production system utilized three of the two-story windowless poultry house and handled 4000 hundred birds (broilers) annually. The egg production system used two of windowless poultry house with two steps floor type for handled 630 hundred birds (layers) and produced 1100t eggs annually. The GHG emissions from the broiler meat production system was estimated to 3.12 [kg-CO2e/kg-broiler meat]. The GHG emissions from the feed production process, fuel consumption of warming at the poultry management process and the manure treatment process were contributed to total GHG emissions from broiler meat production systems. The GHG emissions from the egg production system was 2.86 [kg-CO2e/kg-egg]. The processes contributed to GHG emissions from egg production systems were the feed production process and the manure treatment process.